NATIONAL CENTRE FOR INFORMATION AND DOCUMENTATION

ADVANCES
IN
BULGARIAN SCIENCE

Annual
2013
SOFIA

Published by National Centre for Information and Documentation
52 A, G. M. Dimitrov Blvd.
1125 Sofia, Bulgaria
Phone: +359 2 817 38 62
http: www.nacid.bg
e-mail: advances@nacid-bg.net

Disclaimer
The articles are published as provided by their authors, without additional editing.

ISSN: 1312-6164

CONTENTS

NATIONAL SCIENTIFIC PROGRAMMES WITH EUROPEAN DIMENSIONS **5**

Laser-Induced Fluorescence Spectroscopy – a Contemporary Approach to Cultural Heritage 5

Electromagnetic Systems and Devices with Nano-Ferrofluid 11

Optimization of some Culture Conditions by Response Surface Methodology for Lipase Production from *Aspergillus carbonarius* 20

Selected Lactobacillus Strains Prevent the Adhesion of Pathogenic Bacteria to Human Epithelium 26

Performance Characteristics of two Analythical Assays for Drugs of Abuse 30

Underground Well Temple in Bulgaria: Architectural and Archaeoastronomical Analysis 34

Analysis of Mixed-Mode I/II/III Fracture in Foam Core Composite Sandwich Beams 43

Small-Scale Tests for an Investigation on the Effect of Reinforced Soil 49

BULGARIAN ADDED VALUE TO ERA **56**

Bulgarian Society for Eighteenth-Century Studies 56

MADE IN BULGARIA WITH EUROPEAN SUPPORT **58**

Carbon-Based Nanocomposites with Intermetallic Cu-Sn Nanoparticles as Anode Materials in Li-Ion Batteries 58

EQUAL IN EUROPEAN RESEARCH AREA 66

BULGARIAN VIPs **66**

AWARDS **70**

ARTICLES **72**

EVENTS **75**

NACID

National Centre for Information and Documentation

MAIN OBJECTIVES

NACID is:

- Leading institution in the national information infrastructure in Bulgaria in the sphere of education, science and innovations.
- National Information Centre for Academic Recognition and Mobility - ENIC-NARIC centre for Bulgaria.
- Contact point in terms of Directive 2005/36/EC on the recognition of professional qualifications and delegated coordinator for Bulgaria in Internal Market Information (IMI) system.

PRIMARY FIELDS OF ACTIVITIES:

- Processing and dissemination of bibliographic and reference data and analytical information in support of the policy in the sphere of education, science, technology and innovations;
- Building and maintaining specialized databases;
- Maintaining national stock and DB of dissertations, deposited manuscripts and other scientific publications in Bulgaria.
- Organizing application of ENIC-NARIC network decisions in the field of academic recognition.
- Realizing information assistance in procedures for academic and professional recognition.
- Performing activities resulting from the functions of ENIC-NARIC center.
- Furnishing citizens and contact points in the rest of the member states with information in connection with recognition of professional qualifications and rights for practicing regulated professions in conformity with the Directive 2005/36/EC.
- Performing functions of institutional contact point of the EU's Seventh Framework Programme

INFORMATION PRODUCTS AND SERVICES:

- NACID offers a wide range of information products: subject profiles, paper reviews, subject bibliographic and reference information.
- NACID offers a great variety of information services through its own databases and resources, as well as through information brokerage to external databases. Online access is provided to NACID's own databases grouped in two basic information blocks:

"Bulgarian Science" Databases

- *"SIRENA",* R&D *reports and dissertations;*
- *"Scientific and Technical Publications in Bulgaria";*
- *"Register of the Scientific Degrees and Titles".*

"Science and Industry" Databases

- "*Partnership for Innovation and Development";*
- *"Knowledge for Innovations and Development".*

Information brokerage and servicing from external databases gives access to over 1200 databases of the leading information centers, including STN International – Germany, DIALOG – USA, EBSCO, etc.

- **Library Services**

Central Research and Technical Library (CRTL) with Library and Information Complex in Pedagogics is one of the largest Bulgarian libraries and main supplier of information in the field of science, education, pedagogics, engineering, technology and economy with more than 4 million registered items, including books, periodicals, dissertations, publications on CD ROM, DVD. It offers:

- Lending of library materials;
- Online access to the library catalogues since 1980;
- Searching in electronic catalogues and databases;
- Electronic Document Delivery;
- Interlibrary loan.

INTERNATIONAL ACTIVITY

- Represents the Republic of Bulgaria in international organizations on the subject of its activities.
- Joint actions and projects with related national information and documentation centers in the EU.

NATIONAL SCIENTIFIC PROGRAMMES WITH EUROPEAN DIMENSIONS

LASER–INDUCED FLUORESCENCE SPECTROSCOPY – A CONTEMPORARY APPROACH TO CULTURAL HERITAGE

Victoria Atanassova[1], Stefan Karatodorov[1], Georgi Yankov[1], Peter Zahariev[1], Elitsa Tsvetkova[2]

[1]Institute of Solid State Physics, Bulgarian Academy of Sciences

72, Tzarigradsko Chaussee, Blvd., 1784 Sofia, Bulgaria

[2]National Gallery for Foreign Art

1, 19 February, str., "St. Aleksander Nevsky" Square, 1000 Sofia, Bulgaria

e-mail: vatanassova@issp.bas.bg

Abstract

Laser-induced fluorescence spectroscopy is a nondestructive surface analytical technique widely used for identifying the chemical composition of organic and inorganic compounds. It is applied in many fields of human activity due to the measurements simplicity and quickness. Cultural heritage preservation needs a delicate approach in many cases. This results in establishment of various laser techniques, including LIF, as reliable and adequate methods for studying valuable objects. In this regard, the Institute of Solid State Physics at the Bulgarian Academy of Sciences together with the National Gallery for Foreign Art initiated a project entitled "Laser-induced fluorescence analysis for investigation and preservation of cultural heritage", funded by the Bulgarian Science Fund. The main goal of this project is to study various materials often found in artworks and to create an extensive database of materials characteristics. This will be in favor of conservators-restorers as they will be able to identify easily and quickly the objects surface composition.

INTRODUCTION

Scientific study on cultural heritage objects has its origin in the late eighteenth century, when the German scientist Friedrich Klaproth examined the composition of metal coins. Ever since scientific methods have been applied to study many aspects of the preservation of our cultural heritage (artworks, archaeological findings, historical buildings, etc.). With the technological advance the conservator scientists' needs for nondestructive and non-invasive techniques are increasing, because of the unique character of artifacts. This improves the understanding of their manufacture, evolution and degradation with time, which is necessary knowledge for appropriate conservation- restoration protocols (Bradley & Creagh, 2006). In this paper we present a contemporary nondestructive method for analyzing chemical composition of a given material present on a surface layer. Laser-induced fluorescence (LIF) spectroscopy is based on the absorption of laser light by the material's molecules, being illuminated. Thus excited to higher electronic states, the molecules reemit light, relaxing to the ground electronic state (fig. 1) (Schreiner et al., 2008; Gronlund et al., 2006).

The fluorescence spectrum of every material is unique and reproduces its molecular structure. As shown in fig. 1, both spectra, the absorption and fluorescence, are mirror-images of each other, covering different wavelength regions – the excitation maximum is in the UV-blue wavelengths and the fluorescence maximum is in the

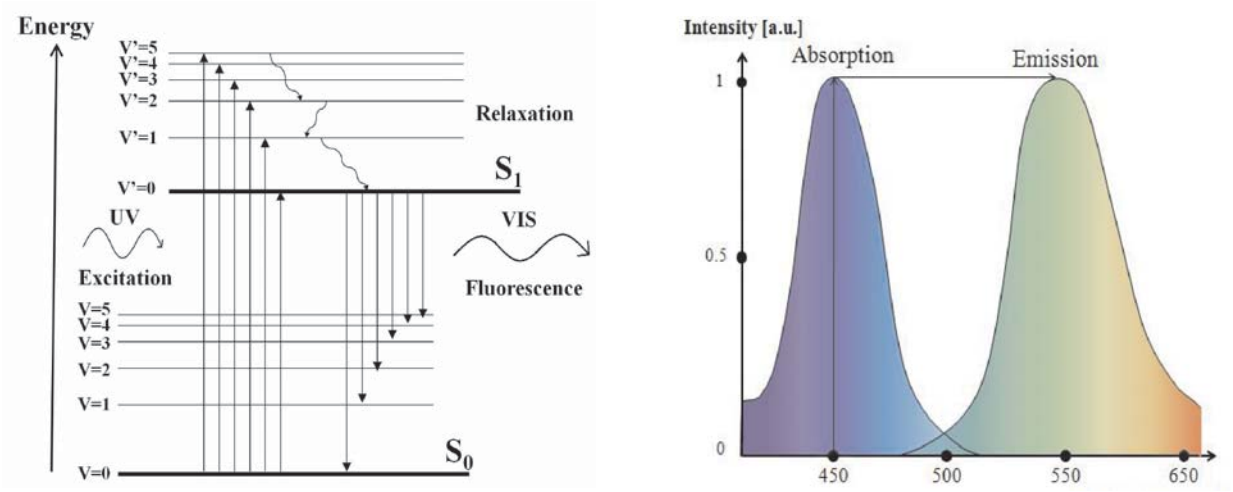

Fig. 1. Mechanism of LIF

blue/green wavelength region. Alterations of materials are displayed as differences in the slopes and wavelength for the maximum fluorescence (Schreiner et al., 2008; Gronlund et al., 2006).

The wavelength-intensity chart gives precise information about the presence of distinct chemical compounds in small or large (LIF imaging) area. As the fluorescence spectra are characterized usually by broad peaks, fluorescence spectroscopy doesn't always guarantee a detailed identification of sample's composition by itself. The analytical capabilities of the method can be improved by measuring the temporal characteristics of the fluorescence signal. Thereby particular species can be identified not only by their fluorescence spectra, but also by the time spent in excited electronic state and the decay profile. This time is of the order of few ns (10^{-9} s) to μs (10^{-6} s) (Schreiner et al., 2008).

A modification of LIF, combining fluorescence imaging and lifetime measurement, named FLIM (Fluorescence Lifetime Imaging Microscopy), increases the sensitivity and the simplicity of the method when applied for large areas (wall paintings, buildings, etc.). Due to the knowledge about temporal properties of the fluorescence emission in every point of the sample's surface, FLIM indicates precisely the chemical compounds in the whole extension of a cultural heritage object, without the need for extensive sampling (Schreiner et al., 2008).

Laser-induced fluorescence is a versatile, selective and very sensitive technique which could provide spatial and temporal information about an object of any size and material (organic or inorganic) in laboratory or in situ, without the need of sampling or preparation. There is also a possibility of remote sensing using optical fibers or light detecting and ranging (LIDAR) system (Valeur, 2001; Schreiner et al., 2008). These features come from the use of lasers as excitation source. Lasers offer the advantage of selective excitation within the absorption spectrum of a material enabling high precision in the identification of species. Furthermore, laser sources have a possibility of high-resolution measurements allowing the detection of small quantities of substances or chemical compounds in small area (Schreiner et al., 2008).

As every other analytical method, there are several limitations and disadvantages in LIF appliance: spectral complexity; limited compound sensitivity, due to the fact that there are materials (pigments or other substances) with weak fluorescence signal that is impossible to detect; decreased sensitivity, because of the broad molecular bands; no available databanks (Schreiner et al., 2008; Fotakis et al., 2007).

Analysis of the molecular composition gives information of original materials used for creating the object (pigments, aging varnish or binder, protective coating, etc.). It characterizes the products of deterioration or the materials added during old restoration procedures. The fluorescence emission also indicates biological growth and detects forgeries. LIF can be combined with other analytical techniques for accurate identifi-

cation of materials or for diagnostics of restoration procedures, as for example laser cleaning (Schreiner et al., 2008). Except in conservation this method is used also in medicine, biology, material analyses and quality control, etc.

Preservation of cultural heritage takes essential place among the activities of our civilization. Analysis of the chemical composition of objects of historical significance is an important step in the conservation process. For that reason the Institute of Solid State Physics together with the National Gallery of Foreign Art started a project entitled "Laser-induced fluorescence analysis for investigation and preservation of cultural heritage", funded by the Bulgarian Science Fund. The project aims at incorporating and developing the technique, studying most of the basic materials (pigments, dyes, adhesives and binders) that have been commonly used in the past and at creating extensive database of characteristic compound spectra which will enable further studies of authentic artworks.

EXPERIMENT

As excitation sources we have used three semiconductor lasers generating 405, 445 and 532 nm. We have also used Q-switched Nd:YAG laser system (Quanta Ray GCR3), oscillating at 355 nm (3rd harmonic) with maximum energy ~ 35 mJ, pulse length 8 ns and variable repetition frequency up to 10 Hz. The fluorescence light, emitted by a small excited area of the sample, passes through broadband filters which cut off the intensive laser radiation and transmit the fluorescence. That light is collected by a lens and through an optical fiber is analysed by a spectrometer. We have used two spectrometers: Avantes 3648 portable spectrometer with operating range 300 – 850 nm and 1 nm resolution; Mechelle 5000 – ANDOR with operating range 220 – 850 nm and spatial resolution about 0.05nm. The latter is equipped with ICCD camera (180 – 850 nm) with temporal resolution 5 ns. The spectrometers are wavelength calibrated. The registered fluorescence spectra are visualized on a computer screen (fig. 2).

With the help of professional restorers we prepared test samples on which different pigments and dyes (cochenille, carmine naccarat, gamboge, turmeric, safflower, indigo blue lake, burnt umber, ivory black, ultramarine, etc.), adhesives and binders (bone glue, isinglass, gum Arabica, dammar, linseed oil, casein, etc.) commonly used in paintings and artworks in the past were painted. Part of the samples is presented in Fig. 3.

The painted rectangles consist of various

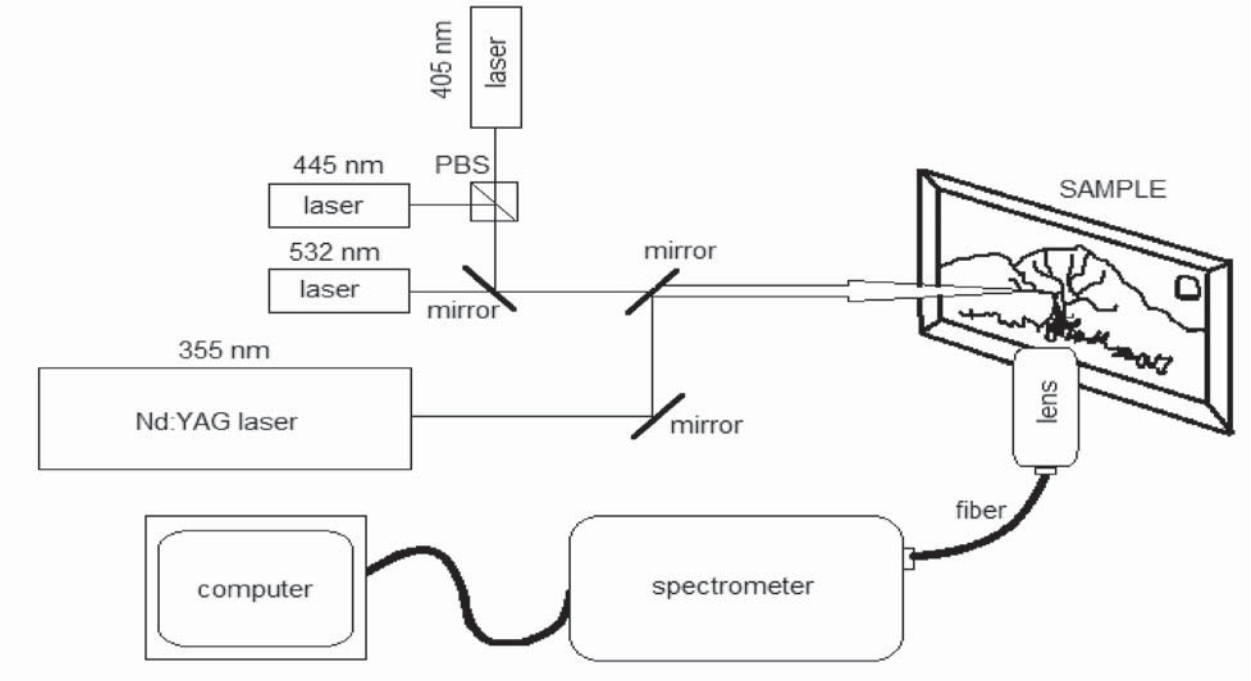

Fig. 2. Experimental set-up of LIF system

combinations of selected pigments and adhesives. Some of them are varnished with dammar dissolved in white spirit because the surface of the majority of authentic paintings is protected by varnish coatings which influence the spectroscopic study. There are also rectangles that consist only of adhesives, one and the same pigment mixed with different adhesives or one and the same adhesive mixed with different pigments. This variety enriches the investigation and the obtained database.

All of the test samples are investigated with three laser wavelengths: 355, 405 and 445 nm. Some of the results are presented in this paper. Spectra of ultramarine mixed with different kinds of adhesives are shown in Fig. 4. There is

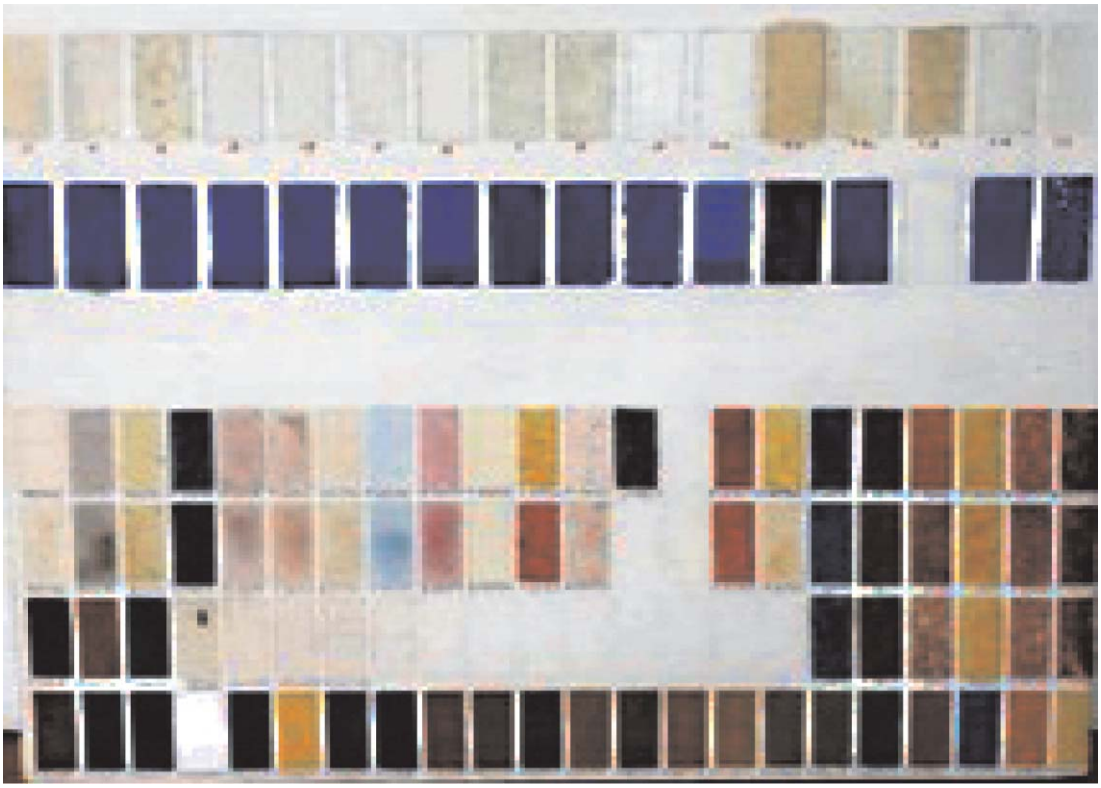

Fig. 3. Part of the test samples.

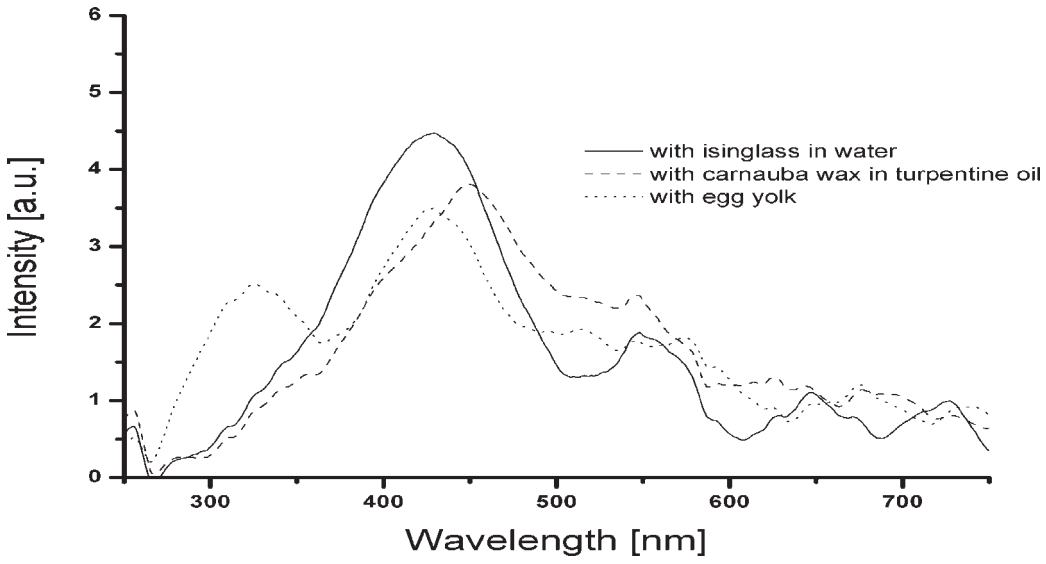

Fig. 4. LIF spectra of Ultramarine mixed with different adhesives.

a significant change in the fluorescence signal from the varied combinations.

The organic adhesives have stronger fluorescence emission than the inorganic.

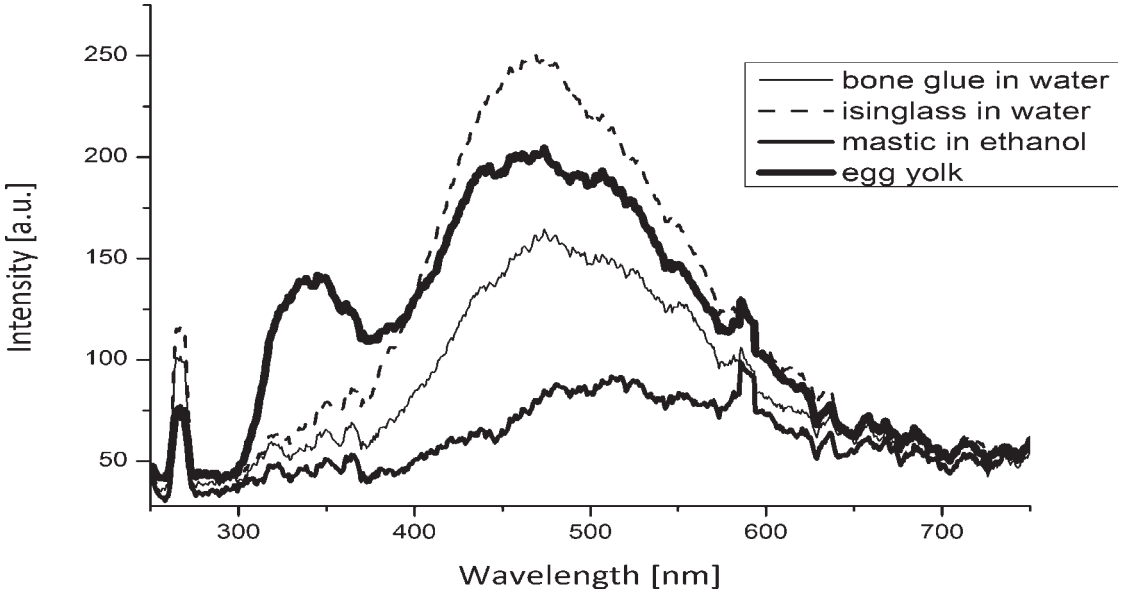

Fig. 5. LIF spectra of some adhesives

Considerable alteration in the spectrum, when the paints are coated with a varnished layer, is observed, too. Due to the transparency of the varnish, most of the exciting light reaches the layer of adhesive and pigment and resultant spectrum is observed. The characteristic light passes through the varnish layer, where it can be partially absorbed and/or reemitted. The obtained spectra are analyzed in order to estimate the sensitivity of the LIF method.

The first steps of collecting comprehensive databanks were done studying variety of widely used adhesives and binders' fluorescence spectra (Fig. 5).

Most of the studied pigments in pure form have very weak signal excited by the used operating energies. Increasing the energy leads to slightly stronger intensity of the signal, but the risk of damaging the surface due to photo-thermal and photo-chemical effects increases, too.

To confirm the results obtained with our system we conducted the same experiments with other LIF set-up, placed in laboratory CERTO – INOE 2000, Bucharest, Romania. The laser system consists of Diode Pumped Solid State (DPSS) laser, generating 266 nm. A comparison between spectra achieved by both set-ups was done. These spectra are shown in fig. 6. As one can

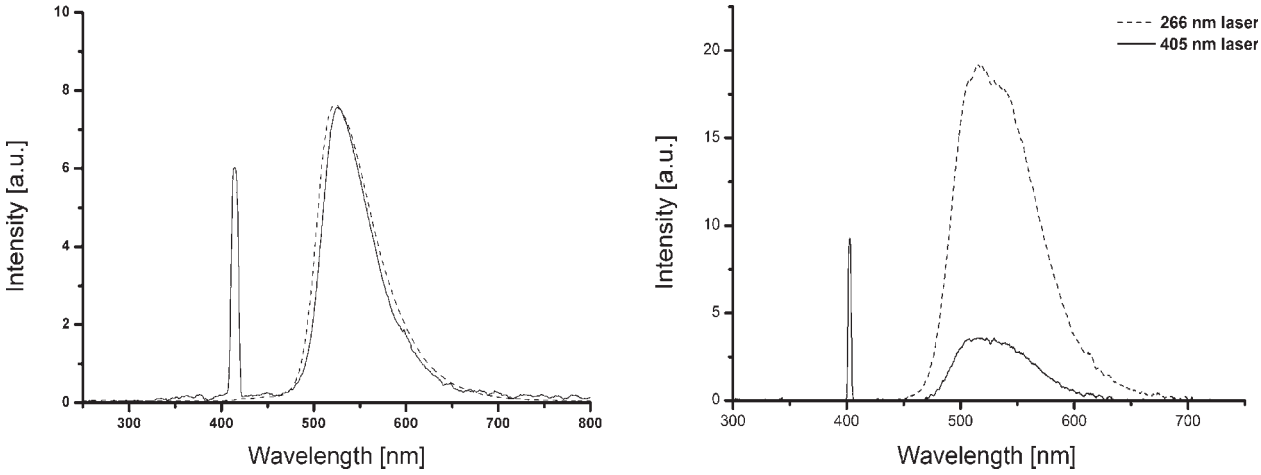

Fig. 6. Comparative LIF spectra from UV and deep UV laser: a) normalized; b) registered by one and the same spectrometer

see, there is a good spectral overlap when both spectra are normalized, i.e. one and the same substance is analyzed by both LIF systems. The influence of the individual set-up components in the experiment was considered as well.

The advantage of using short-wave coherent exciting source with wavelength in the deep UV range (266 nm) is demonstrated. DUV light excites the molecules with higher sensitivity and the intensity of luminescence is an order of magnitude higher than that excited by the UV light. The wavelength dependence of the method is unequivocal.

CONCLUSIONS

In investigation of organic and inorganic compounds the availability of wide variety of narrow-band excitation sources gives the opportunity for high-selective fluorescence measurements. Collecting database of common chemical compounds found in the composition of cultural heritage objects, the conservator scientists will be able to detect specific species on a given surface quickly and selectively. We are planning to enrich the collected database by studying more test samples and improving our experimental set-up, which will involve DUV laser and femtosecond laser equipped with optical parametric amplifier (OPA). This will increase the potential of the method selectivity and sensitivity. Time-resolved measurements are expected to become available as well.

Acknowledgement

The Project is supported by the Bulgarian Science Fund (contract DMU 03/79).

References

[1] Bradley D. & Creagh D. (2006) Physical techniques in the study of Art, Archaeology and Cultural Heritage vol. 1, Elsevier.

[2] Fotakis C., Anglos D., Zafiropulos V., Georgiou S. & Tornari V. (2007) Lasers in the Preservation of Cultural Heritage – Principles and Applications, Series in optics and optoelectronics, v. 2.

[3] Gronlund R., Hallstrom J., Johansson A., Barup K. & Svanberg S. (2006) Remote multicolor excitation laser-induced fluorescence imaging, Lasers in the preservation of Cultural Heritage, Laser Chemistry, Vol. 2006.

[4] Schreiner M., Strlic M. & Salimbeni R. (2008) Handbook on the use of lasers in conservation and conservation science, COST.

[5] Valeur B. (2001) Molecular Fluorescence – Principles and Applications, Wiley-VCH Verlag GmbH.

ЛАЗЕРНО-ИНДУЦИРАНА ФЛУОРЕСЦЕНТНА СПЕКТРОСКОПИЯ – СЪВРЕМЕНЕН ПОДХОД КЪМ КУЛТУРНОТО НАСЛЕДСТВО

Виктория Атанасова[1], Стефан Каратодоров[1], Георги Янков[1], Петър Захариев[1], Елица Цветкова[2]

[1]Институт по физика на твърдото тяло,
Българска академия на науките
бул. „Цариградско шосе" 72, 1784 София
[2]Национална галерия за чуждестранно изкуство
ул. „19 февруари" 1,
площад „Св. Александър Невски", 1000 София

Резюме

Лазерно-индуцираната флуоресцентна (ЛИФ) спектроскопия е недеструктивна повърхностна аналитична техника, широко използвана за определяне на химичния състав на органични и неорганични съединения. Тя намира своето приложение в много области на човешката дейност поради простотата и бързината, с които се извършват измерванията. Опазването на културното наследство в повечето случаи изисква деликатен подход. Различните лазерни техники, включително и ЛИФ спектроскопията, се налагат като надеждни и адекватни за изследване на ценни обекти. Проектът, който осъществява Институтът по физика на твърдото тяло, съвместно с Националната галерия за чуждестранно изкуство, цели изследването на различни материали, които присъстват в състава на обекти с историческа стойност, и създаването на подробна база данни с характеристиките на тези материали. Това ще подобри работата на консерватор-реставраторите и те ще имат възможността бързо и лесно да определят състава на повърхността на дадения обект, което, от една страна, дава историческа информация, а от друга, е начален етап при избора на подходящ консервационно-реставрационен подход.

ELECTROMAGNETIC SYSTEMS AND DEVICES WITH NANO–FERROFLUID

Iliana Marinova*, Valentin Mateev, Aneliya Tezova
Department of Electrical Apparatus, Technical University of Sofia
8 Kliment Ohridski blvd., Block 12, 1756 Sofia, Bulgaria
**E-mail: iliana@tu-sofia.bg*

Abstract

Appearance of the new generation nano-ferrofluid materials dramatically improves operational characteristics of electromagnetic systems and devices. In this work new performance of solenoid type electromagnetic actuator with nano-ferrofluid is investigated and analyzed. Theoretical approach based on 3D multiphysics model of the actuator is developed for fields, processes and phenomena analysis as well as for determination of actuator operational characteristics and parameters. The model couples together electromagnetic field analysis, electric circuit analysis, fluid dynamics analysis and mechanical movement analysis. Transient mode of switching on the electromagnetic actuator is modeled. Measurement system for experimental determination of static and dynamic characteristics of the electromagnetic actuator with ferrofluid is built. Operational electromagnetic characteristics of the actuator are obtained and compared with and without ferrofluid presence in the working gap. Measured results are presented, analyzed and compared with those obtained by developed theoretical model. The developed theoretical and experimental models and investigation approaches could be used in design, optimization and investigation of new effective electromagnetic actuators and devices.

INTRODUCTION

Electromagnetic actuators are widely used in industry [1-5] because of their operational advantages including excellent performance, high reliability, long lifetime, minimal maintenance, etc. They are part of various electromechanical devices, controlling different mechanisms and systems. An electromagnetic actuator with solenoid type electromagnet is utilized in electromagnetic valve actuation systems, fuel injection actuation, exhaust gas recirculation systems, refrigerators, washing machines, etc. [1-4].

Static characteristics are necessary for interoperability of electromagnet operation and counteractions, such as reaction of spring or mass of the armature, etc. Dynamic characteristics are very important because they describe completely performance of the actuator. The static and dynamic characteristics are very sensitive to core shape, electric elements, mechanical elements and magnetic elements. In order to obtain accurate dynamic characteristics of the electromagnetic actuator, it is necessary to perform a transient analysis. To take into account all physical phenomena, it is necessary to couple electromagnetic field analysis, electric circuit analysis, fluid dynamics analysis and mechanical movement [5, 6].

In recent years electromagnetic systems with ferrofluid nanoscale materials [7-11] attract growing interest. These systems have many advantages. Electromagnetic actuators with ferrofluid in the working gap are characterized with better operational characteristics compared with those with air gaps, such as reduced energy consumption, compact in size, etc.

Ferrofluid is a colloidal stable suspension of ferrite nanoparticles in liquid and surfactant. The surfactant molecules covered the solid particles and the fluid behaves as a homogeneous system even in the presence of external forces. Nanoparticles are usually iron oxides or different compounds as manganese-ferrite, zinc-ferrite, manganese-zinc-ferrite, cobalt-ferrite, copper-ferrite, and nickel-ferrite. The liquids are deionized water or a mixture of organic solvents or synthetic oils. The sizes of nanoparticles can vary from 1 nm to 100 nm and determine the properties of ferrofluid. In addition there are two other key parameters used to specify ferrofluids, namely saturation, magnetization

and viscosity. By varying the constituents, a wide diversity of ferrofluids with different properties could be created [12, 13].

Modeling of electromagnetic field distributions in electromagnetic actuators with ferrofluid in its construction must be handled by modern coupled field numerical methods covering all specific properties of modeled applications. Finite element method (FEM) is a powerful numerical method capable to solve such complex problems taking into account all characteristics and special features. Recent achievements of the FEM give possibilities to model fully three-dimensional, nonlinear, inhomogeneous, or anisotropy fields and multi-joint systems.

In this work two investigation approaches are applied for analysis of electromagnetic systems with nano-ferrofluid. The first one is theoretical approach for multiphysics problem modeling; the second one is experimental approach realized via a sophisticated computer-aided measurement system.

In this work new performance of solenoid type electromagnetic actuator with nano-ferrofluid is investigated and analyzed. 3D multiphysics model of the actuator is developed for fields, processes and phenomena analysis as well as for determination of actuator operational characteristics and parameters. The model couples together electromagnetic field analysis, electric circuit analysis, fluid dynamics analysis and mechanical movement analysis. Magnetic field distribution is analyzed by the finite element method. Electromagnetic force over the actuator armature is calculated by the Maxwell stress tensor method. Dynamic behavior of electromagnetic actuator in transient mode is numerically modeled. Measurement system for experimental determination of static and dynamic characteristics of the electromagnetic actuator with ferrofluid is built.

Electromagnetic force and operational characteristics of solenoid type actuator are measured by laboratory measurement system. Operational electromagnetic characteristics are determined for armature moving in ferrofluid in the working gap and they are compared with the characteristics of electromagnet without ferrofluid.

PROBLEM FORMULATION

To take into account all physical phenomena that take place in the actuator construction, it is necessary to couple electromagnetic field analysis, electric circuit analysis, fluid dynamics analysis and mechanical movement analysis. For determination of the dynamic characteristics of the electromagnetic actuator, a multiphysics coupled electromagnetic field – fluid dynamics – dynamic movement model is established. The field distributions inside the electromagnet working gap region depend on the ferrofluid presence there as well as on the electric circuit and kinematics of the device.

Magnetic field modeling

Magnetic field distribution in electromagnet actuator is described by the magnetic vector potential formulation

$$\nabla\times\left(\frac{1}{\mu}\nabla\times\mathbf{A}\right)-\nabla\times\left(\frac{\mu_0}{\mu}\mathbf{M}\right)=\mathbf{J}, \qquad (1)$$

where **A**, **M**, **J** and μ are the magnetic vector potential, magnetization vector, the source current density and magnetic permeability, respectively.

Homogeneous Dirichlet's boundary conditions are imposed over the boundary of buffer zone surrounding the actuator.

Magnetic force acting on armature is calculated by the Maxwell stress tensor method

$$\mathbf{F}_M=\iint_s\left((\mathbf{n}\cdot\mathbf{B})\mathbf{H}-\frac{1}{2}(\mathbf{B}\cdot\mathbf{H})\mathbf{n}\right)ds, \qquad (2)$$

where **B**, **H**, **n**, *s* are the vector of magnetic flux density, vector of magnetic field intensity, unit vector to normal and closed surface, respectively [15].

Magnetic inductance *L* is calculated by stored magnetic field energy – *W* expressed by

$$W=\frac{1}{2}Li^2, \qquad (3)$$

where *i* is the coil current.

Fluid dynamics modeling

The effect of magnetic field on the magnetic nanoparticles volume concentration is governed by the Navier–Stokes equation for fluid velocities **v** and pressure *p*

$$\rho\left(\frac{\partial\mathbf{v}}{\partial t}+\mathbf{v}\nabla\mathbf{v}\right)=\nabla p+\eta\nabla^2\mathbf{v}+\mathbf{F}_M, \qquad (4)$$

where ρ and η are the density and viscosity of ferrofluid, respectively.

Equation (4) is solved with suitable boundary conditions specifying the contact between the fluid and the domain walls, $\mathbf{v} = 0$, and zero traction force at the outflow, $(\rho_{\mathbf{n}}\text{-}\mathbf{v}_{\mathrm{n}}) = 0$ on the fluid domain cross-section.

Dynamic modeling

Dynamic characteristics of electromagnetic actuator system are determined in switching - transient mode. The system of equations which describes the process of switching on the electromagnetic actuator is composed of the electric circuit equation of the actuator coil and motion equation

$$\left| \begin{array}{l} U = Ri + \dfrac{d\Psi}{dt} \\ F_M = m\dfrac{d^2x}{dt^2} + kx + F_{fr} + F_{ff} \end{array} \right. , \quad (5)$$

where in the electric circuit equation U, R, Ψ, x are supply voltage, resistance of the coil, flux linkage and displacement of the armature, respectively. In the motion equation m, k, F_M, F_{fr}, F_{ff} are mass of the armature, stiffness coefficient of the spring, electromagnetic force, friction force with core and resistive force of ferrofluid, respectively [15, 18]. Magnetic flux linkage is determinate by the coil inductance, depending on coil current and armature gap.

The system is solved by the Euler method, which is first-order numerical procedure for solving ordinary differential equations. For each time step of the integration procedure the current values of electromagnetic force and coil inductance are acquired by the FEM magnetic field model.

COMPUTER AIDED MEASUREMENT SYSTEM

Computer measurement laboratory test system is developed for determination of static electromagnetic and dynamic characteristics of electromagnetic solenoid type actuator. Block diagram with main elements of the developed measurement system is shown in Fig. 1.

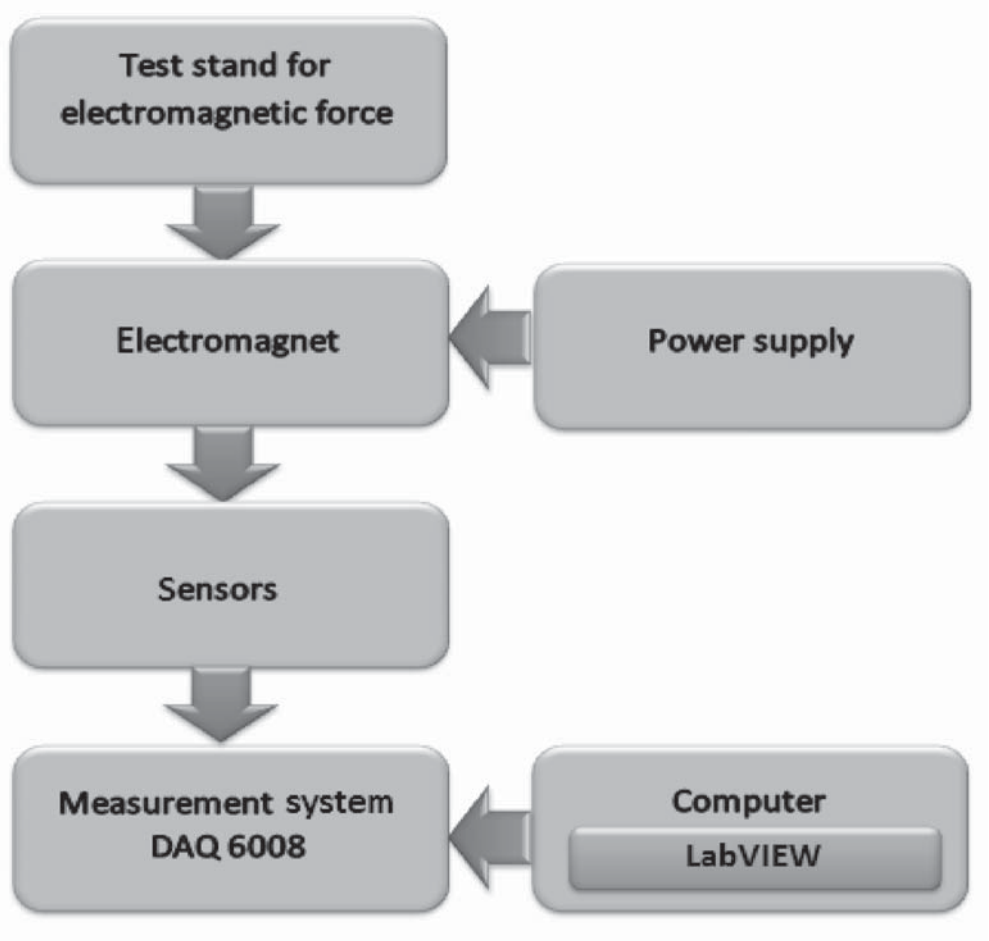

Fig. 1. Block diagram of the experimental computer measurement system.

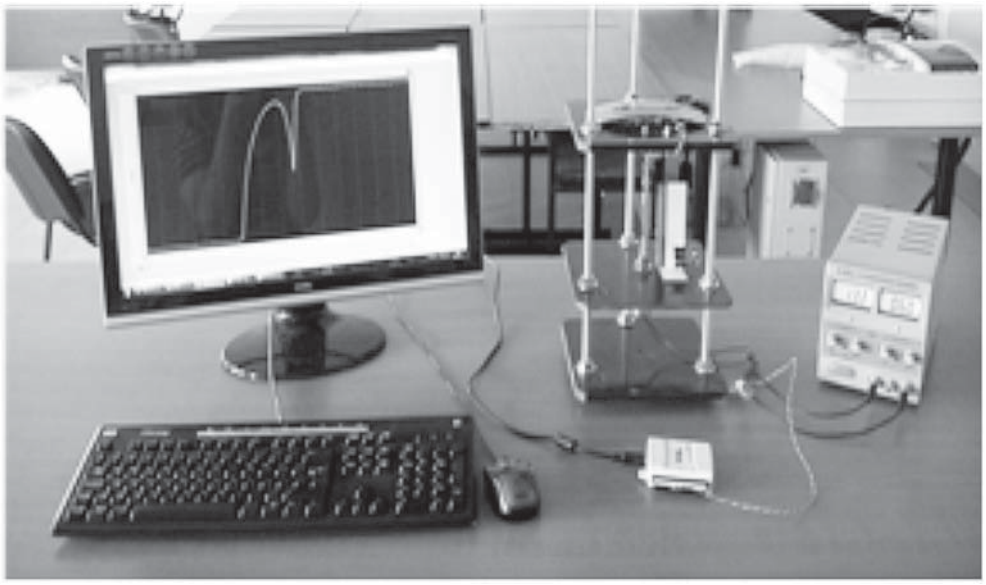

Fig. 2. Computer measurement system.

Computer measurement system is composed of test bench/fixture, measurement sensors and transducers, controllable power supply, data acquisition measurement module and computer unit with LabVIEW software, shown in Fig.2.

Constructed test bench/fixture is shown in Fig.3.

The main elements of the test bench are

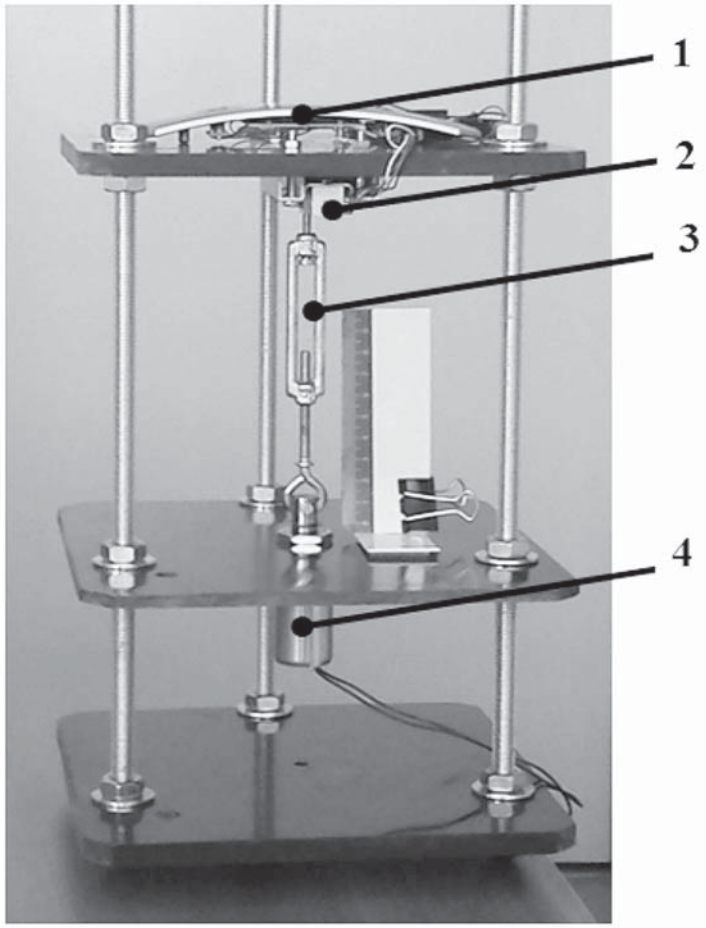

Fig. 3. Test bench

1 - digital display; 2 - weight sensors 3 –spring; 4 – solenoid type electromagnet.

force/strain gauge, holder for fixing armature, injector for ferrofluid. A force/strain gauge for measuring the strength/pressure at range ± 30N with accuracy of 0,001 N is used. The computer measurement system is supplied by DC electric power supply HY3005D [17]. Automation of the measurement process is done by using the program LabVIEW [17].

SOLENOIDAL ELECTROMAGNETIC ACTUATOR

The electromagnetic actuator under consideration is solenoid type construction and consists of a stationary ferromagnetic core, a movable cylindrical ferromagnetic part (armature) with cone end, magnetic gap filled with ferrofluid, opening spring and supporting elements. Cross-section with dimensions of the electromagnetic actuator is shown in Fig. 4.

The material of core and armature is electrical steel with non-linear B-H characteristic [3]. The air gap is filled with ferrofluid and is considered as a magnetic gap. The coil consists of 600 turns, copper wire with diameter 1mm is used. Average current density at coil region is J = $7x10^6$ A/m^2. The mass of the armature is m = 0.042 kg. The used spring is with stiffness coefficient k = 300 N/m. The ferrofluid is with relative magnetic permeability μ = 1.21; saturation flux density B_s = 44 mT (± 10%); magnetization M = 107 kA/m; viscosity < 6 mPa•s; density 1.1 g/cm^3; boiling point 230 °C (± 10 %) [14]. Electric power of the coil energizes the magnetic circuit. Magnetomotive force (mmf), determined by the rated current I = 1.66A and number of turns w, creates magnetic flux. Magnetic flux creates electromagnetic force attracting the armature. Ferrofluid is used to reduce the dissipation of magnetic flux in the working gap of the electromagnet.

IMPLEMENTATION

For solving the electromagnetic problem the finite element method by ANSYS 12.1 software is employed [16]. 3D geometrical model of electromagnetic actuator (Fig. 4 – c) is built and im-

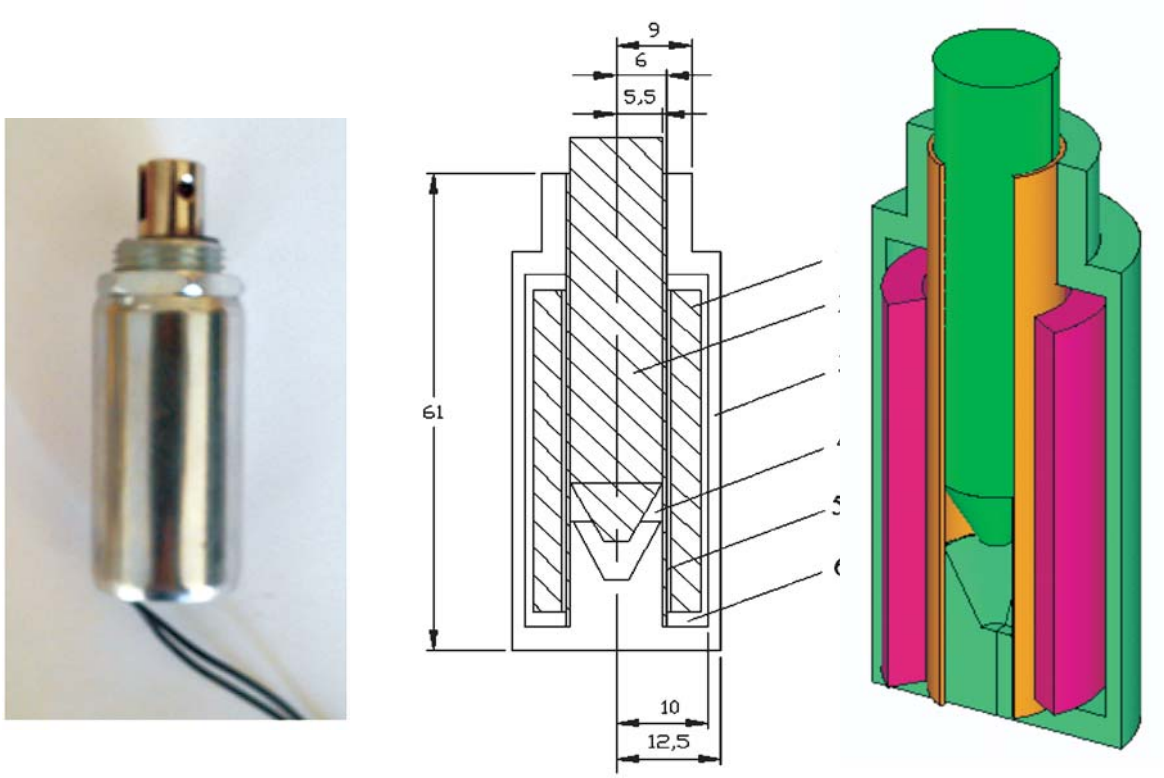

a) outlook b) cross-section c) 3D model

Fig. 4. Electromagnetic actuator
1 – coil; 2 - ferromagnetic armature; 3 - ferromagnetic core; 4 – magnetic gap; 5 - brass tube; 6 - insulation of the coil.

plemented for determination of static and dynamic characteristics. Magnetic, electric and motion equations are coupled for determination of dynamic characteristics. Computational process uses iterative technique, the time is divided into subintervals equal to 0.001s. The current of the coil, velocity and displacement of the armature are calculated in each time step. Values of electromagnetic force and inductance of the coil are obtained from magnetic problem by finite element method. The results from the current step are used to obtain the solution in the next time step. The initial conditions used for dynamic characteristics calculations at $t_0=0$ are $\delta_0=\delta_{in}$, $x_0=0$, $i_0=0$, $U=6V$, $R=3.7\Omega$. The calculations are made for different initial working gaps δ_{in} = 6ч18 mm. Computations were automated using ANSYS Parametric Design Language (APDL).

Electromagnetic actuator is investigated in static and dynamic mode. Static electromagnetic force is calculated at working gap δ = 1÷18 mm. Dynamic characteristics are obtained at various working gaps. Distributions of magnetic flux density of the electromagnetic actuator at several values of the magnetic gap are determined.

In Fig. 5 – a, b, c, d magnetic flux density distributions for electromagnet with air gap and with ferrofluid at δ = 1 mm and δ = 18 mm are shown. The maximum value of the magnetic flux density obtained with ferrofluid at working gap δ = 1 mm is B_{max}=1.75 T and with air gap B_{max}=1.74 T. At working gap δ = 18 mm the maximum value of the magnetic flux density with ferrofluid is B_{max}=1.020 T and with air gap B_{max}=0.97 T.

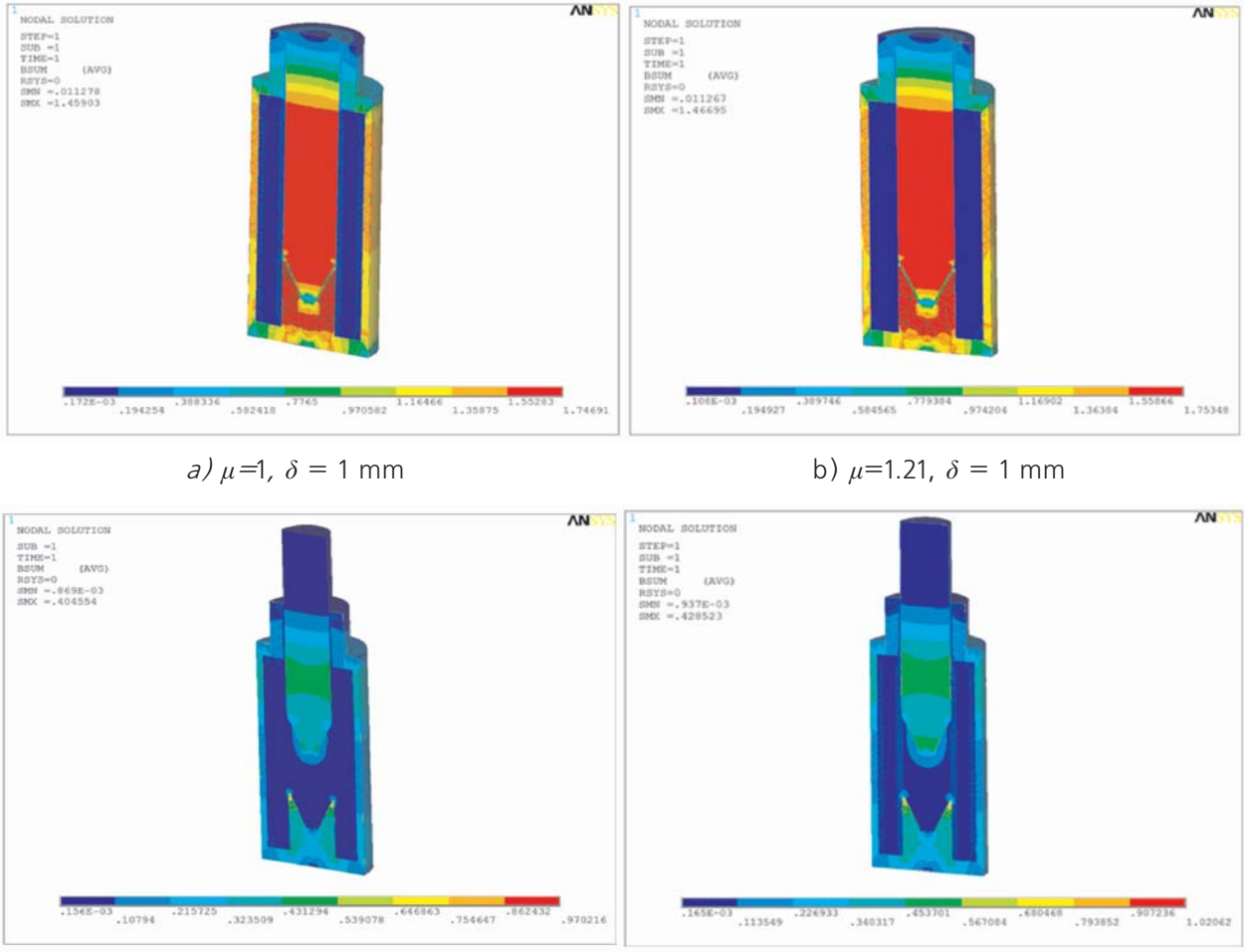

a) μ=1, δ = 1 mm

b) μ=1.21, δ = 1 mm

c) μ = 1, δ=18 mm

d) μ = 1.21, δ=18 mm

Fig.5. Distribution of magnetic flux density

In Fig. 6 – a, b the dynamic characteristics of the current changing with time in switching mode of the electromagnet are given. Calculations are made for electromagnet with air gap and with working gap filled with ferrofluid. In Fig. 7 characteristics of electromagnetic force changing with time are shown, and in Fig. 8 the characteristic of inductance changing with time is shown.

The presence of ferrofluid in electromagnet leads to increasing of the magnetic force acting on the armature at greater working gaps. Moreover, the value of ferrofluid permeability affects on the shape of the corresponding curve, the characteristic becomes flatter. In switching on mode the current in the electromagnet with ferrofluid is lower than in electromagnet with air gap (Fig. 6). The coil inductance is higher when the electromagnet operates with ferrofluid. The switching time of solenoid is almost not influenced. These results are experimentally investigated [17].

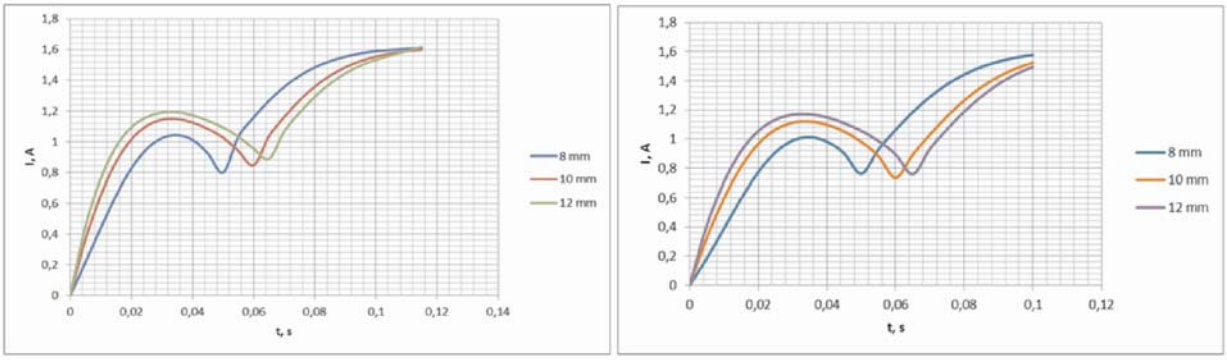

a) air gap b) magnetic gap with ferrofluid

Fig. 6. Time dependence of the current in switching mode of the electromagnet.

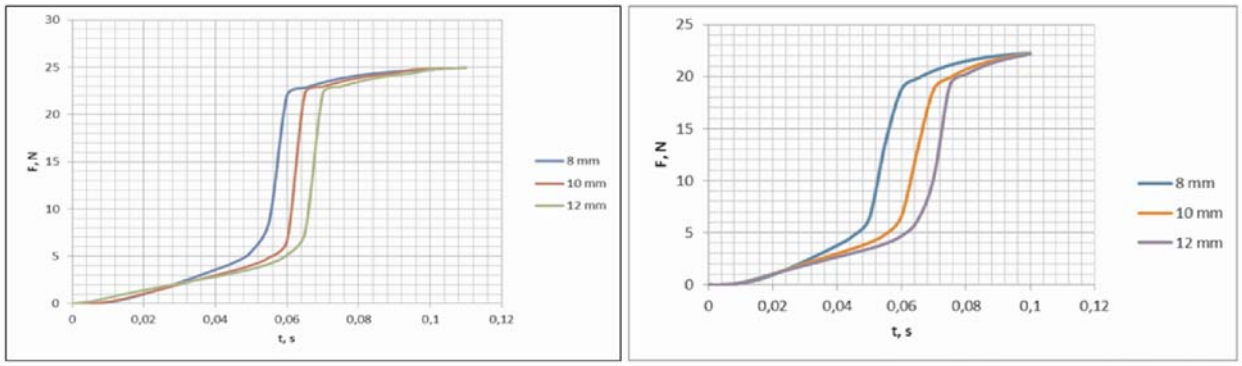

a) air gap b) magnetic gap with ferrofluid

Fig. 7. Time dependence of the electromagnetic force in switching mode of the electromagnet.

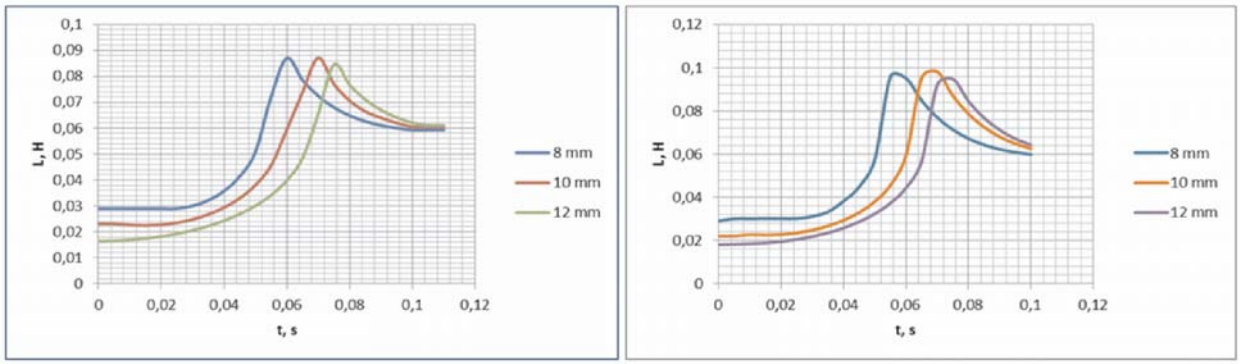

a) air gap b) magnetic gap with ferrofluid

Fig. 8. Time dependence of the inductance in switching mode of the electromagnet.

EXPERIMENTAL INVESTIGATION

Dynamic characteristics of the electromagnetic actuator are measured by the developed computer measurement system. Dynamic characteristics are determined in switching - transient mode for electromagnet's armature. For this purpose the holder device for fixing actuator armature in the stationary position has been replaced by a spring mechanism.

In Fig. 9 the dynamic characteristics of the current changing with time in switching mode of the electromagnet are given. Rated current of the solenoid type electromagnet is 1.66 A.

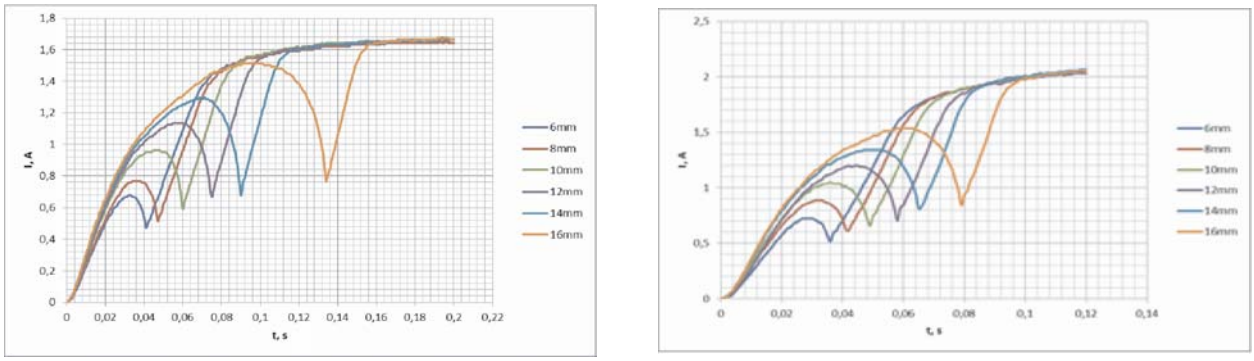

(a) (b)

Fig. 9. Dynamic characteristics of the actuator at various gaps at supply current of I =1.66A - a) and I = 2.075A – b)

Dynamic characteristics of the electromagnet are determined also at current 25% higher than the rated one (I = 2.075 A). The results obtained for transient process are shown in Fig.9-b.

The response time of the electromagnet for air gap δ = 6 mm with current I = 1.66A is t = 0.041s and with current I = 2.075A, t = 0.036s. For air gap δ = 16 mm and I=1.66 A the response time is t = 0.134 s and for I = 2.075A, t=0.079 s.

It is seen that for larger air gaps with increasing current by 25%, the response time of the electromagnet decreases almost by half.

CONCLUSIONS

Investigation approach for solenoid type electromagnetic actuator with nano-ferrofluid is developed and performed. 3D multiphysics model of the actuator is developed and applied for operational characteristics determination. Operational electromagnetic characteristics are determined for armature moving in ferrofluid in the working gap and they are compared with the characteristics of the electromagnet without ferrofluid. Computer measurement system for experimental determination of static and dynamic characteristics of the electromagnetic actuator with ferrofluid is built. The developed and implemented computer measurement system is characterized with simplicity, with easy operation and high accuracy according to force measurements (0.001 N), distance measurements (0.1 mm) and electric voltage measurement (1.47 mV). Measurement process could be further improved by applying a more sophisticated virtual instrument and accurate sensors. Developed computer measurement system is suitable for investigation of electromagnetic actuators as well as for scientific and educational research.

The developed model can be applied for explorations of characteristics of such electromagnetic devices. The developed theoretical and experimental models and investigation approaches could be used in design and optimization of new effective electromagnetic devices.

Acknowledgement

Parts of this research were supported by the National Research Fund of the Republic of Bulgaria at the Ministry of Education, Youth and Science (contract DO 02-157/2008) and project 132PD0047-01 – 2013 of the R&D Sector of Technical University of Sofia, Bulgaria.

References

[1] Cazacu D., Stanescu C. (2011), Performance analysis of a solenoidal electro-magnet, Scientific Bulletin of the Electrical Engineering Faculty, "Valahia" University of Targoviste, Romania, Vol. 2 (16) 2011, 5-10.

[2] Terzova A., Mateev V., Marinova I. (2013), Modelling of electromagnetic actuator with ferrofluid, Proceeding of full paper of 7th International PhD Seminar on Computational electromagnetics and bioeffects of electromagnetic fields – CEMBEF 2013, August 28-31, 2013, Niљ, Serbia, 75-78.

[3] Terzova A., Mateev V., Marinova I. (2013) Static and dynamic characteristics of actuator with ferrofluid, Proceedings of the Technical University - Sofia, v. 64, book 2, 2013.

[4] Lee J., Dede E., Banerjee D., Iizuka H. (2012), Magnetic force enhancement in a linear actuator by air-gap magnetic field distribution optimization and design, Finite Elements in Analysis and Design, Vol. 58, 2012, 44R52.

[5] Mateev V., Marinova I., Terzova A. (2011), Transient electromagnetic modeling of electromagnetic system, Proceedings of the Technical University - Sofia, Vol. 61, book 2, 2011, 113–121.

[6] Shin D., Choi M., Kwon J., Jung H. (2007), Analysis of an Electromagnetic Actuator for Circuit Breakers, Journal of Electrical Engineering and Technology, Vol. 2, No. 3, 2007, 346-352.

[7] Sreedhar B., Kumar R., Sharma P., Ruhela S., Philip J., Sundarraj S., Chakraborty N., Mohana M., Sharma V., Padmakumar G., Nashine B., Rajan K. (2013), Development of active magnetic bearings and ferrofluid seals toward oil freesodium pumps, Nuclear Engineering and Design, Vol. 256, 2013, 1166t1174.

[8] Andт B., Baglio S., Beninato A. (2012), A ferrofluid inclinometer with a time domain readout strategy, Proc. Eurosensors XXVI, Krakyw, Poland, 2012, 586 – 589.

[9] Horak W., Szczęch M. (2013), Experimental and numerical determination of the static critical pressure in ferrofluid seals, Journal of Physics: Conference Series No. 412, 2013, 1-6.

[10] Yoon T., Lee J., Kim D., Lee Y., Park M. (2012), Experimental Investigation of Magnetic Fluid used in Tandem mode for Underwater Vehicle System, 16-th International Conference on Mechatronics Technology, Tianjin, China, 2012, 59-61.

[11] Schultheis T., Hoheisel D., Xiao W., Molella L., Reithmeier E., Rissing L., Hardt S. (2012), Performance of an adaptive liquid microlens controlled by a microcoil actuator, Microfluid Nanofluid, Vol. 13, 2012, 299–308.

[12] Scherer C., Figueiredo A. (2005), Ferrofluids: Properties and Applications, Brazilian Journal of Physics, 2005, 718-727.

[13] Raj K., Moskowitz B., Tsuda S. (2004), New commercial trends of nanostructured ferrofluids, International Journal of Engineering and Materials Sciences, 2004, 241-252.

[14] Mateev V., Marinova I., Saito Y. (2013), Coupled Field Modeling of Ferrofluid Heating in Tumor Tissue, IEEE Transactions on Magnetics, Vol. 49, Issue 5, 2013, 1793–1796.

[15] Yatchev I., Marinova I. (2007), Numerical Analysis and modeling of circuits and fields, Technical University of Sofia, 2007.

[16] ANSYS Release 12.0 Documentation, 2010.

[17] Terzova A., Mateev V., Marinova I. (2013), Computer measurement system for determination of static and dynamic characteristics of electromagnetic actuator with ferrofluid, Proceedings of 23-th National Scientific Symposium with international participation on Metrology and Metrology Assurance, Sozopol, 2013, 205-208.

[18] Yatchev I., Hinov K., Gueorgiev V. (2004), Dynamic Characteristics of a Bi-stable Linear Actuator with Moving Permanent Magnet, Serbian journal of electrical engineering Vol. 1, No. 2, June 2004, 207–214.

ЕЛЕКТРОМАГНИТНИ СИСТЕМИ И УСТРОЙСТВА С НАНОФЕРОФЛУИДИ

Илиана Маринова, Валентин Матеев, Анелия Терзова

Катедра „Електрически апарати", Технически университет - София
бул. „Климент Охридски" №8, бл. 12, 1756 София

Резюме

Появата на нови наноферофлуидни материали подобрява значително работните характеристики на електромагнитните системи и устройства. В тази статия е изследвана работата на соленоиден електромагнитен изпълнителен механизъм с наноферофлуид. Формулирана е задачата за моделиране на работните характеристики на изследвания електромагнитен изпълнителен механизъм. Разработен е 3D модел, използващ метода с крайни елементи, за изследване на свързаните физични полета на електромагнитната система. Моделът съчетава задачите за анализ на магнитно поле, електрическа верига, флуидна динамика и кинематика на подвижните части. Преходният процес на включване на електромагнитния изпълнителен механизъм е изследван посредством прецизна компютърна измервателна система за експериментално определяне на електромагнитните работни характеристики на устройството. Моделираните и експериментално измерени работни характеристики, със и без ферофлуид, са сравнени и анализирани. Разработените и разгледани модели и измервателна система формират обобщен изследователски подход, който може да се използва при проектирането и оптимизацията на нови ефективни електромагнитни устройства и изпълнителни механизми.

OPTIMIZATION OF SOME CULTURE CONDITIONS BY RESPONSE SURFACE METHODOLOGY FOR LIPASE PRODUCTION FROM *ASPERGILLUS CARBONARIUS*

Georgi Dobrev*, Boriana Zhekova, Valentina Dobreva, Hristina Strinska
University of Food Technologies
Department of Biochemistry and Molecular biology
26 Matitsa Blvd., 4000 Plovdiv, Bulgaria
**E-mail: g_dobrev2002@yahoo.fr*

Abstract

The influence of initial pH of the nutrient medium and cultivation temperature on lipase biosynthesis from Aspergillus carbonarius was studied. It was found that the strain produced considerable amount of lipase enzyme in the range of pH 3.0-7.0 and temperature of 27-30°C. By carrying out a planned experiment and a mathematical realization of optimal composite design a regression model was developed. It was used for prediction of the optimal values of the factors – cultivation temperature (28.5°C) and initial pH of the medium (6.5), at which maximum predicted lipase activity was $\hat{Y}$ *= 2864.89 U/L. The mathematical model was adequate at a confidence level 6 = 0.05 and it was characterized by a high value of the correlation coefficient* R^2*=0.99. Five consecutive experiments at the predicted optimal values?of the factors were carried out. A mean value* $\hat{Y}$ *= 2779.90 U/L of lipase activity with a standard deviation* $\sigma = \pm$ *103.63 was achieved, which experimentally confirmed the results obtained from the mathematical model.*

INTRODUCTION

The group of lipolytic enzymes includes lipases or also called "true lipases" (EU 3.1.1.3), which catalyze the hydrolytic cleavage of ester bonds in water-insoluble long chain triacylglycerols (chain length higher than 10 carbon atoms), a large number carboxylesterases (EU 3.1.1.1), which hydrolyze small ester-containing molecules at least partly soluble in water, and phospholipases (EC 3.1.4.X) (Arpigni & Jaeger, 1999).

The catalytic action of lipases in aqueous media is a typical example of a heterogeneous catalysis. Due to the hydrophobic nature of the substrate, enzyme reaction takes place at the interface of water-oil emulsions. Interfacial surface has a significant effect on the rate of the reaction, and therefore its kinetics can not be described by the Michaelis-Menten equation (Reis et al., 2009). Besides hydrolytic activity, in aqueous free media lipases have the ability to catalyze esterification, interesterification, alcoholysis, acidolysis and aminolysis (Pahoja & Sethar, 2002).

The variety of substrates and the nature of reactions catalyzed by lipases, determined their application in various fields of industry. They are used in dairy industry, where as a result of their hydrolytic activity volatile products are produced, which form and amplify a specific taste and aroma. In baking industry the hydrolytic activity of lipases is used for preparation of biosurfactants, which improve bread structure. Most large-scale applications of lipases are their inclusion in the composition of detergents and their use for transesterification of vegetable oils in the production of biodiesel (Ghosh et al., 1996).

Because of the huge variation in applications, the availability of lipases with specific characteristics is still a limiting factor. Thus searching for new lipases with different characteristics and improving lipase production continue to be important research topics (Uppada et al., 2012).

The properties of lipases from various sources (plants, animals and microorganisms) are known and studied. Manufacture of commercial lipases is based on a submerged cultivation of bacteria, yeasts or fungi. Fungal lipases attract considerable research interest, because they are extracellular enzymes and in some cases they are characterized by a high thermal stability (Ghosh

et al., 1996). Microbial biosynthesis of lipases is significantly influenced by fermentation conditions – cultivation temperature and pH of the nutrient medium (Kumari et al., 2009; Sharma et al., 2012). Improving fermentation conditions is the most frequently used operation in biotechnology to obtain maximum cell density, high yields of the desired metabolic product, or enzyme levels in the microbial system. This approach is not only time consuming, but also ignores combined interactions between physicochemical parameters. Hence response surface methodology (RSM), which includes factorial design and regression analysis, helps in evaluating effective factors and in building models to study interaction and select optimum conditions of variables for a desirable response (Adinarayana et al., 2004; Kaushik et al., 2010).

The aim of the study is by using RSM to determine the optimal cultivation temperature and initial pH of the nutrient medium for achieving maximum lipase activity from *Aspergillus carbonarius* in a submerged cultivation.

MATERIAL AND METHODS

Microorganism

A strain of *Aspergillus carbonarius* NRRL369 from ARS Culture Collection was used for lipase biosynthesis. The strain was cultivated on a slant agar medium containing (g/L): glucose 20.0, yeast extract 10.0, agar-agar 15.0. Preparation of the medium included pH adjustment to 7.0 and sterilization at 121 ºC for 30 min. The inoculated tubes were incubated at 27 ºC for 7 days and were stored at 4ºC.

Inoculum preparation

For inoculum preparation the following nutrient medium was used (g/L): malt extract 10.0, yeast extract 4.0, glucose 4.0, K_2HPO_4 1.0, $NaNO_3$ 2.5. Cultivation was performed in 500-ml Erlenmeyer flasks, containing 100 mL nutrient medium with pH 6.5. The flasks were inoculated with 2.5 mL of 7 day-old culture, containing 3.10^7-3.10^8 spores/mL and the strain was grown at 27 °C for 48 h with a 180 rpm rotary shaking.

Lipase biosynthesis

Submerged cultivation of the strain was performed in 500-mL Erlenmeyer flasks, containing 50 mL nutrient medium with composition (g/L): rapeseed oil 20.0, meat extract 5.6, $MgSO_4$ 1.0, KH_2PO_4 4.0 and Tween 80 20.0. After sterilization the medium was inoculated with 5.0 mL inoculum and the strain was grown at 27 °C for 64 h with a 180 rpm rotary shaking. Biomass was removed by filtration and the culture liquid was tested for lipase activity. The influence of initial pH of the nutrient medium on lipase biosynthesis was studied in the range of pH 3.0-9.0, and the effect of cultivation temperature was studied in the range of 23-30 °C.

Response surface methodology

Optimal composite design 2^2 was used to find the optimal cultivation temperature and pH of nutrient medium for lipase production from *Aspergillus carbonarius*. The quadratic regression models are one of the most widely used in practice. They are expressed as follows:

$$\hat{Y} = b_0 + \sum_{i=1}^{m} b_i . x_i + \sum_{i=1, j=i+1}^{m} b_{ij} . x_i . x_j + \sum_{i=1}^{m} b_{ii} . x_i^2 \quad (1)$$

where $\hat{Y}$ is the response variable, b – the regression coefficients of the model, and– coded levels of the independent variables (Vuchkov & Stoyanov, 1980).

Independent variables participating in the 2^2 and their values are presented in Table 1.

Table 1
Values of independent variables at different levels of the optimal compsite design 2^2

Independent variables	Levels		
	-1	0	1
x_1– Temperature (°C)	25.0	27.0	29.0
x_2 - pH	5.0	7.0	9.0

The coding of the independent variables is done by using:

$$x_i = \frac{(x_i - x_{io})}{\Delta x_i} \quad (2)$$

x_i is the current value of the i –factor, x_{io}– is the current value of the i –factor in the center point of the design, Δx_i – is the step of variation of the i –factor.

Determination of lipase activity

For lipase activity determination the method proposed by (Kaushik et al., 2006) was adapted. The method is based on the use of a synthetic substrate c-nitrophenyl palmitate. Substrate solution was prepared by dissolving 30 mg ρ-nitrophenyl palmitate in 10 mL isopropanol and addition of phosphate buffer with pH 6.0 to 100 mL total volume. 2.4 mL of the substrate solution were incubated at 35 ^{o}C for 10 min and 0.1 mL suitably dissolved enzyme was added. The enzyme reaction was performed at 35 ^{o}C for 30 min and the enzyme was inactivated by addition of 1.0 mL 10 % solution of NaOH. The reaction mixture was centrifuged at 3000 min^{-1} for 10 min and the absorbance at 405 nm was measured in accordance to a reference sample with an inactivated enzyme.

One unit (U) of lipase activity was defined as the amount of enzyme releasing 1 μmol ρ-nitrophenol for 1 min at 35 ^{o}C and pH 6.0.

EXPECTED RESULTS

The effect of initial pH of the nutrient medium on lipase biosynthesis from *Aspergillus carbonarius* is presented on Fig. 1.

Maximum lipase activity 2524.27 U/L was achieved at initial pH 7.0 of the nutrient medium. The optimal pH value of the nutrient medium for lipase biosynthesis varies for different strains. Some authors found that the optimal initial pH of the nutrient medium during cultivation of *Aspergillus* sp. is in the range of pH 6.0-7.0 (Adinarayana et al., 2004; Falony et al., 2006; Hosseinpour et al., 2011). Ghosh et al. (1996) established that in the acidic pH range lipase activity decreased.

In contrast to the results in the literature, in the cultivation of *Aspergillus carbonarius* significant lipase activity (about 80%) was detected at pH 3.0 (Fig. 1). These results are prerequisite for production of a lipase enzyme with specific characteristics.

Lipase biosynthesis was significantly influenced by cultivation temperature (Fig. 2).

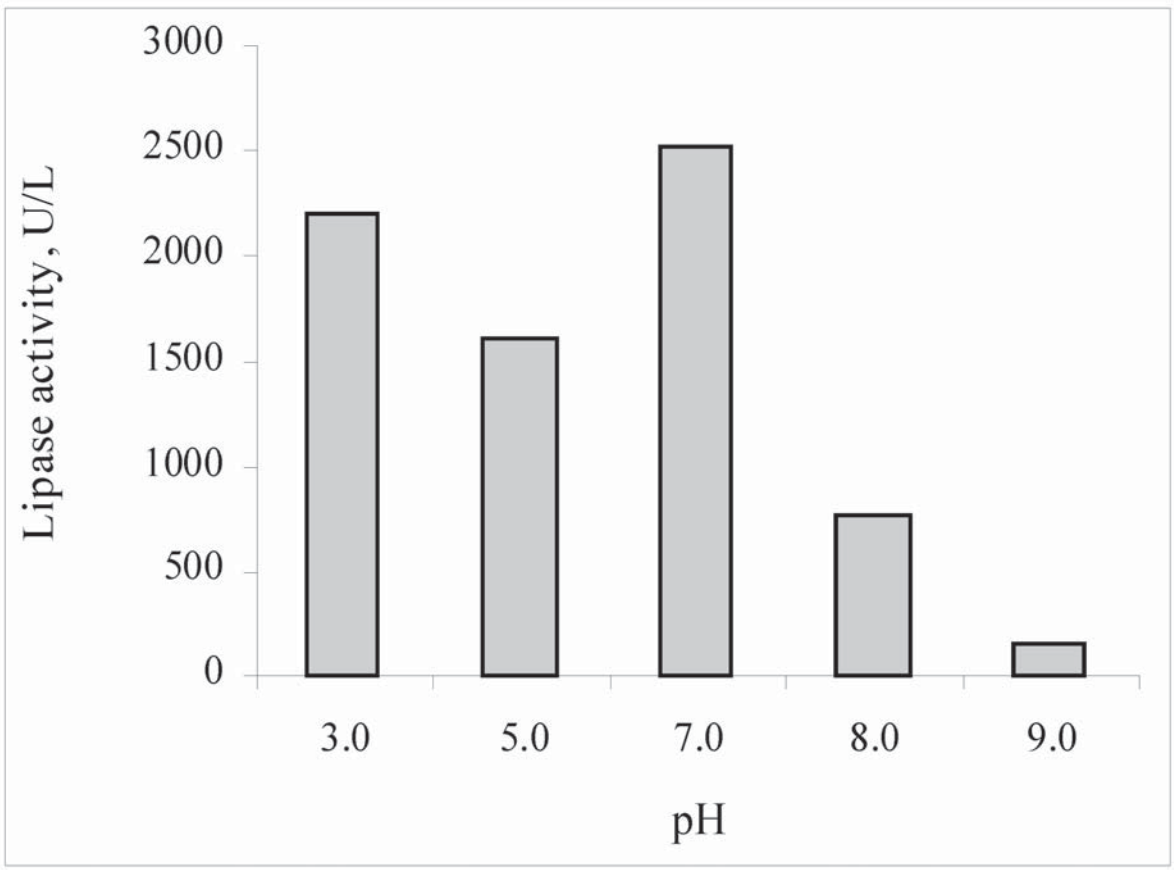

Fig. 1. Effect of initial pH of the nutrient medium on lipase biosynthesis

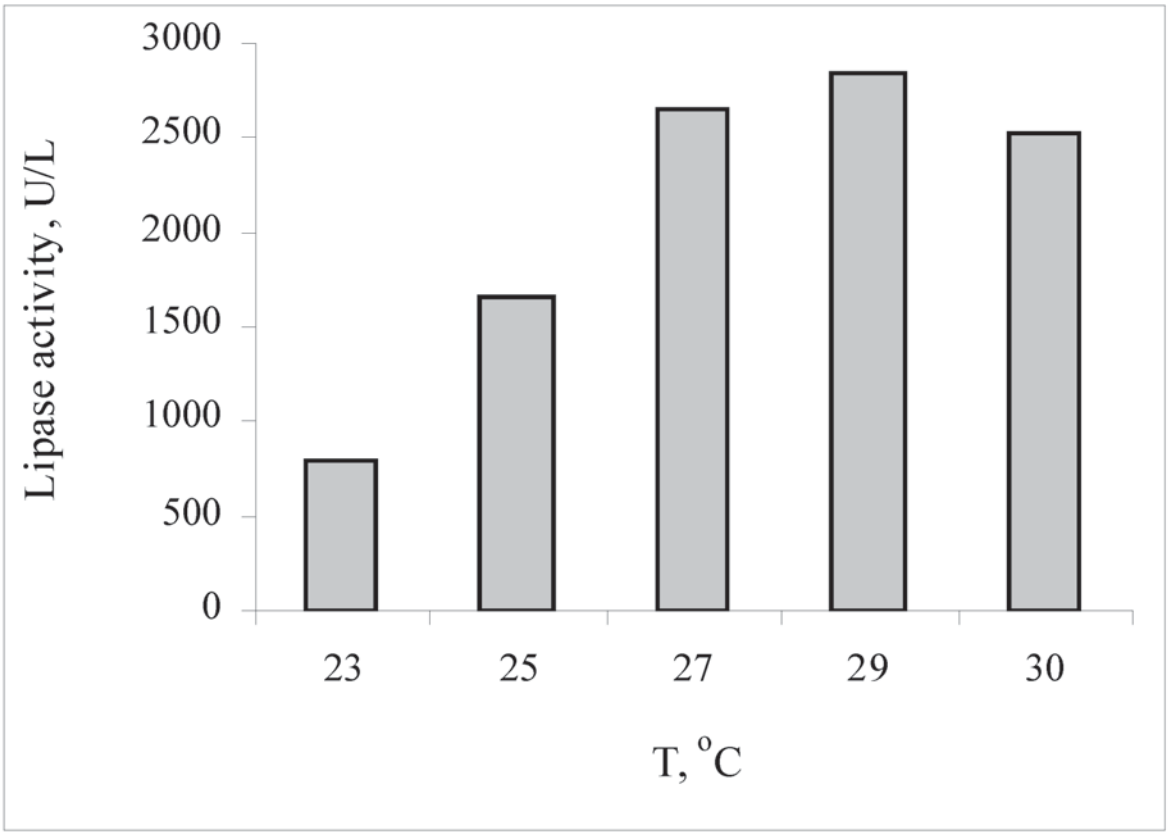

Fig. 2. Effect of cultivation temperature on lipase biosynthesis

Maximal lipase activity was achieved at cultivation temperature of 29 °C, but it should be noted that no considerable difference in lipase biosynthesis was observed in the range of 27-30 °C. According to some authors the optimal temperature for lipase production from fungi strains from the genus *Aspergillus* is in the range of 30-40 °C (Adinarayana et al., 2004; Falony et al., 2006; Hosseinpour et al., 2011).

In order to determine the optimal values of the initial pH of the nutrient medium and the temperature of cultivation, taking into account their interaction effects, an optimal composite design 2^2 was performed (Table 2).

Table 2

Experimental data and results of the optimal composite design 2^2

Run numbers	Coded levels		Lipase activity, U/L	
	x_1	x_2	Y[a]	$\hat{Y}$
1	1	1	1620.25	1533.81
2	-1	1	370.51	407.02
3	1	-1	2230.81	2377.20
4	-1	-1	1360.35	1250.40
5	1	0	2850.56	2790.61
6	-1	0	1590.37	1663.81
7	0	1	1290.42	1340.35
8	0	-1	2220.18	2183.74
9	0	0	2610.64	2597.15

x_1 – cultivation temperature;

x_2 – initial pH of the nutrient medium;

[a] results are a mean value of three replications

The results from the regression analysis are presented in Table 3.

Table 3

Results from the regression analysis

Coefficients	Value	Standard Error	t Stat	P-value
b_o	2597.15	59.861	43.386	$2.7*10^{-5}$
b_1	563.40	32.787	17.183	0.001
b_2	-421.69	32.787	-12.862	0.001
b_1*b_2	94.82	40.156	2.361	0.099
b_1^2	-369.94	56.789	-6.514	0.007
b_2^2	-835.10	56.789	-14.705	0.001

After investigation of the confidence level of the regression coefficients, only coefficients with *P-value* ≤ 0.05 were included in the model (3).

$$\hat{Y} = 2597.15+563.40.x_1-421.69.x_2-369.94.x_1^2-835.10.x_2^2 \quad (3)$$

The predicted values of lipase activity by model (3) are marked with $\hat{Y}$ in Table 2.

The analysis of variance and the F-ratio test have been performed to justify the goodness of fit for this RSM model (Table 4).

Table 4

Analysis of variance for the regression equation for lipase biosynthesis

	df	SS	MS	F	Significance F
Regression	4	4639962	1159990	83.88487	0.000413
Residual	4	55313.45	13828.36		
Total	8	4695275			

The mathematical model developed was characterized by value of *Significance F = 0.000413*, which indicated that the model was adequate at confidence level $\alpha=0.05$. R^2 value of 0.99 showed a good fit of the model with the experimental data. Analyzing the regression equation (3) it was found that the maximum predicted lipase activity was $\hat{Y}$= 2864.89 U/L. It was achieved at the following coded values of the factors: x_1 (temperature) = 0.76 and x_2 (pH) = -0.25 (Fig. 3).

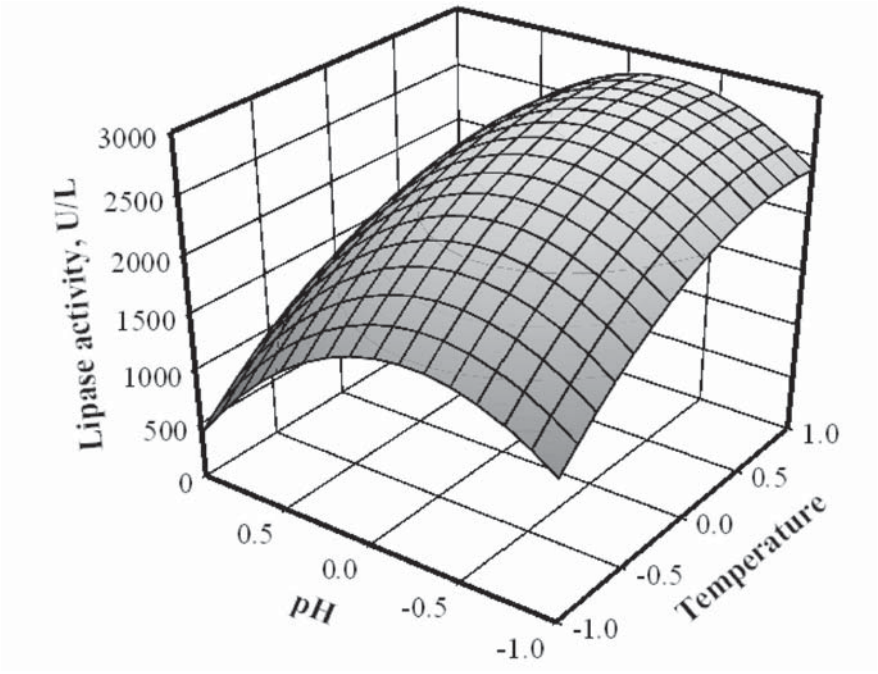

Fig. 3. Response surface plot indicating interaction effects of cultivation temperature and initial pH of the nutrient medium on lipase biosynthesis

After decoding of the levels of the initial factors, their optimal values were determined – cultivation temperature 28.5 °C and initial pH of the nutrient medium pH 6.5. They insured achievement of maximum lipase activity.

In order to determine the fitness of the model, cultivation experiments of the strain for achieving maximum lipase biosynthesis were performed using the determined optimal conditions. Maximum lipase activity of 2779.90 U/L (mean value of 5 consecutive experiments with a standard deviation $\sigma = \pm 103.63$) was obtained experimentally, and this was close to the predicted value 2864.89 U/L (Table 5).

Table 5

Validation of the model for lipase biosynthesis at determined optimal values of the investigated factors

Factors	Optimal value	Predicted activity, U/L	Observed activity, U/L
Temperature, °C	28.5	2864.89	2779.90
pH	6.5		

CONCLUSION

A significant effect of cultivation temperature and initial pH of nutrient medium on lipase biosynthesis from *Aspergillus carbonarius* was established. In the range of pH 3.0-7.0 the strain produced considerable amount of lipase activity. It should be noted that in the highly acidic region at pH 3.0 *Aspergillus carbonarius* synthesized significant lipase activity, which is not common for strains from the genus *Aspergillus*, producing lipases. These results are prerequisite for the isolation of a lipase enzyme with specific characteristics. By carrying out a planned mathematical design a model was derived, with the aid of which optimum values of cultivation temperature (28.5 °C) and initial pH of the nutrient medium (pH 6.5) were predicted. Experimentally obtained lipase activity at the optimum levels of the tested factors was 2769.90 U/L.

Acknowledgements

The research is financed by the Bulgarian Science Fund at the Ministry of Education and Science of the Republic of Bulgaria (number of project ДМУ 03/59).

References

[1] Adinarayana K., Raju K., Zargar M., Devi R. & Ellaiah P. (2004). Optimization of process parameters for production of lipase in solid-state fermentation by newly isolated *Aspergillus* species. Indian J. Biotechnol. 3, 65-69.

[2] Arpigny J. & Jaeger K. (1999). Bacterial lipolytic enzymes: classification and properties. Biochem. J. 343, 177-183.

[3] Falony G., Armas J., Mendoza J. & Hernandez J. (2006). Production of extracellular lipase from *Aspergillus niger* by solid-state fermentation, Food Technol. Biotechnol. 44, 235–240.

[4] Ghosh P., Saxena R., Gupta R., Yadav R. & Davidson S. (1996). Microbial lipases: production and application, Sci. Prog. 79, 119-157.

[5] Hosseinpour M., Najafrpour G., Younesi H. & Khorrami M. (2011). Submerged culture studies for lipase production by *Aspergillus niger* NCIM 584 on soya flour, Middle-East J. Sci. Res. 7, 362-366.

[6] Kaushik R., Marwah R., Gupta P., Saurabh S., Saso L., Parmar V. & Saxena R. (2010). Optimization of lipase production from *Aspergillus terreus* by response surface methodology and its potential for synthesis of partial glycerides under solvent free conditions. Indian J. Microbiol. 50, 456-462.

[7] Kaushik R., Saurabh S., Isar J. & Saxena R.. (2006). Statistical optimization of medium components and growth conditions by response surface methodology to enhance lipase production by *Aspergillus carneus.* J. Mol. Catal. B: Enzym. 40, 121–126.

[8] Kumari A., Mahapatra P. & Banerjee R. (2009). Statistical optimization of culture conditions by response surface methodology for synthesis of lipase with *Enterobacter aerogenes*. Braz. Arch. Biol. Technol. 52, 1349-1356.

[9] Pahoja V. & Sethar M. (2002). A review of enzymatic properties of lipase in plants, animals and microorganisms. Pakistan J. Appl. Sci. 2, 474-484.

[10] Reis P., Holmberg K., Watzke H., Leser M. & Miller R. (2009). Lipases at interfaces: A review. Adv. Colloid Interface Sci. 147H148, 237P250.

[11] Sharma C., Sharma P. & Kanwar S. (2012). Optimization of production conditions of lipase from *B. Licheniformis* MTCC-10498. Res. J. Recent. Sci. 1, 25-32.

[12] Uppada S., Gupta A. & Dutta1 J. (2012). Statistical optimization of culture parameters for lipase production from *Lactococcus lactis* and its application in detergent industry. Int. J. Chem. Tech. Res. 4, 1509-1517.

[13] Vuchkov I. & Stoyanov S. (1980). Mathematical modeling and optimization of technological objects, Technics, Sofia, 135Q151.

ОПТИМИЗИРАНЕ НА НЯКОИ УСЛОВИЯ НА КУЛТИВИРАНЕ ЧРЕЗ ИЗПОЛЗВАНЕ НА МЕТОД С ПОВЪРХНИНА НА ОТКЛИКА ЗА ПОЛУЧАВАНЕ НА ЛИПАЗА ОТ *ASPERGILLUS CARBONARIUS*

Георги Добрев, Боряна Жекова, Валентина Добрева, Христина Стринска
Университет по хранителни технологии
Катедра "Биохимия и молекулярна биология"
бул. "Марица" 26, 4000 Пловдив

Резюме

Изследвано е влиянието на началното pH на хранителната среда и температурата на култивиране върху биосинтеза на липаза от Aspergillus carbonarius. Установи се, че изследваният Aspergillus carbonarius продуцира значителна липазна активност в интервала на pH 3.0-7.0 и на температура 27-30 °C. Чрез провеждане на планиран математически експеримент и реализиране на оптимален композиционен план се изведе регресионен модел, с помощта на който се предсказаха оптималните стойности на температура на култивиране – 28.5 °C и начално pH на хранителната среда 6.5, като предсказаната максимална липазна активност е $\hat{Y}$=2864.89 U/L. Изведеният математически модел е адекватен при ниво на доверие б=0.05 и се характеризира с висока стойност на корелационен коефициент R^2=0.99. Проведоха се пет последователни експеримента при предсказаните оптимални стойности на изследваните фактори, като се постигна средна стойност на липазна активност Y=2779.90 U/L със стандартно отклонение σ=±103.63, което експериментално потвърждава резултатите, получени от математическия модел.

SELECTED LACTOBACILLUS STRAINS PREVENT THE ADHESION OF PATHOGENIC BACTERIA TO HUMAN EPITHELIUM

Zhechko Dimitrov
LB-Bulgaricum Plc., R&D Center, 12-A Malashevska Str., 1202, Sofia, Bulgaria
e-mail: jechkoelby@yahoo.com

Abstract

Adhesion is one of the most important properties of probiotic bacteria included in the functional foods. One of the possible protective mechanisms of probiotics is connected to the competition with pathogenic bacteria for adhesion to the epithelium layer. In this article we evaluated the ability of three preliminary selected probiotic strains to inhibit the adhesion and to displace pathogens using Caco-2 cells model. The ability to inhibit the adhesion of pathogens or to displace already adhered pathogenic bacteria was strain dependant on both the probiotic strains and the pathogen bacteria used. The main objective of the present study was to evaluate the concurrent adhesion abilities of the probiotic strains using three ways: simultaneous incubation of probiotic and pathogenic bacteria on the epithelium cells; treatment with probiotic bacteria to preliminary adherent pathogens; and treatment with pathogenic bacteria to preliminary adherent probiotic strains to epithelium cells. According to the results the highest suppression of the adhesion of the pathogens was achieved by simultaneous action of the probiotic strains and pathogens. The worst result, attempting to decrease the adhesion of the pathogens, was received when pathogenic strains acted after the adhesion of probiotics. Our results suggest that in order to remarkable decrease the adhesion of the pathogenic bacteria, a relatively high number of probiotic strains in the intestinal tract should be maintained.

INTRODUCTION

Probiotics are viable bacteria that have beneficial effects on the health of the host (1, 2). Many of the probiotic bacteria are lactic acid bacteria and are useful in the treatment of dysfunctions with disturbed intestinal microflora and abnormal gut permeability (3). Proposed mechanisms through which the ingested probiotic microbes may subsequently benefit their host include the production of antimicrobial factors, competition for nutrients, degradation of toxins and immunomodulation (4). However, of the main criteria for selecting probiotic strains, adherence to intestinal epithelia is thought to be paramount (5, 6). Indeed, adhesion to epithelial cells and/or mucus appears to mediate coloniza-

tion of the gastrointestinal tract by lactobacilli and may be a prerequisite for competitive exclusion of enteropathogenic bacteria (7) and immunomodulation of the host (8, 9). Successful probiotic bacteria are usually able to colonize the intestine, at least temporarily, by adhering to the intestinal mucosa (10, 11). Studies have also suggested that adhesive probiotic bacteria could prevent the attachment of pathogens, such as coliform bacteria and clostridia, and stimulate their removal from the infected intestinal tract (12). Laboratory models using human intestinal cell lines such as Caco-2 (13, 14) and HT-29 (15) have been developed to study the adhesion of probiotic lactic acid bacteria and their competitive exclusion of pathogenic bacteria. Moreover, it has been shown that certain lactobacilli share carbohydrate-binding specific sites with some entero-pathogens, and inhibition of pathogen adhesion by steric hydrance has also been reported (7). This provides the rationale for the use of lactobacilli to prevent infection at an early stage by inhibiting the adhesion of pathogens by competitive exclusion.

The main objective of this work was to evaluate the adhesive properties of pre-selected *Lactobacillus* strains and to assay their ability to inhibit the adhesion or to displace pathogens, attempting to select probiotics with the ability to compete the adhesion of intestinal pathogens.

MATERIAL AND METHODS

Bacterial strains

The *Lactobacillus* strains were isolated after plating of 0.1-ml of respective dilutions of fecal or milk/cheese homogenates on MRS agar (Merck, Darmstadt, Germany). The plates were incubated at 37 °C for 3 days under anaerobic conditions (10% CO_2, 80% N_2, 10% H_2). The single colonies were purified trice and the species belonging and strain identity were determined by help of species-specific PCR, Amplified Ribosomal DNA Restriction Analysis, sequencing of hyper variable rDNA V6-V8 regions, and Pulsed field gel electrophoresis, according to Dimitrov et al. (16, 17). The bacterial pathogens used were *Salmonella* typhimurium ATCC 29631, *Escherichia coli* NCTC 8603 and *Listeria monocytogenes* ATCC 15313. The bacterial pathogens were grown in Gifu anaerobic medium (GAM; Nissui Pharmaceutical, Japan).

Quantitative assessment of adherence of lactobacilli and pathogenic bacteria

The intestinal cell culture Caco-2 was used in the adhesion assay. This human colon adenocarcinoma cell line was obtained from the American Type Culture Collection. The cells were cultured in Dulbecco's modified Eagle's minimal essential medium (DMEM) (GIBCO-BRL), containing 25 mM glucose, 20% (vol/vol) heated inactivated fetal calf serum (GIBCO-BRL), and 1% nonessential amino acids (GIBCO-BRL). The cells were grown at 37°C in 5% CO_2. At approximately 95% confluence, the monolayers were passaged by incubating with a 0.25% trypsin solution (Gibco) for 5 min at 37°C. For the adhesion assay, monolayers of Caco-2 cells were prepared in two-chamber slides (Lab-Tek chamber slide; Nunc Inc.) by inoculating 2.8 x 10^5 viable cells into 2 ml of culture medium. The medium was replaced every two days.

Fifteen-day-postconfluent Caco-2 monolayers were washed five times with 1 ml of sterile PBS before the adhesion assay. One ml of the test bacteria at concentrations between 1 x 10^5 and 4 x 10^8 CFU ml^{-1} were added to 1 ml of complete Caco-2 medium. This suspension (2 ml) was added to each chamber of the two-chamber slide and incubated at 37°C, in a 5% CO_2-95% air atmosphere, with gentle rocking. After incubation for 60 min, the monolayers were washed twice with sterile PBS (pH 7.2), fixed with methanol, Gram stained, and examined microscopically. Visual counting of adhered cells was adopted in this study, for it allows differentiation of the gram-positive *Lactobacillus* and gram-negative *E. coli*. Each adherence assay was conducted in triplicate, and the number of adherent bacteria was counted on about 1,000 Caco-2 cells, in 60 randomly selected microscopic fields. To stimulate the physiological pH condition of the gastrointestinal tract, all experiments were done at pH 7.

In the study of the competition for adhesion on Caco-2 cells, *Lactobacillus* and *E. coli* were added simultaneously or sequentially to the Caco-2 cultures before counting. In the latter case, free cells of the first bacterium were removed by

washing with PBS (pH 7.2) before the second bacterium was added.

RESULTS AND DISCUSSION

Three ways for evaluation of the competitive adhesion were applied. The first one was connected with a direct competition between probiotics and pathogenic bacteria for the adhesive sites. This was achieved by simultaneously incubation of the two kinds of bacteria on epithelium layer. The second way was a prevention of the adhesion of pathogens from preliminary adherent probiotic strains. In this case, initially the selected Lactobacillus strains adhere to the epithelium cells, and after washing up of the non-adherent bacteria incubation follows with the pathogenic strains. Following this way it is possible to receive information if the preliminary consumption of probiotics can prevent the subsequent adhesion of pathogens. The third way, studying the competitive adhesion, was connected with the ability of probiotics to displace already attached to epithelium pathogenic bacteria. The assay of this effect was achieved by initial incubation of epithelium monolayer with pathogenic bacteria and, after washing, subsequent incubation with probiotic strains. This way helps to receive information if certain probiotic is able to detach already adherent pathogenic bacteria.

Assessing the competitive adhesion, a final concentration of *E. coli* and *Salmonella* of $1x10^8$ was maintained. The concentration of the probiotic strains during the experiments was the same. Three pre-selected probiotic strains demonstrating high adhesion level were used in this study: *L. plantarum* F12, *L. gasseri* G4/13 and *L. helveticus* AC. The results of the competitive adhesion of the selected strains against *E.coli* are summarized in Table 1, and these against *Salmonella* – in Table 2. The results from triplicate assays are expressed as a number of adherent bacteria on 100 Caco-2 cells.

On Figure 1 two microscopic pictures of the competitive adhesion against *E.coli* are presented – *L.helveticus* AC (left) and *L. plantarum* F12 (right). The adhesion abilities of *L. plantarum* F12 are much higher than those of *L. helveticus* AC, which is clearly seen in the Figure 1. This fact

Table 1. Competitive adhesion of the selected strains against *E.coli*.

	L. plantarum F12	*L. gasseri* G4/13	*L. helveticus* AC
Adhesion of single strains. The adhesion of *E.coli* is 240 ± 8.	2100 ± 17	1700 ± 14	890 ± 11
Simultaneous adhesion: pathogen and probiotic.	41 – *E.coli* / 730 – p F12	17 – *E.coli* / 360 – G4/13	93 – *E.coli* / 124 – hAC
Adhesion of pathogen on epithelium with preliminary adherent probiotic	194 – *E.coli* / 540 – p F12	112 – *E.coli* / 240 – G4/13	214 – *E.coli* / 82 – hAC
Adhesion of probiotic on epithelium with preliminary adherent pathogen	110 – *E.coli* / 610 – p F12	80 – *E.coli* / 290 – G4/13	142 – *E.coli* / 106 – hAC

Table 2. Competitive adhesion of the selected strains against *Salmonella typhi murium*.

	L. plantarum F12	*L. gasseri* G4/13	*L. helveticus* AC
Adhesion of single strains. The adhesion of *Salmonella* is 170 ± 8	2092 ± 16	1689 ± 13	887 ± 11
Simultaneous adhesion: pathogen and probiotic.	32 –*Salmonella*/ 820 – p F12	12 –*Salmonella*/ 390 – G4/13	68 –*Salmonella*/ 166 – hAC
Adhesion of pathogen on epithelium with preliminary adherent probiotic	142 –*Salmonella*/ 580 – p F12	66 –*Salmonella*/ 294 – G4/13	136 –*Salmonella*/ 98 – hAC
Adhesion of probiotic on epithelium with preliminary adherent pathogen	48 –*Salmonella*/ 710 – p F12	26 –*Salmonella*/ 326 – G4/13	120 –*Salmonella*/ 124 – hAC

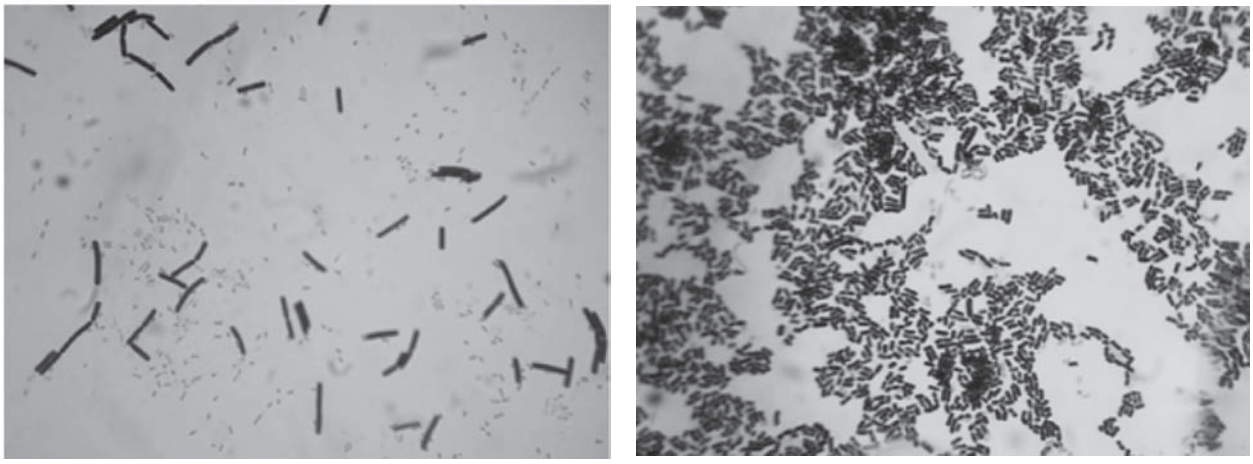

Figure 1. Microscopic pictures of the competitive adhesion against *E. coli* of *L. helveticus* AC (left) and *L. plantarum* F12 (right).

leads to higher suppression of the adhesion of the pathogens by *L. plantarum* F12. As it is seen in the Tables 1 and 2, the most significant is the effect of suppression against the two pathogens by simultaneous incubation of the probiotics and the pathogens with the epithelium cells. The reduction of the adhesion of both *Salmonella* and *E. coli* was the most significant using every of the three probiotics. The smallest was the reduction of the adhesion of the two pathogens when the probiotics were preliminary adherent on the epithelium. It could be supposed that in order to decrease the probability of adhesion of the pathogens, it is necessary to maintain relatively high concentration of the probiotic cells. The results in the tables point that the most adherent strain *L. plantarum* F12 does not lead to higher reduction of the adhesion of the pathogens than *L. gasseri* G4/13. The probable cause for these phenomena could be the greater affinity between the adhesion sites of the *L. gasseri* G4/13 and the epithelium cells on the one hand, in comparison with the affinity between the adhesion sites of pathogens and epithelium cells, on the other hand.

CONCLUSION

The adhesion rate of the probiotic strain is one of the factors for successful competition to the adhesion of pathogens. Another factor is the affinity between the adhesion sites of the probiotics and the epithelium cells. The competitive adhesion is a strain-dependant property and should be evaluated for every probiotic strain.

Acknowledgement

This work was supported by National Innovation Fund, project № 6ИФ-02-33/15.12.2012.

References

[1] Lee, Y. K., K. Nomoto, S. Salminen, and S. L. Gorbach. 1999. Handbook of Probiotics. John Wiley & Sons, New York, N.Y.

[2] Salminen, S., A. Ouwehand, Y. Benno, and Y. K. Lee. 1999. Probiotics: how should they be defined? Food Sci. Technol. 10:107-110.

[3] Lee, Y. K., and S. Salminen. 1995. The coming of age of probiotics. Trends Food Sci. Technol. 6:241-244.

[4] Hirayama K, Rafter J. The role of probiotic bacteria in cancer prevention. Microbes Infect 2000; 2:681-686

[5] Collins J.K., Thornton G., O'Sullivan G.C. Selection of probiotic strains for human applications. Int Dairy J 1998; 8:487-490

[6] Blum S., Reniero R., Schriffrin E., Crittenden R., Mattila-Sandholm T., Ouwehand A.C., Salminen S., von Wright A., Saarela M., Saxelin M., Collins K., Morelli L. Adhesion studies for probiotics: need for validation and refinement. Trends Food Sci Technol 1999; 10: 405-410

[7] Bernet M.F., Brassart D., Nesser J.R., Servin A.L. Adhesion of human bifidobacterial strains to cultured human intestinal epithelial cells and inhibition of enteropathogen-cell interactions. Appl Environ Microbiol 1993; 59: 4121-4128

[8] Blum S., Delneste Y., Alvarez S., Haller D., Perez P.F., Bode Ch., Hammes W.P., Pfeifer A.M.A., Schiffrin E.J. Interactions between commensal bacteria and mucosal immunocompetent cells. Int Dairy J 1999; 9: 63-68

[9] Erickson K.L., Hubbard N.E. Probiotic immunomodulation in health and disease. J Nutr 2000; 130: 403-409

[10] Saxelin, M., T. Pessi, and S. Salminen. 1995. Fecal recovery following oral administration of *Lactobacillus* strain GG (ATCC 53103) in gelatine capsules to healthy volunteers. Int. J. Food Microbiol. 25:199-

203.

[11] Tamura, N., M. Norimoto, K. Yoshida, C. Hirayama, and R. Nakai. 1983. Alteration of fecal bacterial flora following oral administration of bifidobacterial preparation. Gastroenterol. Jpn. 18:17-24.

[12] Benno, Y., and T. Mitsuoka. 1992. Impact of *Bifidobacterium longum* on human fecal microflora. Microbiol. Immun. 36:683-694.

[13] Greene, J. D., and T. R. Klaenhammer. 1994. Factors involved in adherence of lactobacilli to human Caco-2 cells. Appl. Environm. Microbiol. 60:4487-4494

[14] Raza, S., S. M. Graham, S. J. Allen, S. Sultana, L. Cuevas, and C. A. Hart. 1995. *Lactobacillus* GG promotes recovery from acute non bloody diarrhea in Pakistan. Pediatr. Infect. Dis. J. 14:107-111

[15] Ouwehand, A. C., P. Niemi, and S. J. Salminen. 1999. The normal fecal microflora does not affect the adhesion of probiotic bacteria in vitro. FEMS Microbiol. Lett. 177:35-38

[16] Dimitrov Z., Minkova S., and Michaylova M. 2008. Comparative evaluation of three molecular typing methods in their applicability to differentiate *Lactobacillus* strains with human origin. World Journal of Microbiology and Biotechnology 24:1305-1312

[17] Dimitrov Z., Michaylova M., and Minkova S. (2005). Characterization of *Lactobacillus helveticus* strains isolated from Bulgarian yogurt, cheese, plants and humane fecal samples by SDS-PAGE of cell-wall proteins, Ribotyping and PFGE fingerprinting. International Dairy Journal, 15: 998-1005

ПОДБРАНИ ЩАМОВЕ LACTOBACILLUS ПРЕДОТВРАТЯВАТ АДХЕЗИЯТА НА ПАТОГЕННИ БАКТЕРИИ КЪМ ЧОВЕШКИЯ ЕПИТЕЛ

Жечко Димитров
ЕлБи-Булгарикум ЕАД, Център за НИРД, ул. "Малашевска" 12-А., 1202, София, България
e-mail: jechkoelby@yahoo.com

Резюме

Адхезията е едно от най-важните свойства на пробиотиците, включвани във функционалните храни. Един от възможните протективни механизми на пробиотиците е свързан с конкурентната адхезия спрямо патогенните бактерии към епителния слой. Изследвана е възможността на три предварително подбрани пробиотични щама да потискат адхезията и да изместват вече адхезирали патогени, използвайки Caco-2 моделната система. Способността за потискане на адхезията и изместване на вече адхезирали патогени е щамово-специфична, както по отношение на пробиотичните щамове, така и за патогените. Главна цел е изследването на конкурентната адхезия на пробиотични щамове по три начина: едновременно инкубиране на пробиотичните и патогенните бактерии с епителни клетки; третиране с пробиотични бактерии на предварително адхезирали патогенни бактерии; третиране с патогенни бактерии на предварително адхезирали пробиотични бактерии към епителен слой. Съгласно резултатите най-значимо потискане на адхезията на патогенните бактерии се постигна чрез едновременното действие на пробиотиците с патогенните бактерии. Най-слабо бе редуцирането на адхезията на патогенни бактерии, когато третирането с патогени бе осъществено спрямо предварително адхезирали пробиотични бактерии. Резултатите сочат, че значимо редуциране на адхезията на патогенни бактерии се постига, когато се поддържа сравнително висока концентрация на пробиотични бактерии в интестиналния тракт.

PERFORMANCE CHARACTERISTICS OF TWO ANALYTICAL ASSAYS FOR DRUGS OF ABUSE

Ralitsa Atanasova–Bozhikova, Alexandrina Venkova, Radi Karadjov,
Toxico-chemical laboratory*, Clinic of Toxicology- UMBALSM "N.I.Pirogov",
bul. Gen. Totleben 21, 1606 Sofia, Bulgaria
e-mail: r_bozhikova@abv.bg

Abstract

Many situations require immediate testing and results for drugs of abuse. Hospital emergency departments have an immediate need for detecting drug overdoses. The increased prevalence of drug use has prompted the development of diverse drug screening technology that will produce results in as little as 10 minutes. The aim of the study is to present performance characteristics of two assays for drugs of abuse in patients in the Clinic of toxicology in UMBALSM "N.I. Pirogov": thin-layer chromatography (TLC) and immunoassay tests (IAT) including sensitivity, accuracy, urine detection times. TLC is selective

and sensitive enough to detect the drugs: benzodiazepines, narcotic analgetics, tricyclic antidepressants, phenothiazines, anxiolytics, non-steroid anti-inflammatory agents. Our experience shows that in cases with mixed intoxications, especially intoxications in children, TLC is more informative and gives more reliable and comprehensive drug screen. In situations when the target drug is unknown, and TLC or IAT alone do not give sufficient data, a combined use of both methods is necessary.

INTRODUCTION

Many situations require immediate testing and results for drugs of abuse. Hospital emergency departments have an immediate need for detecting drug overdoses. The increased prevalence of drug use has prompted the development of a new drug screening technology that will produce results in as little as 10 minutes. A number of different laboratory methods are available for comprehensive drug screening (Gymez et al., 2006; Hawks, 1986). When the drug abuse habit of a patient is unknown, physicians usually request a "comprehensive drug screen".

Aim of the study:

The aim of the study is to present performance characteristics of two assays for drugs of abuse in patients in the Clinic of toxicology UMBALSM "N.I. Pirogov": thin-layer chromatography (TLC) and immunoassay tests (IAT): sensitivity, accuracy, urine detection times.

MATERIALS AND METHODS

Thin-layer chromatographic screening for presence of drugs and metabolites in urine includes:

Materials:

1. Methanol: concentrated ammonium hydroxyde; 2. ethanol-sulfuric acid reagent – mix of sulfuric acid, water, ethanol; 3. sodium nitrite – mixture of sulfuric acid and sodium nitrite; 4. Bratton Marshall reagent – solution of N – (1-Naphthyl) ethylenediamine dihydrochloride in ethanol and water; 5. Dragendorff reagent – solution of potassium bismuth subnitrate), acetic acid and water /solution I /; aqueous solution of potassium iodide /solution II /. Mix solutions I and II with glacial acetic acid and water; 6. TLC silica gel plates / MERCK / - 5 x 10 cm; 7. chromatographic container; 8. sprayer for visualization of the spots; 9. UV–lamp; 10. anhydrous sodium sulfate; 11. ammonium chloride buffer– ammonium chloride saturated with conc. ammonium hydroxide up to pH 9; 12. solution of ammonium hydroxide / 0.5 mol/l /; 13. aqueous hydrochloric acid / 1 mol/l /.

Standards **–** extracts of tablets and ampoules in chloroform for comparison of results.

Methods:

1. Acidic extraction – isolation and concentration of acidic drugs from the probe: preparation of an acidic extract by means of hydrochloric acid and chloroform; separation of the lower, organic layer, evaporation to dryness. 2. Basic extraction – isolation and concentration of the basic drugs: preparation of a basic extract with ammonium hydroxide and chloroform; evaporation to dryness.

Thin–layer chromatography process:

1. Application of the probe-extract (in chloroform) and the respective standards, evaporation to dryness and place in the container with methanol and ammonium hydroxide; 2. Remove the plate and dry; 3. View the plate under the ultraviolet light / 254 и 365 nm / and note any fluorescent and non-fluorescent spots. If appearance of yellow spots - presence of benzodiazepines 4. Spray plate with ethanol/sulfuric acid, which colors phenothiazines. 5. Second observation of the plate under UV-light for appearance of yellow-fluorescent spots of benzodiazepines. 6. Heating of the plates at 100є C for 5 min for performance of acid hydrolysis. 7. Processing with nitrogen oxides. 8. Processing of the plate with N_1 - reagent. The aromatic amine is coupled with the diazonium salt received in the previous step and obtaining of azodyes in the presence of benzodiazepines 9. Processing with Dragendorff reagent for testing of availability of basic compounds.

Sensitivity of TLC: A general limit of sensitivity of 1 mg/l is reasonable.

Immunoassay tests for drugs directly in urine

Tests of Innovacon–USA are used:

MOR – for detecting of morphine as metabolite of codeine and heroine, THC - Δ9 – tetrahydrocannabinol, the active substance of marihuana, cannabis, MTD – methadone, AMP – amphetamine, MET – metamphetamine, COC – cocaine, TCA – tricyclic antidepressants, BZO – benzodiazepines, BAR – barbiturates.

Principle:

The immunoassay is based on the principle of competitive binding. Drugs which may be present in the urine specimen compete against their respective drug conjugate for binding sites on their specific antibody.

A drug, if present in the urine specimen below its cut-off concentration, will not saturate the binding sites of its specific antibody. The antibody will then react with the drug-protein conjugate and a visible colored line will show up in the test line region. The presence of a drug above the cut-off concentration will saturate all the binding sites of the antibody.

A drug-positive urine specimen will not generate a colored line in the test region because of drug competition, while a drug-negative urine specimen will generate a line in the test region because of the absence of drug competition.

Transfer 3 full drops of urine to the specimen well and read the result in 5 minutes.

RESULTS AND DISCUSSION

TLC is selective and sensitive enough to detect the drugs: benzodiazepines, narcotic analgetics, tricyclic antidepressants, phenothiazines, anxiolytics, nonsteroid anti-inflammatory agents /Fig. 1/. Table 1 shows the performance characteristics of both types of assays for drugs of abuse. The selectivity, sensitivity and the turnaround times of the used methods in the screening were demonstrated. Table 2 illustrates the typical screening confirmation cut-off concentrations and the expected time scales of detection for some commonly abused drugs. The drugs detected with TLC are: BZO, OPD, CVD, NAD and drug detected with IAT is CAN.

Negative reports based on IAT other TLC alone are not conclusive due to lack of sensitivity. If the screening method is IAT, the cut-off may have been set too high.

Our experience shows that in cases with mixed intoxications and especially in intoxications in children, TLC is more informative and gives more reliable and comprehensive drug screen. This applies especially to poisonings in children because of the small quantities of drugs (usually half to one tablet).

Intravenous use of drugs of abuse provides nearly instantaneous absorption into the bloodstream and excretion of the drug and/or metabolites in urine occurs almost immediately. Inhalation or oral use of drugs will result in slower absorption and excretion in urine may not be detected immediately after use (Verebey et al., 1997). According to our and other data (Gheorghe M. et al. 2008; Rezai-Basiri et al., 2010), TLC is not sensitive enough to detect marihuana, amphetamine, cocaine, phencyclidine, etc., and in these cases IAT as screening method is preferable. In situations when the target drug is unknown, and TLC or IAT alone does not give sufficient data, a combined use of both methods is necessary.

References

[1] Gheorghe M., Balalau D., Ilie M. et al. (2008). Qualitative analysis of confiscated illegal drugs by thin-layers chromatography. Farmacia LVI, 5, 541-546.

[2] Gómez M.J., Petrović M., Fernández-Alba A.R., et al. (2006). Determination of pharmaceuticals of various therapeutic classes by solid-phase extraction and liquid chromatography-tandem mass spectrometry analysis in hospital effluent wastewaters, J. Chromatogr A. 2; 1114(2):224-33.

[3] Hawks R.L. (1986). Analytical methodology. In: Hawks R.L., Chiang N.C., eds. Urine testing for drugs of abuse. NIDA Res. Monogr.; 73:30-42.

[4] Rezai-Basiri M., Ghazi-khansari M., Faghih A, Sadeghi M. et al. (2010). Eur. .J Gen. Med. 7(2):192-196.

[5] Verebey K.G., Buchan B.J. (1997). Diagnostic laboratory. In: Substance abuse, 1997, 369-377.

ХАРАКТЕРИСТИКИ НА ДВА МЕТОДА ЗА АНАЛИЗ НА ВЕЩЕСТВА ПРИ ПАЦИЕНТИ С ИНТОКСИКАЦИИ

Ралица Атанасова-Божикова, Александрина Венкова, Ради Караджов

Токсикохимическа лаборатория, Клиника по токсикология, УМБАЛСМ „Н.И. Пирогов", бул. "Тотлебен" 21, София 1606

Резюме

Много ситуации изискват експресно тестиране и резултати за вида на веществата при пациенти с интоксикации. Спешните отделения/клиники имат спешна необходимост за детекция на веществата/лекарствата, причини за отравянията. Бързото доказване на наличието или отсъствието на дадена токсична субстанция в рамките на 10 минути е довело до развиването на различни методи за бърз скрининг. Целта на настоящото изследване е да бъдат представени характеристиките на два от методите, които се използват в Токсикохимическата лаборатория към Клиниката по токсикология на УМБАЛСМ „Н.И. Пирогов": тънкослойна хроматография /ТСХ/ и имунотестовете /ИМТ/, а именно: чувствителност, точност, времена на детекция. ТСХ е селективна и чувствителна за откриването на следните вещества: бензодиазепинови препарати, някои наркотични аналгетици, трициклични антидепресанти, фенотиазини, анксиолитици, нестероидни противовъзпалителни средства. Опитът ни е показал, че при смесени интоксикации, особено при деца, ТСХ е по-високо информативен метод и предоставя по-достоверна и в общи линии повече информация за вида на отравянето. В ситуациите, в които веществото, причина за интоксикацията е неизвестно, и прилагането само на ТСХ или ИМТ не дава достатъчно информация, се оказва необходимо използването на двата метода в комбинация.

Table 1

Characteristics of TLC И IAT for drugs of abuse

Assay	Sensitivity	Specificity	Accuracy	Turn-around time
TLC	Moderate-high	High	Qualitative	1-4 h
IAT	Moderate-high	Moderate	Low-high	1-4 h

Table 2

Screening and confirmation cut-off concentrations and detection times for drugs of abuse

Drug	**Cut-off** (ng/ml)	**Tested analyte**	**Urine detection time**
Amphetamine	1000	Amphetamine	1-4 days
Barbiturate	300	Secobarbital, amobarbital, other barbiturates	1-4 days for short acting; up to 30 days for long acting
Benzodiazepines	200-300	Diazepam	1-7 days
Cocaine	300	Benzoylecgonine	1-3 days
Codeine	300	Codeine Morphine	1-3 days
Marihuana	50	Tetrahydrocannabinol	1-3 days-casual use; 30 days for chronic use (data from other authors)
Methadone	300	Methadone	1-3 days
Metamphetamine	1000	Metamphetamine Amphetamine	1-4 days
Heroin	300	Morphine, 6-acetylmorphine	1-3 days

Fig. 1. Drugs detected with TLC: BZO, OPD, CVD, NAD; drugs detected only with IAT - CAN, TVS detected with gas chromatography in the Clinic of toxicology for 2013

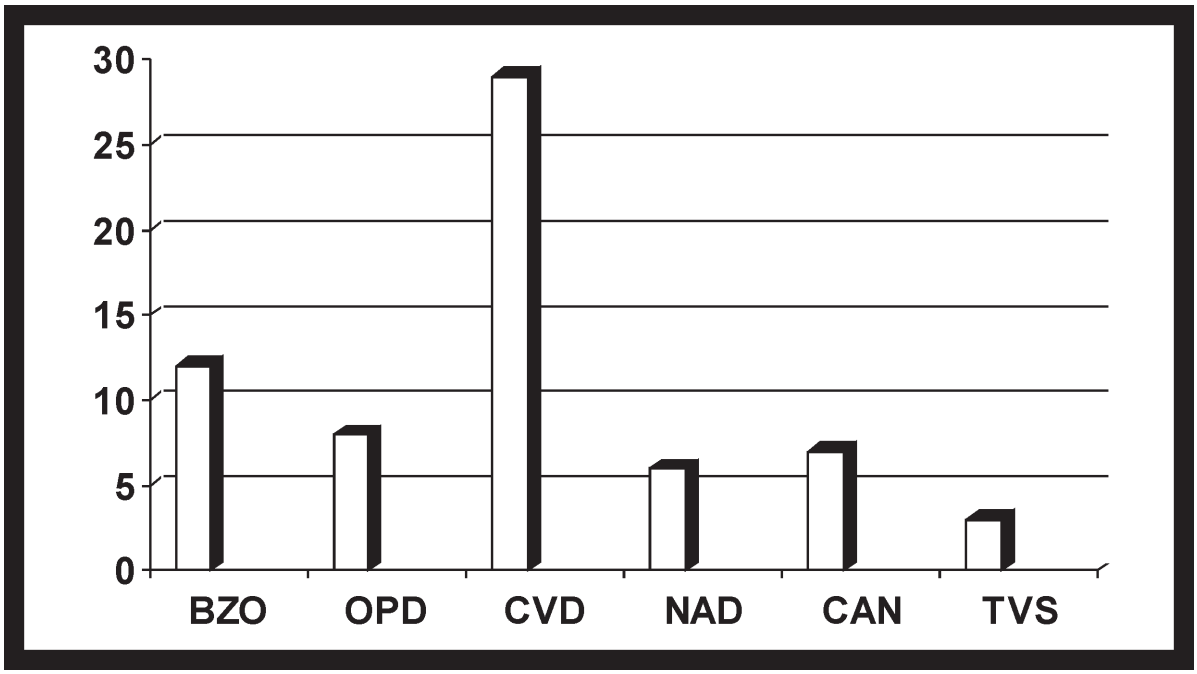

Legend:
BZO – benzodiazepines
OPD – other psychotropic drugs
CVD – cardiovascular drugs
NAD – non-steroidal anti-inflammatory *drugs*
CAN – cannabinoids
TVS – toxic volatile substances

UNDERGROUND WELL TEMPLE IN BULGARIA: ARCHITECTURAL AND ARCHAEOASTRONOMICAL ANALYSIS

Lyubomir Tsonev
Institute of Solid State Physics, Bulgarian Academy of Sciences,
72 Tzarigradsko Chaussee blvd, 1784 Sofia, Bulgaria
e-mail: ltsonev@abv.bg

Abstract

An ancient underground well temple of Sardinian type was found in Bulgaria in 1971 near the village of Garlo. This curious monument demonstrates some architectural and localization peculiarities which still do not have any satisfactory explanation in the framework of pure archaeology. For the first time these specific features are analyzed here from the view point of archaeoastronomy. This approach allows us to propose a new hypothesis interpreting the temple as a sacred ritual object which connects symbolically the Sun god with the underground water as a marker of the perpetual cycle of life. Preliminary indirect measurements support this hypothesis.

WELL TEMPLES IN ARCHAEOLOGY

The unique underground well temple in Bulgaria is located at Garlo village, Pernik region

(about 40 km Northwest from Sofia: N = 42° 47′ 14.80″, E = 22° 50′ 52.62″). It was discovered in 1971 by Dimitrina Mitova-Dzhonova (Митова-Джонова 1984, 2007). She dates the object in XIV-XIII c. BC. We shall denote it shortly as "Garlo temple".

From the architectural and religious viewpoint it has neither predecessors nor followers in the Balkan Peninsula. There is only one analogous monument in East Europe – near the town Kerch (antique Panticapaeum), the Crimean Peninsula (Гайдукевич 1949). Practically all temples of the underground water of this kind (about 30-40) are located on the island of Sardinia. The cult of the underground water has its origins in Mesopotamia, in the Sumerian god Enki – god of the underground water, god of fertility and keeper of the world order. Obviously this cult has flourished in Sardinia especially in II-I mill. BC (Atzeni 1980, Lilliu 1980). Technical development of the Sardinian well temples continues throughout one millennium. The most ancient monuments are supposed to be created in the Middle Bronze Age XIV-XIII c. BC. They are realized in a crude cyclopic technique of dry masonry which is similar to the fortress walls in Mycenae, Tiryns (continental Greece) and Hattusa (the capital of the Hittite Empire in Asia Minor). The most advanced well temples in Sardinia appear in the Late Bronze and in the Iron Age IX - VI c. BC; they are built of high quality quadrae and have false vaults.

The Bulgarian temple was investigated and partially restored in 1972. In 1983 a big protecting building with a special shelter and with an exhibition platform for the public was constructed around the temple. At the same time an additional and not entirely correct restoration was carried out. In 2007 the shelter collapsed. Till the end of 2010 the temple was cleared out again. In 2012 the ministry of culture of Bulgaria took a decision to rebuild the shelter and to restore the tholos floor damaged by treasure hunters. Since 2009 the temple has obtained the statute of an "archaeological object of national value".

The architectural Sardinian objects devoted to the underground water have various but similar constructions without firm architectural rules. Generally, they can be divided into two basic types. The smaller objects [sacred pits, sacred sources, pozzi sacri] are designed as modest over-ground shrines around the springs. They do not have underground parts; they consist most often of a façade built of high quality quadrae. The larger objects have complex, sophisticated and very impressive construction [well temples, sacred wells, temples at pit]. In their present form they include several obligatory components: (1) underground staircase corridor [dromos]; (2) underground tholos roofed with a spherical or parabolic axially symmetrical vault; (3) suitable designed underground water source. The water source itself can be formed as a shallow captation of a spring, but it can represent also a deep well of stone masonry. The tholos vault has an opeion in most cases – a circular opening at the vault's apex allowing the light of the sun, moon and stars to penetrate the tholos. Archaeologists suppose that some of the well temples had authentically an over-ground part designed in the nuraghi style [temenos]. Some of the well temples display traces of over-ground input tray [exedra, vestibule, atrium], which is not an obligatory element. In any case the underground sources and wells of Sardinian type have obviously religious but not profane character.

Sizes and proportions of well temples vary within certain limits. The orientation and the length of the dromos, for example, are not strongly prescribed by the cult. The dromos is directed predominantly to the south semi-horizon. The well depth also varies in a rather wide interval. However, it is worth paying attention to the inclination of the dromos staircase. The dromos inclination in respect to the horizon angle is 40° ± 2° in all Sardinian temples. The staircase of Garlo temple in its present reconstructed state has an inclination of 30° and so it seems to make an exception from the general rule. However, according to Дерменджиев 2007 the authentic, not restored, staircase has been steeper with inclination of 40°.

D. Mitova-Dzhonova interprets the Garlo temple as a manifestation of the cult to the Sumerian god Enki. She supposes that this temple was created on the Balkan Peninsula accidentally when a group of Sumerian origin migrated westwards looking for raw materials suitable for

development of high quality bronze metallurgy. After crossing Balkan Peninsula the migrants settled permanently in Sardinia, Balearic Islands and Iberian Peninsula where they developed the rich "Nuraghi" culture including about one hundred underground well temples. (Митова-Джонова 1984, 2007).

ARCHITECTURAL CHARACTERISTICS OF GARLO TEMPLE

The most important architectural characteristics of Garlo temple are described here.

The first unique building achievement realized in Garlo temple is the extraordinary complicated location on the terrain. All temples at pit in Sardinia as well as the asclepieion in Panticapaeum are situated on flat horizontal terrain. Garlo temple is tangentially semi-dug along a steep mountain slope. This is the most difficult disposition for a building at all. The underground well temples in Sardinia and the Crimea are located on flat terrain.

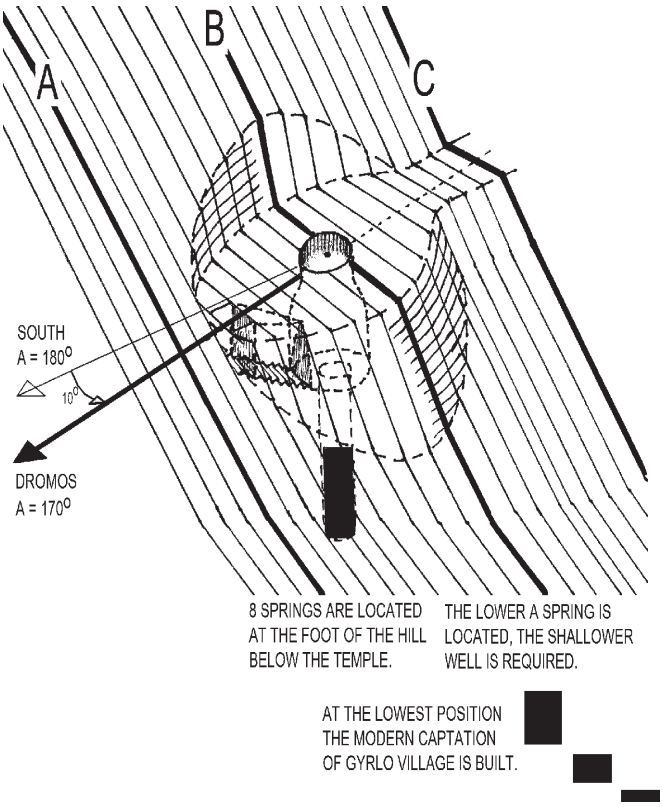

A visitor enters the temple through a **covered staircase – dromos**. In the upper part the staircase begins as an open air construction, but its lower part is covered in a quasi-megalithic manner, with big rough stone plates, giving a trapezoidal cross section of the corridor. When the corridor goes deeper under the ground the load on the ceiling increases and the width of the cover plates decreases respectively. At the lower end the corridor obtains already a triangular cross section crowned with a tapered cotter. The dromos changes significantly its architectural character (from a flat ceiling to a key stone arch) along a distance of 4 m only in order to adapt itself to the change in the pressure of the stone mass overlay. This is the **second extraordinary building achievement** in Garlo temple.

The core of the building is the vaulted cylindrical tholos (height and diameter of about 4 m). **The vault is the third extraordinary building achievement** in Garlo temple. This is not a false vault (layered masonry of quadrae, the upper layer sticking out a little bit inside), but a real vault (rough stones are ordered in a wedge-like manner). The restoration has affected only 0.5 m in the very upper part of the vault. The walls

from the tholos floor up to a height of 3 m are preserved in their original state.

SPIRITUAL BACKGROUND OF GARLO TEMPLE – CULT OBJECTS IN THRACE

It has been already proven with a high degree

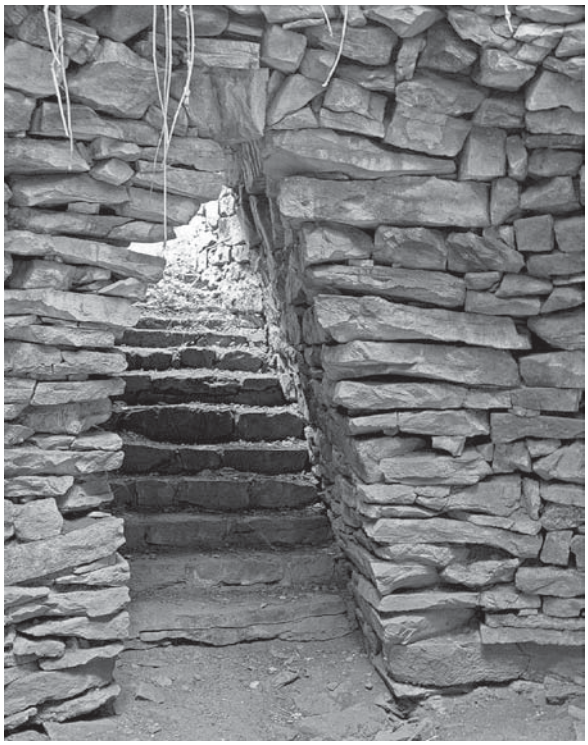

of reliability that THE SOLAR CULT is most widely represented in sacred monuments over the territory of ancient Thracia - north and central part of the Balkan Peninsula (*ИИ* 1990, 1991). Some artifacts originating from V - IV mill. BC allow to be interpreted as solar and lunar calendars: decorated clay figurines from Ovcharovo village near Targovishte, North-East Bulgaria, and golden plates with symbolic scenes from Letnitsa village near Lovech, Central North Bulgaria. Traces from solar cults are detected in numerous ancient rock-cut shrines dated in II mill. BC: Belintash, Harman-kaya and Angel voyvoda in the Rhodope Mountains, rock-cut ritual complex in Sliven region in the Balkan Mountain Range.

Solar monuments are found from I mill. BC till the Roman time IV c. AC: Thracian cult buildings, rock-carvings near Burgas, southern Black sea coast, rock tombs near Kavarna, northern Black sea coast, Sarmizegetusa ritual complex in Romania.

In the period XII-VI c. BC in the East part of the Balkan Peninsula a relatively big and multiform megalithic field appears, including several hundreds of dolmens, menhirs, cromlechs, etc. The Thracian dolmens are studied from an archaeoastronomical viewpoint in the beginning of XXI c. (Kolev et al 2008, Cézar González-García et al 2009, Цонев 2010, Tsonev et al 2011, Tsonev & Kolev 2012). They do not demonstrate well-defined orientation, but they are obviously predominantly directed to the South semihorizon, i.e. to the culmination of the sun, to the Sun god in his maximum power.

In the interval V - II c. BC the megalithic technique in Thracia is replaced by masonry of quadrae and fired bricks. Typical sacred objects created in Thracia in this period are monumental tombs and/or temples under tumuli. They combine the horizontal plans of the most developed Thracian two-camera dolmens with dromos (the local tradition) with the older pattern of Aegean vaulted constructions (the Mycenaean tradition) and with the tumular coverage of Scythian origin. (Китов & Агре 2002, Русева 2002). The classic Thracian temples under tumuli from the period V c. BC - III c. AC demonstrate the same predominantly South orientation of the dromos.

LUNAR OR STELLAR CULTS are not noticeably documented in ancient cult monuments in Thracia with one curious exception - the Baylovo cave near Sofia (ИИ 1991). A good review about the astronomical knowledge in the classical Thracian society from the middle of I mill. BC till the end of the Roman time as described by ancient authors is presented in (ИИ 1991).

As for the WATER CULT, its existence is also proved in Thracia in pre-Roman time already, but never in the form of sacred wells, of underground pits or wells. It is expressed in honoring numerous small springs in their natural appearance, always over-ground situated and without significant architectural envelope (Nekhrizov, 2005).

Shrines devoted to sacred springs in Bulgarian territory provided with impressive architectural envelopes are very rare and appear in late Roman times only. Let us mention two examples: /1/ the sanctuary of the three nymphs at the village Kasnakovo, near Haskovo (Аладжов, 1997; Nekhrizov, 2005; Венедиков, 1950) and /2/ the sanctuary devoted to Asclepius at the village of Batkun/Patalenitsa near Pazardzhik (Tsontchev, 1941; Zontschew, 1940).

CONCLUSION: the general sacred conception of Garlo temple is connected, although not very tightly, with the main ancient cults represented over the Thracian lands, but its architectural realization is unique on the Balkan Peninsula and even in East Europe. At the same time the similarity of Garlo temple architecture with numerous Sardinian well-temples is obvious and still needs a reasonable explanation.

NEW ARCHAEOASTRONOMIC HYPOTHESIS ABOUT GARLO TEMPLE

Beside the analysis of the inherent proportions of the monument, Mitova-Dzhonova noticed two curious peculiarities of its terrain localization.

SPECIFIC POINT 1. The temple builders display a special interest to the South direction. Building the real dromos in Garlo in approximately South direction, i.e. tangentially to the mountain slope, is a very complex technical problem. If the dromos was intended as an entrance to the tholos only, the builders could choose a much simpler approach. The East side of the temple is not dug into the hill but is built freely over the terrain. The entrance could be realized there by a simple arch, without any corridors and staircases and this would simplify greatly the construction! So, the South orientation is an essential characteristic of the temple.

SPECIFIC POINT 2. The monument is placed *at a very high level* above the surrounding terrain. Nine springs exist in the locality, most of them at the foot of the hill. The highest spring has

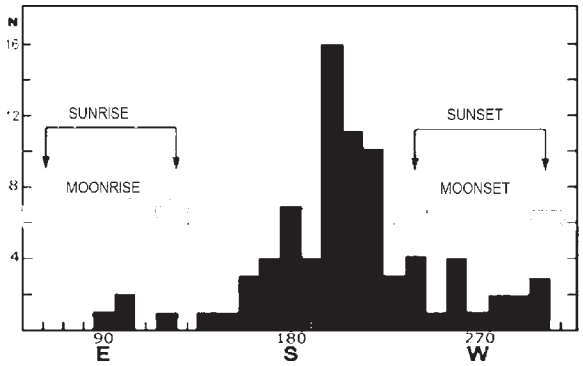

Orientation of 80 dolmens in Bulgaria XII-VII c. BC

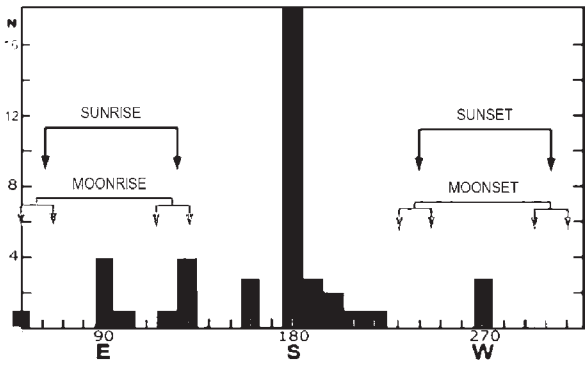

Orientation of 47 classic undertumular temples on the Balkan Peninsula VII c. BC – III c. AD

been chosen for the construction of the temple instead of the lower situated springs. This unexpected choice increased essentially technical complexity of the building requiring the deepest well.

Dermendzhiev has undertaken the only serious attempt till now to analyze Garlo temple from an archaeoastronomical viewpoint (Дерменджиев 2007). He supposed that the ancient people used the temple as an exact solar calendar measurement instrument over the whole year. They examined closely how the sunlight penetrates the temple through the dromos-corridor and marked the position of the lintel shadow on the floor – *observer situation No.1*. At the winter solstice the sunlight penetrates the temple in a most inclined manner and projects the lintel on the North wall of the tholos. When the time passes the lintel shadow moves over the well opening towards the lower end of the dromos. At the summer solstice the sunlight penetrates the temple most abruptly, does not enter the tholos at all and projects the lintel on the middle point of the staircase.

Unfortunately, the incorrect restoration did not allow proving accurately this calendar hypothesis. Dermendzhiev measured also the azimuthal orientation of the dromos 170°, but he did not comment the small deviation from the exact South. And in our opinion this is the third special feature of Garlo temple - *Specific point 3*.

We propose here the idea that the sunlight penetration into the tholos through the dromos corridor was considered in antiquity as a ritual action. The priest in the tholos observed the sunlight (*observer situation No.2*) and combined it symbolically by a

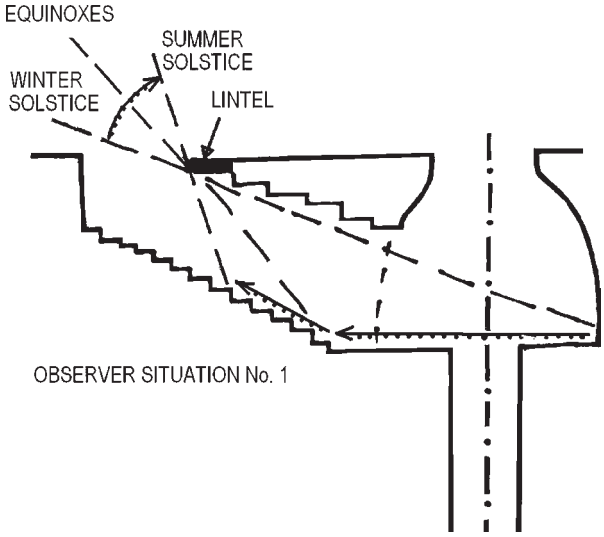

proper ceremony with the underground water and this combination has been believed to produce the life-giving power, to celebrate the start of a new life cycle of the nature. The South orientation of the dromos evidences special interest to the solar culmination. From this viewpoint Garlo temple plays the role of a marker of the solar culmination at winter solstice only and not the role of a precise calendar measuring instrument. Therefore our hypothesis includes the *Specific point 1* as a basic element from the very beginning.

In *observer situation No.2* the priest has an observation window, which is limited above by the lintel, below by the highest staircase step and laterally by both dromos walls. Through this window the priest sees the V-like overlap of the contours of two mountain hills – the hill where the temple is built AA' and the neighboring hill BB'. According to our hypothesis through this window the observer could see the solar culmination during the winter solstice only and not

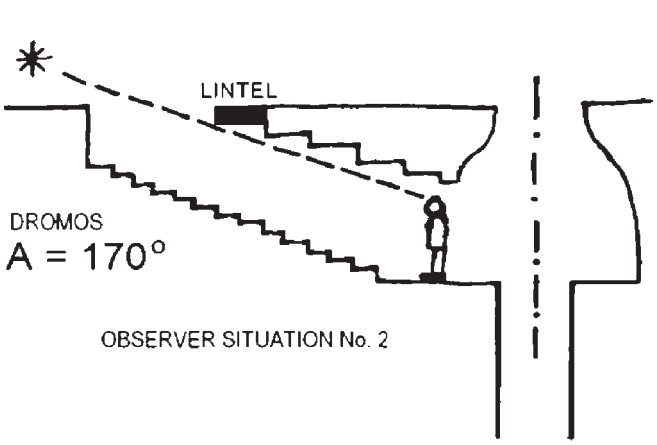

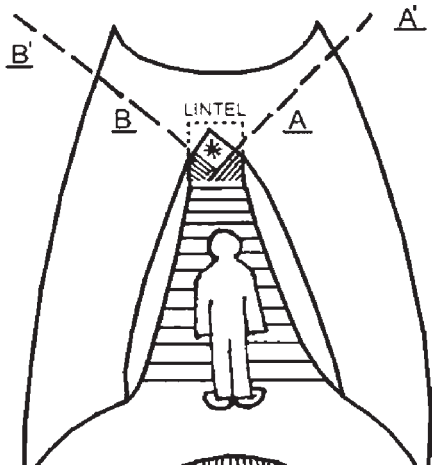

during the summer solstice and during the vernal and autumnal equinoxes. If the temple was situated *lower* than its actual position, the priest could not observe the solar culmination at the winter solstice because the temple would be in a shady position during the whole day. The temple builders were forced in this situation to choose the most complex building process placing the monument *over the highest spring* at the hill slope and to build the deepest possible well. So, our hypothesis explains the *Specific point 2*.

Let's assume that the builders have already chosen the exact place for the tholos – over the highest spring. In this situation it turned out that the local relief hindered the observation of the sun culmination *exactly* in south direction. Two ways out of this difficulty were possible:

(I) to make the well deeper and to place the tholos higher at the hill slope (in respect to its actual position today) – in this case the technical complexity of the building process would increase drastically; or (II) to rotate the dromos slightly - 10^{o} - eastwards in order to direct it towards the saddle between the contours of the neighboring hills AA' and BB' at an azimuth of 170^{o}, allowing the observation of the solar culmination at winter solstice not exactly, but with a small inaccuracy which does not disturb the ritual intention. The temple builders decided to use the second variant utilizing the specific character of the local landscape. This original technical solution stays in very good agreement with the real relief of the temple area. So, our hypothesis explains also the *Specific point 3.*

The verification of the hypothesis by means of direct measurements cannot be done due to two obstacles: /1/ the protective building around the monument blocks the south horizon; /2/ the dense forest around the protective building also prevents direct observations and measurements through the dromos. Therefore we were forced to use a complicated two-stage experimental procedure in summer 2013. At the first stage we found from the *observation position No.2* that point, where the dromos axis hits the wall of the protective building from inside. At the second stage we made our measurements from the additional *observer point No.3*, located outside the building. The results stay in good agreement with our hypothesis.

At the same time our hypothesis makes no claim to interpret *all* well temples of Sardinian

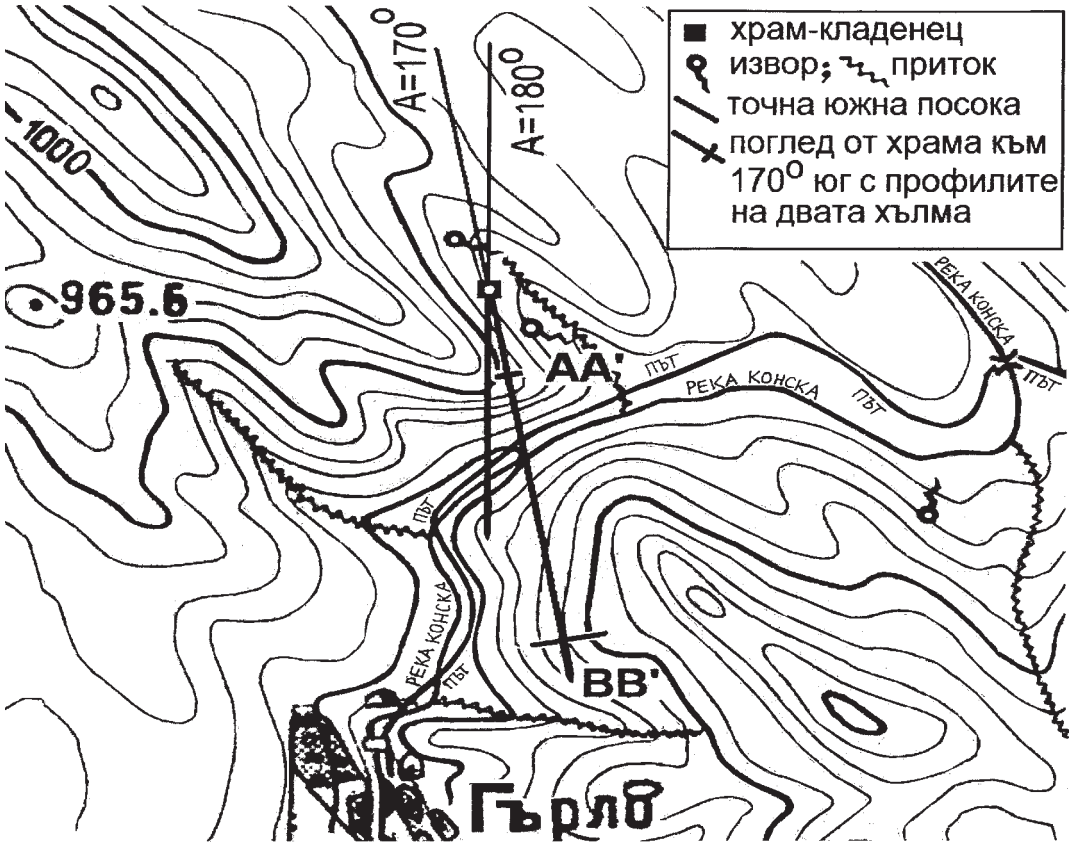

type. Every monument of this kind needs a separate investigation. As an example illustrating this statement we can mention the Nuraghic well temple of Santa Cristina in Paulilatino (Oristano, Sardinia), where a connection of the WATER cult with the LUNAR cult has been found out (Lebeuf 2008).

The dating of Garlo temple proposed by the discoverer Mitova-Dzhonova on the basis of some stone and clay artifacts (XIV-XIII c. BC) seems not very convincing from architectural viewpoint due to the fact that the real vault was invented and applied as late as in the Roman Empire only. Therefore, Garlo temple needs to be dated by some more objective physical method, e.g. by *optically stimulated luminescence - OSL* (Aitken 1998, Liritzis 2011). In order to examine the possibility of such procedure we for the first time measured the vertical profile of the mountain slope at three places.

1/ Profile "B" crosses the temple exactly through the center of the opeion where the intervention in the authentical environment was most considerable not only in the remote past, but also in the years 1972-1983;

2/ Profile "A" crosses the hill 50 m southwards from the temple where the terrain has kept its original state more than three thousand years;

3/ Profile "C" crosses the hill 50 m northwards from the temple where the road necessary for the restoration of the temple was traced in 1983.

The result is exceptionally interesting; it reveals the authentic picture of the building process. First, a 15 m deep conical pit has been excavated. The stone masonry has been carried out from the deepest point up to the zero level: at the beginning the well has been formed, then the tholos and at the end – the vault with the opeion. The entire "unnecessary" mass of stones and earth removed from the artificial cavity has

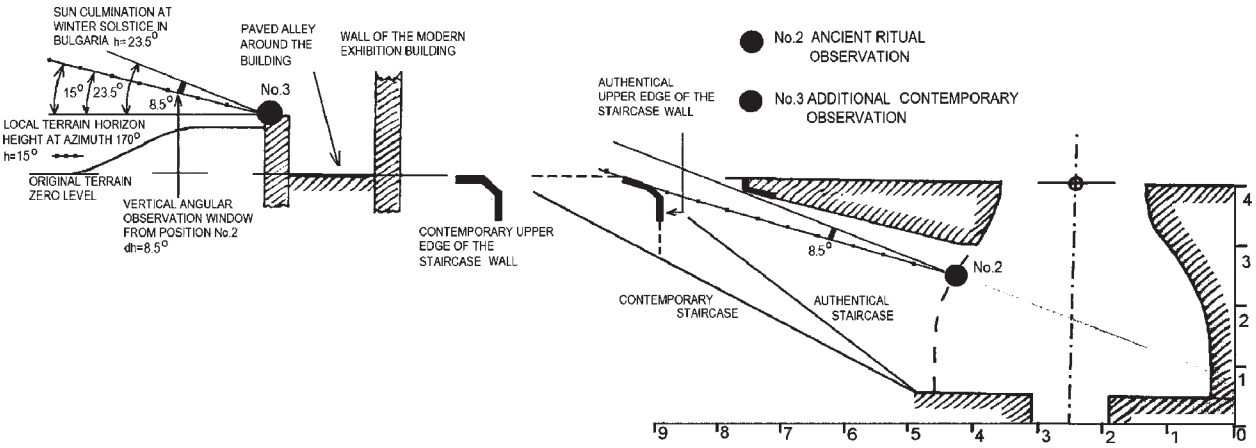

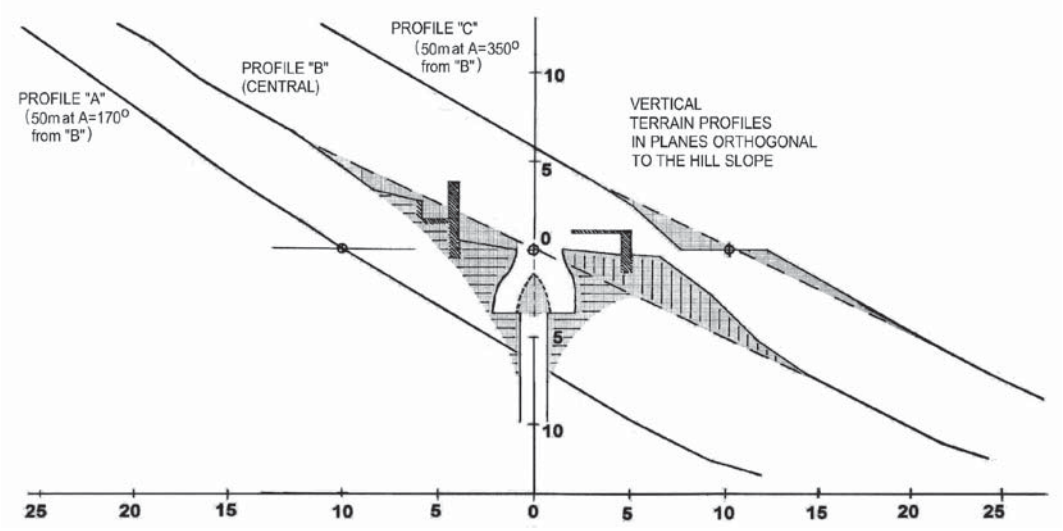

been piled up on the slope below the level of the temple opeion (zero level of the contemporary terrain). The excavated material has been sufficiently long time irradiated by the solar UV radiation and the geological luminescence signal accumulated by the quartz grains on the stone surface has been totally bleached. Then the last surface rock and soil layer has covered the bleached material and the accumulation of the new archaeological luminescence energy started there again. So, the necessary and sufficient conditions for the OSL dating procedure are fulfilled and this method could be applied here some day.

DEDICATION: The author dedicates the present article in the memory of N. Dermendzhiev.

References:

[1] Митова-Джонова Д.: *Мегалитен храм-кладенец при с. Гърло, Пернишки окръг*, изд. НИПК, София 1984.

[2] Митова-Джонова Д.: *Произход и същност на протосардинските сакрални кладенци III-I хил. пр. Хр.*, изд. Иврай, София 2007 (на български и италиански паралелно).

[3] Гайдукевич В.Ф.: *Боспорское царство*, изд. АН СССР, Москва-Ленинград 1949, стр. 170-171.

[4] Atzeni E.: Vornuragezeit – In: *Kunst Sardiniens*, Berlin-Scharlottenburg 1980, pp.15-43.

[5] Lilliu G.: Nuragenkultur – In: *Kunst Sardiniens*, Berlin-Scharlottenburg 1980, pp. 44-85.

[6] Дерменджиев Н.В.: *Методология на археоастрономическите изследвания. Анализ на обекти и находки от територията на България*, докторска дисертация 2007, депозирана в библиотеката на сектор "Слънце" при Институт по астрономия - БАН.

[7] ИИ = *Интердисциплинарни изследвания: Доклади от Първия национален симпозиум по археоастрономия в България (1988),* ред. П.Вълев, М.Гюрова, изд. НАИМ-БАН и Министерството на културата, София: Том XVII - 1990, Том XVIII – 1991.

[8] Kolev D., L.Tsonev, A.C.Gonzalez-Garcia and V.Koleva: Orientation of the dolmens in Bulgaria – In: *Proceedings of the International Conference 'Geoarchaeology and Archaeomineralogy', Oct. 29-30 2008*, *Sofia*; Publ. House "St. Ivan Rilski", Sofia 2008, pp. 169-174.

[9] Cézar González-García A., Dimiter Z. Kolev, Juan A. Belmonte, Vesselina P. Koleva and Lyubomir V. Tsonev: On the Orientation of Thracian Dolmens - *Archaeoastronomy. The Journal of Astronomy in Culture*, Volume XXII (2009), pp.21-33.

[10] Цонев Л.: *Мегалитите в България*, изд. Фараго, София 2010.

[11] Tsonev L.V., D.Kolev, Y.Dinchev: Dolmens in Sakar Mountain – In: *Proceedings of the Conference 'Man and Universe'*, Union of Scientists in Bulgaria, Smolyan 07.10.2011, publ. in Smolyan 2011.

[12] Tsonev L.V., D.Z.Kolev: Bulgarian megaliths: present state and perspectives for further research *Mediterranean Archaeology and Archaeometry Journal, Rhodes University*, Vol.12 (2012), No.2, pp. 15-19.

[13] Китов Г. & Д.Агре: *Въведение в тракийската археология*, изд. Авалон, София 2002.

[14] Русева М.: *Тракийската гробнична архитектура в българските земи през V-IIIв.пр.н.е.*, изд.Я, Ямбол 2002.

[15] Nekhrizov G.: Cult places of the Thracians in the Eastern Rhodope Mountains (End of the 2nd – 1st millennium BC) – In: *The Culture of Thracians and their Neighbours, Proceedings of the International Symposium in Memory of Prof. M.Domaradski*, Ed. by J.Bouzek, L.Domaradska, BAR International Series Vol. 1350 (2005).

[16] Аладжов Д.: *Селища, паметници, находки от района на Хасково,* Хасково 1997.

[17] Венедиков И.: Разкопките при с. Каснаково през 1945-1946г. - *Известия на археологическия институт,* София 1950, стр. 105-115.

[18] Zontschew D.: Das Thrakische Heiligtum von Batkun - *Wiener Jahreshefte*, Band XXXII (1940), Kolonnen 81-106.

[19] Tsontchev D.: *Le sanctuaire thrace pres du village de Batkoun*, Institut archeologique bulgare, Fonds du department du Plovdiv, Tome II, Sofia 1941.

[20] Lebeuf A.: The Nuraghic well of Santa Cristina Paulilatino, Oristano, Sardinia. A verification of the Astronomical Hypothesis: Work in Process, Preliminary Results – In: Archaeologica Baltica Vol.10 (2008), pp.155-161.

[21] Aitken M.J.: *An Introduction to Optical Dating*, Oxford University Press, 1998.

[22] Liritzis I.: Surface Dating by Luminescence: An Overview – *Geochronometria*, Vol. 38, No.3 (2011), pp.292-302.

ПОДЗЕМЕН ХРАМ-КЛАДЕНЕЦ В БЪЛГАРИЯ: АРХИТЕКТУРЕН И АРХЕОАСТРОНОМИЧЕН АНАЛИЗ

Любомир Цонев
Институт по физика на твърдото тяло, Българска академия на науките,
бул. "Цариградско шосе" 72, 1784 София,
e-mail*: ltsonev@abv.bg*

Резюме

През 1971 г. в България е открит древен подземен храм-кладенец от сардински тип близо до с.Гърло, Брезнишко. Този любопитен паметник има някои архитектурни и ситуационни особености, които все още нямат задоволително обяснение в рамките на чистата археология. Тук за пръв път споменатите особености са анализирани от гледище на археоастрономията. Този подход позволи да бъде предложена нова хипотеза, която интерпретира храма като свещен ритуален обект, който символично свързва бога Слънце с подземните води като маркер за вечно повтарящия се цикъл на живота. Предварителните непреки измервания поддържат тази хипотеза.

ANALYSIS OF MIXED-MODE I/II/III FRACTURE IN FOAM CORE COMPOSITE SANDWICH BEAMS

Victor Rizov
Department of Technical Mechanics, University of Architecture, Civil Engineering and Geodesy,
1 Chr. Smirnensky blvd., 1046 – Sofia, Bulgaria,
E-mail:V_ RIZOV_ FHE@UACG.BG

Abstract

The capacity of the Split Cantilever Beam (SCB) for characterization of mixed-mode I/II/III fracture behavior of foam core composite sandwich constructions is evaluated theoretically. The sandwich SCB was obliquely-loaded with respect to the crack plane in order to induce general mixed-mode I/II/III crack loading conditions. The influence of the loading angle on the fracture behavior was analyzed. The method of linear-elastic fracture mechanics was applied. Three-dimensional finite element model of the sandwich SCB was developed. Within the finite element simulations, the fracture was studied in terms of the strain energy release rate using the virtual crack closure technique. The analysis revealed non-uniform distribution of the strain energy release rate mode components along the crack front. It was found that the obliquely-loaded sandwich SCB is an efficient specimen for investigating mixed-mode I/II/III fracture in foam core composite sandwich constructions over a broad mixed-mode ratio range.

INTRODUCTION

Foam core sandwich composite structures are finding increasing use in modern engineering (Wang et al., 2010). A sandwich structure typically consists of two thin stiff composite faces bonded to a relatively thick light-weight core. The faces carry bending moments as compressive or tensile stresses, while the role of the core is to support the faces against backing and wrinkling and to transfer the transverse forces as shear stresses. Basic advantage of sandwich structures is their superior stiffness and strength per weight in comparison with conventional metal structures.

The load-bending ability of sandwich structures is highly dependent on the properties of the rigid foam used as a core material. The strength of the core may be considerably decreased by the presence of inherent imperfections in the foam material as flaws and voids or by defects which arise during lifetime of the sandwich structure due to impacting events or fatigue. These imperfections and defects act as stress concentrators from which cracks may initiate and propagate in the core. That is why the fracture properties of the foam core have significant influence on the structural performance of the sandwich. Therefore, fracture analyses of rigid foams (used as core materials) are of great importance in the design of sandwich structures.

However, relatively little attention has been given to the problem of fracture in the foam core of sandwich structures. The fracture behavior of cellular foam materials was studied under static loading (Ashby et al., 1984). Fatigue crack propagation in polyurethane foams was investigated using Compact Tension (CT) test specimens (Noble et al., 1981). They related the fatigue crack growth rates to the cyclic stress intensity factor range using the Paris' law equation. Environmental effects were analyzed on the fatigue fracture behavior of polycarbonate foams (Yau et al., 1986). Fracture toughness of rigid foams was characterized using an anti-clastic plate bending test method (Farshad et al., 1998). Modified double cantilever beam and shear fracture sandwich specimens were used for studying face/core debond fracture (Prasad et al., 1994). The fracture specimens were analyzed by finite element method models. A delamination crack along the face sheet/core interface in a foam core sandwich structure was simulated using a two-dimensional finite element model (Goswami et al., 2001). Mode I fracture behaviour of syntactic foam used as light core material for composite sandwich panels was studied using Three Point Bending (TPB) fracture

specimens (Rizzi et al., 2000). Two-dimensional finite element simulations of the TPB specimen were performed. Fracture behaviour of closed cell rigid polymeric foam frequently used as core material in sandwich structures was investigated (Bazhant et al., 2003). Mode I fracture was studied using single edge-notched prismatic specimens. The results obtained were compared with data from three-point bending fracture specimens. An analysis of mode I fracture in holed rigid foam panels was also performed. It was found that linear-elastic fracture mechanics can be applied to analyze the fracture behaviour of rigid foams.

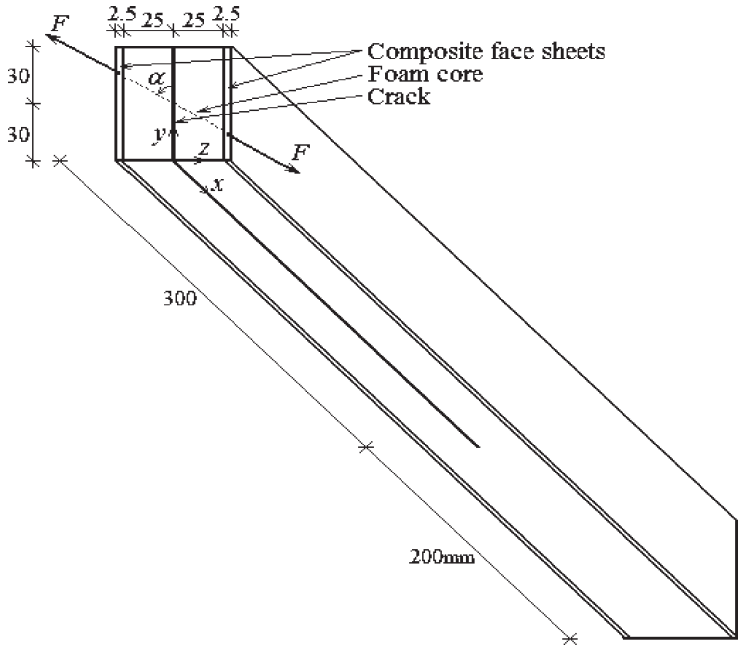

Fig. 1. Obliquely-loaded sandwich SCB.

It can be summarized that most of publications in the filed of fracture behavior are focused on pure modes of fracture. However, in real situations a fracture may occur under general mixed-mode I/II/III crack loading conditions due to the complex character of the loads applied on the sandwich constructions. It is obvious that investigations are needed of fracture behavior under combined loadings. Therefore, the basic purpose of the present work is to evaluate theoretically the capacity of the sandwich SCB for characterization of fracture behavior of foam core composite constructions under general mixed-mode I/II/III crack loading conditions. In order to generate such loading conditions, the sandwich SCB was obliquely-loaded with respect to the crack plane. Fracture analysis was carried out in terms of the strain energy release rate. The concepts of linear-elastic fracture mechanics were applied. Three-dimensional finite element model was developed to simulate the mechanical response of the sandwich SCB. Within the finite element simulations, the virtual crack closure technique was applied in order to analyze the strain energy release rate mode components distribution along the crack front. The influence of the loading angle on the fracture was investigated.

ANALYSIS OF STRAIN ENERGY RELEASE RATE IN OBLIQUELY–LOADED SANDWICH SCB

The obliquely-loaded foam core polymer composite sandwich SCB analyzed in the present paper is illustrated in Fig. 1. The sandwich consists of two polymer composite face sheets with thickness of 2.5 mm adhesively bonded to a rigid foam core with width of 50 mm. The height and the length of the sandwich beam are 60 mm and 500 mm, respectively. The sandwich has in its mid-plane, *xy*, a crack with length of 300 mm (Fig. 1). In order to generate mixed-mode I/II/III loading conditions, the two crack arms of the sandwich SCB were obliquely-loaded in opposite directions in such a way that the load line was through the centroid of the specimen (the loading is situated in the *yz* coordinate plane).

The influence of the loading angle, б, on the fracture behavior was investigated. For this purpose, four values (0^0, 30^0, 60^0, and 90^0) of б, measured from the vertical axis were considered in the analysis. The strain energy release rate mode components distribution along the crack front at different loading angles was studied using a three-dimensional finite element model of the obliquely-loaded sandwich SCB. The model was developed using the ANSYS finite element program system. The geometry of the model corresponded to the geometry of the SCB shown in Fig. 1. Three-dimensional continuum brick fi-

nite element SOLID45 defined by eight nodes, having three degrees of freedom per node, i.e. translations in the *x*, *y*, and *z* directions was used in order to mesh the model. The mesh was refined in the crack front zone in order to obtain a more accurate picture of the strain energy release rate mode components distribution along the crack front. In total, 4860 elements were used. It should be specified that before carrying out further computations, a mesh sensitivity study was conducted with respect to the number of elements in order to ensure that the mesh was fine enough to give reliable results. The results reported in the present paper were obtained by the finite element mesh depicted in Fig. 2. The boundary conditions and the loading in the finite element model corresponded to these in Fig. 1. The free end (x=500 mm) of the sandwich SCB was fixed in order to prevent rigid body movement of the model.

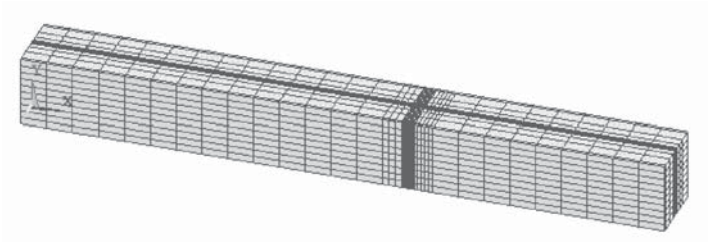

Fig. 2. Three-dimensional finite element mesh for discretization of the obliquely-loaded sandwich SCB.

It was assumed that the face sheets of the sandwich SCB are made of unidirectional glass/epoxy composite (the fibers are oriented in longitudinal direction, i.e. parallel to *x*-axis). The equivalent elastic properties of the composite used in the finite element simulations are reported in Table 1. The properties are given with respect to the coordinate axes *x*, *y*, and *z* defined in Fig. 1.

E_x, MPa	E_y, MPa	E_z, MPa	G_{xy}, MPa	G_{yz}, MPa	G_{zx}, MPa	ν_{xy}	ν_{xy}	ν_{xy}
45000	12000	12000	4500	3600	4500	0.3	0.3	0.3

Table 1. Elastic properties of the composite face sheets used in the finite element analysis. The subscripts refer to the principal material axes *x*, *y*, and *z* defined in Fig. 1.

The sandwich core itself was assumed to be an isotropic linear-elastic foam material with elastic modulus, E= 85 MPa, and Poisson ratio, ν=0.42.

Within the finite element simulations of the sandwich SCB, the strain energy release rate mode components and their distribution along the crack front at different loading angles were studied applying the virtual crack closure technique. This technique assumes validity of linear-elastic fracture mechanics (Davidson et al., 1996). The main advantage of the virtual crack closure technique is that it uses only one analysis step of the finite element model. The nodal forces along the crack front and the nodal displacements behind it generated by the finite element analysis are needed in order to calculate the strain energy release rate mode components (G_I, G_{II}, and G_{III}) associated with the three basic modes of crack growth (I, II, and III). A fragment of the crack front three-dimensional finite element mesh in the vicinity of the node *i* is illustrated in Fig. 3.

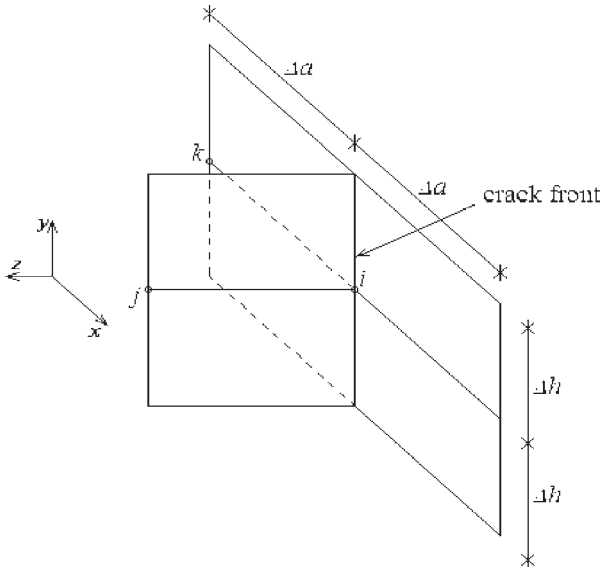

Fig. 3. Scheme of the crack front three-dimensional finite element mesh in the vicinity of node *i*.

The virtual crack closure technique is based on the assumption that the work done to closure the crack by one element is equivalent to the strain energy release rate when the crack grows by one element length. Therefore, at node *i* in Fig. 3 the strain energy release rate mode components G_I, G_{II}, and G_{III} can be calculated using the formulae

$$G_I = \frac{1}{2\Delta a \Delta h} Z_i \left(w_j - w_k\right), \quad (1)$$

$$G_{II} = \frac{1}{2\Delta a \Delta h} X_i \left(u_j - u_k\right), \quad (2)$$

$$G_{III} = \frac{1}{2\Delta a \Delta h} Y_i \left(v_j - v_k\right) \quad (3)$$

where *X*, *Y*, and *Z* are the nodal force components, and *u*, *v*, and *w* are the nodal displacement components in the *x*, *y*, and *z* directions, respectively. The subscripts in Eqs. (1) – (3) denote the corresponding nodes in Fig. 3. The strain energy release rate mode components distribution was obtained by applying Eqs. (1) – (3) for each node along the crack front.

The distribution is displayed in Fig. 4 for the four values of the loading angle (0^0, 30^0, 60^0,

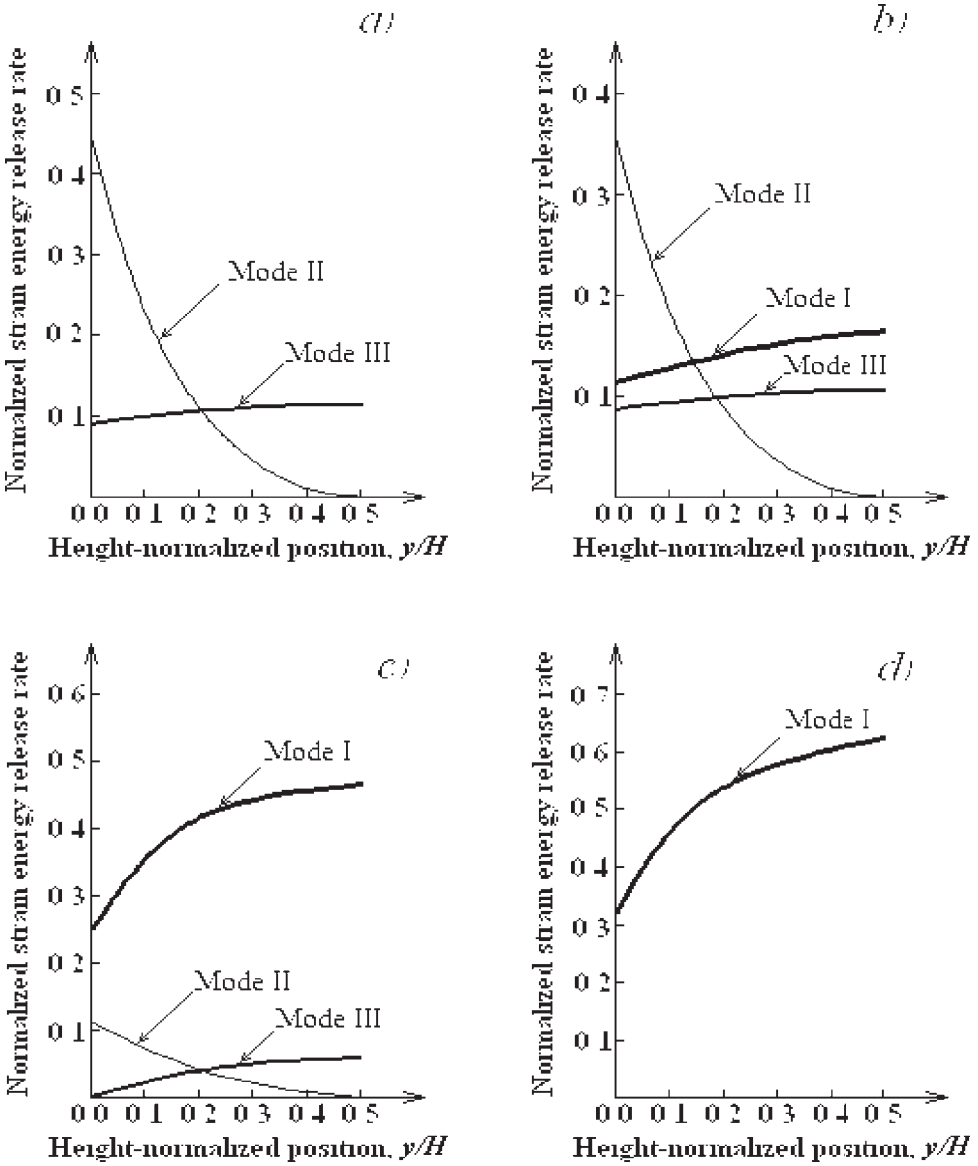

Fig. 4. Distribution of the normalized strain energy release rate mode components along the crack front in the sandwich SCB loaded at: (*a*) $\alpha = 0^o$, (*b*) $\alpha = 30^o$, (*c*) $\alpha = 60^o$, and (*d*) $\alpha = 90^o$ (the loading angle, α, is defined in Fig. 1). Here *H* is the height of the sandwich SCB cross-section. Only half the crack front is plotted, because the distribution is symmetrical about the crack front centre.

and 90^0) considered in the analysis (the strain energy release rate mode components are normalized using the formula $G_i^N = G_i H / F$, where H is the height of the sandwich SCB cross-section, and i=I, II, and III). Only half the crack front is plotted, because the distribution is symmetrical about the center of the crack front. The horizontal axis in Fig. 4 is defined such that $y/H = 0.0$ is at the low edge of the sandwich SCB cross-section. Thus, $y/H = 0.5$ corresponds to the crack front centre.

As expected, the distribution is non-uniform. The mode I component is maximum at the center of the crack front, while the mode II component increases towards the edge of the sandwich SCB cross-section. The mode III component is distributed almost uniformly in the central area of the crack front and slightly decreases near the sandwich SCB cross-section edge. The strain energy release rate mode components distribution can be explained in the following way.

Loading Angle, α	G_I^a / G^a	G_{II}^a / G^a	G_{III}^a / G^a
0^o	0.000	0.609	0.391
30^o	0.404	0.321	0.275
60^o	0.834	0.087	0.079
90^o	1.000	0.000	0.000

Table 2. Mixed-mode ratios of the average values of the strain energy release rate mode components (G_I^a / G^a, G_{II}^a / G^a, and G_{III}^a / G^a) in the sandwich SCB specimen loaded at different loading angles.

The mode I crack growth is associated to the deformation behavior in the crack front area induced by the bending of the two crack arms around the *y*-axis by the *z* component of the two forces applied on the specimen (the loading and the coordinate axes *x*, *y*, and *z* are shown in Fig. 1). The fact that G_I decreases towards the edge of the sandwich SCB cross-section can be explained with the laterally less constrained strains along the crack front.

The mode II loading conditions are generated by the bending of the two crack arms around the *z*-axis by the *y*-component of the two forces applied on the sandwich SCB (Fig. 1). The increase of the G_{II} component towards the edge of the SCB should be attributed to the fact that the longitudinal displacements induced by the bending of the crack arms around the *z*-axis increase towards the edge. The diagrams shown in Fig. 4 indicate that the mode II component of the strain energy release rate is zero at the crack front centre. This finding is related to the fact that the longitudinal displacements of the crack arms are zero at the centre.

Mode III crack growth is associated to the shear stress, τ_{xy}, along the crack front (induced by the *y*-component of the loading).

The influence of the loading angle on the mixed-mode I/II/III fracture behavior was evaluated by analyzing the mixed-mode ratios of the average values of the strain energy release rate mode components: G_I^a / G^a, G_{II}^a / G^a, and G_{III}^a / G^a. Such mixed-mode ratios were computed for the four values of the loading angle considered in the analysis. The results are summarized in Table 2. It should be specified that the average values of the strain energy release rate mode components along the crack front used for calculation of mixed-mode ratios were obtained as

$$G_I^a = \frac{\int_0^H G_I(y)dy}{H}, \quad (4)$$

$$G_{II}^a = \frac{\int_0^H G_{II}(y)dy}{H}, \quad (5)$$

$$G_{III}^a = \frac{\int_0^H G_{III}(y)dy}{H}, \quad (6)$$

where $G_I(y)$, $G_{II}(y)$, and $G_{III}(y)$ are the strain energy release rate mode components distributions along the crack front obtained by the virtual crack closure technique, H is the height of the specimen cross-section. The integrals in formulae (4), (5), and (6) were solved numerically.

The average value of the total strain energy release rate was obtained as

$$G^a = G_I^a + G_{II}^a + G_{III}^a \quad (7)$$

Table 2 shows that there is significant increase in the relative amount of mode I component of the strain energy release rate with increase of the loading angle, i.e. at large loading angles the fracture is mode I dominated. At $\alpha = 90^o$ pure mode I crack loading conditions are induced ($G_I^a / G^a = 1$). The data in Table 2 indicate also that the obliquely-loaded sandwich SCB can be used for characterization of fracture behavior over the complete mixed-mode ratio range: $0 \le G_I^a / G^a \le 1$. Concerning the relative amount of mode II and mode III components of the strain energy release rate, Table 2 shows that they decrease when the loading angle increases. The decrease of mode II is due to the fact that the bending moments in the crack arms induced by the *y*-component of the loading decrease with increase of the angle α (Fig. 1). The decrease of mode III component can be attributed to the decrease of the vertical shear force in the crack arms with increase of the loading angle.

CONCLUSIONS

The capacity of obliquely-loaded SCB for characterization of the mixed-mode I/II/III fracture in the core of sandwich composite structures was evaluated. The concepts of linear-elastic fracture mechanics were applied. Three-dimensional finite element simulations of obliquely-loaded sandwich SCB were carried out. The strain energy release rate mode components distribution along the crack front was analyzed by the virtual crack closure technique. The influence of the loading angle on the mixed-mode I/II/III fracture was investigated. The analysis revealed that the strain energy release rate mode components distributions are non-uniform along the crack front.

This finding was related to the global deformation behavior of the obliquely-loaded sandwich SCB specimen. The relative amount of the mode I component of the strain energy release rate increases with increase of the loading angle. This was attributed to the increase of the bending moments in the crack arms induced by the *z*-components of the loading with increase of the angle α (Fig. 1). It was found also that the sandwich SCB can be used to characterize the fracture in the core over the complete mixed-mode range, i.e. $0 \le G_I^a / G^a \le 1$. The relative amounts of the mode II and mode III components of the strain energy release rate decrease with increase of the loading angle. This was explained with decrease of the *y*-component of the loading with increase of the angle α. In general, the finite element simulations indicate that the obliquely-loaded SCB can be used for investigation of mixed-mode I/II/III fracture in the core of sandwich structures. The basic advantage of the sandwich SCB is that mixed-mode I/II/III fracture can be studied over a broad range of mixed-mode ratios (Table 2) using only one type of specimen.

References

[1] Wang Can, Chen Hao-ran, Lei Zhen-kun (2010) Experimental investigation of interfacial fracture behaviour in foam core sandwich beams with viscous-elastic adhesive interface. Compos. Struct. 92, 1085-1091.

[2] Ashby M. F., Gibson L. J., Mati S. K. (1984) Fracture Toughness of Brittle Cellular Solids. Scr. Metall. 18, 213-217.

[3] Noble F. W., Lilley J. (1981) Fatigue Crack Growth in Polyurethane Foam. J. Mater. Sc. 16, 1801-1808.

[4] Yau S. S., Mayer G. (1986) Fatigue Crack Propagation in Polycarbonate Foam. J. Mater. Sc. Eng. 78, 111-114.

[5] Farshad M., Floeler P. (1998) Investigation of mode III fracture toughness using an anti-clastic plate bending method. Eng. Fract. Mech. 60, 597-603.

[6] Prasad S., Carlson L. A. (1994) Debonding and crack kinking in foam core sandwich beams – I. Analysis of fracture specimens. Eng. Fract. Mech. 47, 823-824.

[7] Prasad S., Carlson L. A. (1994) Debonding and crack kinking in foam core sandwich beams – II. Experimental investigation. Eng. Fract. Mech. 47, 825-841.

[8] Goswami S., Becker W. (2001) The effect of face sheet/core delamination in sandwich structures under transverse loading. Compos. Struct. 54, 515 – 521.

[9] Rizzi E., Papa E., Corigliano A. (2000) Mechanical behaviour of syntactic foam: experiment and modelling. Int. J. Solids. Struct. 37, 5773-5794.

[10] Bazhant Z. P., Zhou Y., Zi G., Daniel I.M. (2003) Size effect and asymptotic matching analysys of fracture of closed-cell polymeric foam. Int. J. Solids. Struct. 40, 7197-7217.

[11] Davidson B. D., Sundararaman V. A. (1996) A single leg bending test for interfacial fracture toughness determination. Int. J. Fract. 78, 193-210.

АНАЛИЗ НА ПУКНАТИНА ПО СМЕСЕНА ФОРМА I/II/III В КОМПОЗИТНА САНДВИЧ ГРЕДА СЪС СЪРЦЕВИНА ОТ ПЯНА

Виктор Ризов
Катедра „Техническа механика", Университет по архитектура, строителство и геодезия, бул. „Хр. Смирненски" 1, София – 1046

Резюме

Направено е теоретично изследване на възможността на раздвоената конзолна греда за характеризиране на пукнатина по смесена форма I/II/III в композитни сандвич конструкции. Сандвич гредата е натоварена косо по отношение на равнината на пукнатината, за да се генерира натоварване по смесена форма I/II/III. Анализирано е влиянието на ъгъла на наклона върху пукнатината. Приложен е методът на линейната теория на пукнатините. Разработен е обемен модел на гредата по метода на крайните елементи. Скоростта на освободената потенциална енергия на деформацията е изследвана по метода на виртуално затваряне на пукнатината. Установено е неравномерно разпределение на компонентите на скоростта на освободената потенциална енергия на деформацията по фронта на пукнатината. Изследването показва, че косо натоварената раздвоена конзолна греда е ефикасно опитно тяло за характеризиране на пукнатина по смесена форма I/II/III в композитни сандвич конструкции.

SMALL–SCALE TESTS FOR AN INVESTIGATION ON THE EFFECT OF REINFORCED SOIL

Elvina Stoynova
Department of Geotechnics, University of Architecture, Civil Engineering and Geodesy
Hristo Smirnenski Boul. 1, Sofia

Abstract

Results of a small-scale test for the ultimate bearing capacity of circular foundation on geogrid-reinforced sand are presented. The number of layers of geogrid varied from 1 to 3 and the length of geogrid was from 2 to 4 times the diameter of the model foundation. The results apply to foundations placed on the surface.

Introduction

In the last 30 years several small-scale tests were conducted with small plates simulating footings on reinforced soil foundation (RSF). The reinforcement is mostly connected with the increasing of the bearing capacity (estimated by BCR) and reducing of the settlements (estimated by SRF). The aim of the researchers is to investigate the effect of the reinforcement and at the same time to determinate the optimum ratio of the parameters.

The first researchers Binquet and Lee [1] and Guido et al. [2] have proved that maximum effect of the reinforcement was for values of u/B <0,67 and recommended the values (b=B)cr=2÷3; (d/B)cr = 1,25. In 1994 Yetimoglu et al. [3] indicated the critical values of u/B=0,25; h/B=0,2 and b/B=4,5. The optimum values of the parameter of RSF after Das and Shin [4] are b/B=5÷6; u/B≈0,35 and d/B=2. Boushehrian and Hataf [5] investigated experimentally the influence of the reinforcement on the bearing capacity. Chang et al. Cascante [6] determined the depth of the first layer of geogrids on u=(0,3-0,5). B. Puri et al. [7] specified the critical values of u/B=0,33, b/B=4 and N=4.

Model foundations with different shapes and dimensions are used – square plates from 40/40 to 200/200 mm, circular plates with Ø50÷Ø240 mm or strip plates with dimensions from 50/300 to 200/600 mm. The test material is dry sand with friction angle from 32,5° to 38° and ρ=1,45÷1,72 g/mi. The test tanks are circular with diameter Ø300 mm or rectangular with length up to 1200 mm. The systems are with static or dynamic, with direct or hydraulic loading – with or without pressure control. The measuring system is mechanical or electronic. The geogrids are standard or not, with various cells dimensions, material and tensile strength.

Reinforced soil

The parameters of RSF in the area of the investigations and practices were implemented by Binquet and Lee [1]. In Fig. 1 are shown basic parameters.

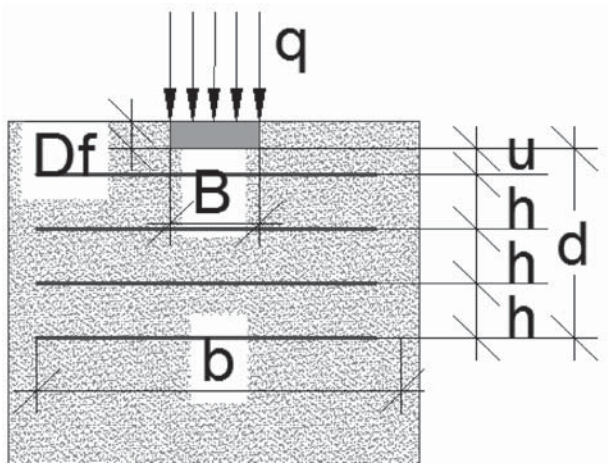

Fig. 1. Geometric parameters for RSF

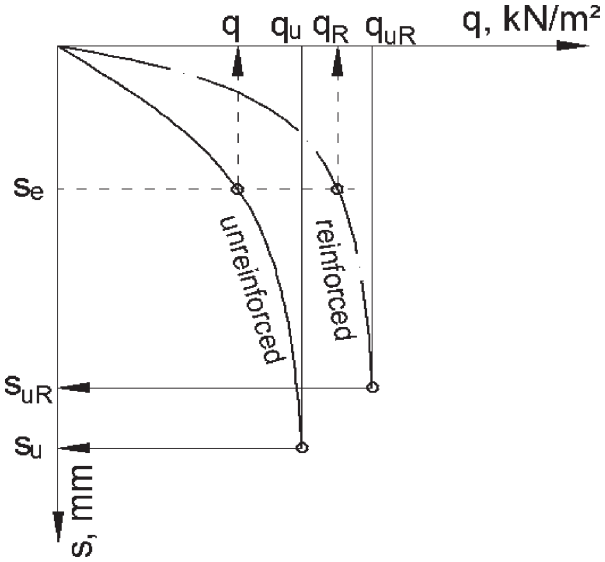

Fig. 2. Settlements vs. loading in case of reinforced and unreinforced soil foundation

q - load

B, m –width of the foundation

b, m –width of the geogrid

Df, m – depth of the foundation

d, m – thickness of reinforcement zone below the bottom of the foundation

u, m – depth of the geogrid below the bottom of the foundation;

h – vertical distance between the layers of the geogrid;

N, бр. – layers of the geogrid;

T_u, kN/m – strength of the geogrid

Fig. 2 shows the general behaviour of reinforced and unreinforced soil foundation. The load-settlement curve of unreinforced soil is closer to the settlement axis compared to those of reinforced soil. The shown relations are of principle and are standard for estimation of the variation of the settlement as a function of the loading for reinforced and unreinforced soil.

The Bearing Capacity Ratio (BCR) is a non-dimension parameter for estimation of the effect of reinforcement for increasing the bearing capacity. There are two possibilities to evaluate BCR: with respect to the ultimate bearing capacity $BCR_u=q_{uR}/q_u$ or the allowable bearing capacity $BCRs=q_R/q$, where q_{uR} and qu are the bearing capacity of reinforced and unreinforced soil and q_R and q are the pressure for reinforced and unreinforced soil at a given settlement level $s=s_e$.

The effect of reinforcement to reduce the settlement is expressed by the Settlement Reduction Factor (SRF). The factor is defined as $SRF=s_{u,R}/s_u$, where s_{uR} is settlement of reinforced soil for load q_{uR}, and s_u – settlement of unreinforced soil for load q_u.

Experimental tests

The test set-up consisted of steel base plate, steel cylinder tank and steel collar – see Fig. 3. The parts were connected by studs. The dimensions of the base plate were 310x250x10 mm. The outside diameter of the cylinder tank was 250 mm, thickness of the wall 8 mm and height 150 mm. The inside walls of the tank were marked so that the level of the geogrid can be kept. After the sand was placed and compacted the steel collar was removed.

The tank with the base plate was placed on a work table. The axial load was applied on the model foundation – steel plate with diameter ø55 mm. The load was increased incrementally until reaching the load of failure. The loading steps (25 kPa) were realized with concrete plates measuring 30x30x25 mm and weight 6 kg each. During each load step the settlements were recorded at time intervals 1, 2, 5, 10, 15, 30 min. The maximum speed of the displacements was 1# / 30 min.

a)

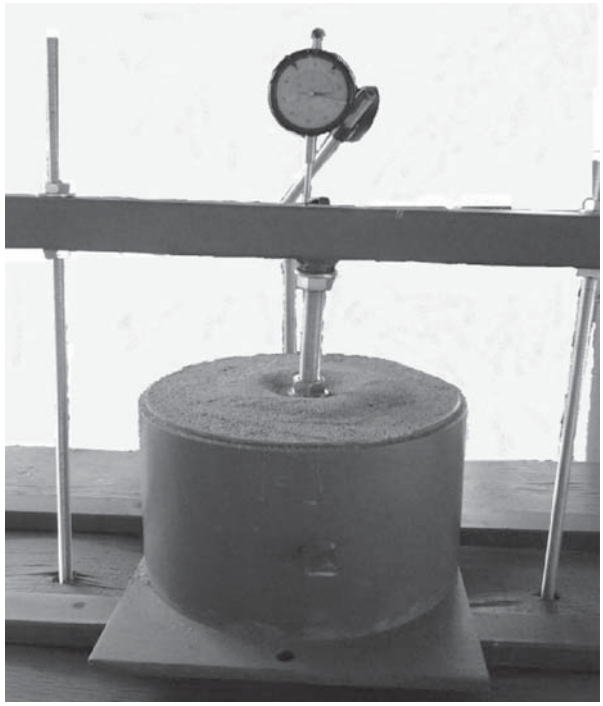

b)

Fig. 3. Test set-up – a) steel cylindrical tank; b) load step before the failure

The sand used for the test had grain-size distribution as shown in Fig. 4. The sand parameters are: specific density ρs=2,65 g/cmi, porosity n=0,434, coefficient of uniformity U=8,4, friction angle φ = 38°. The sand was dry with the relative density of compaction Dr= 0,63 for all tests.

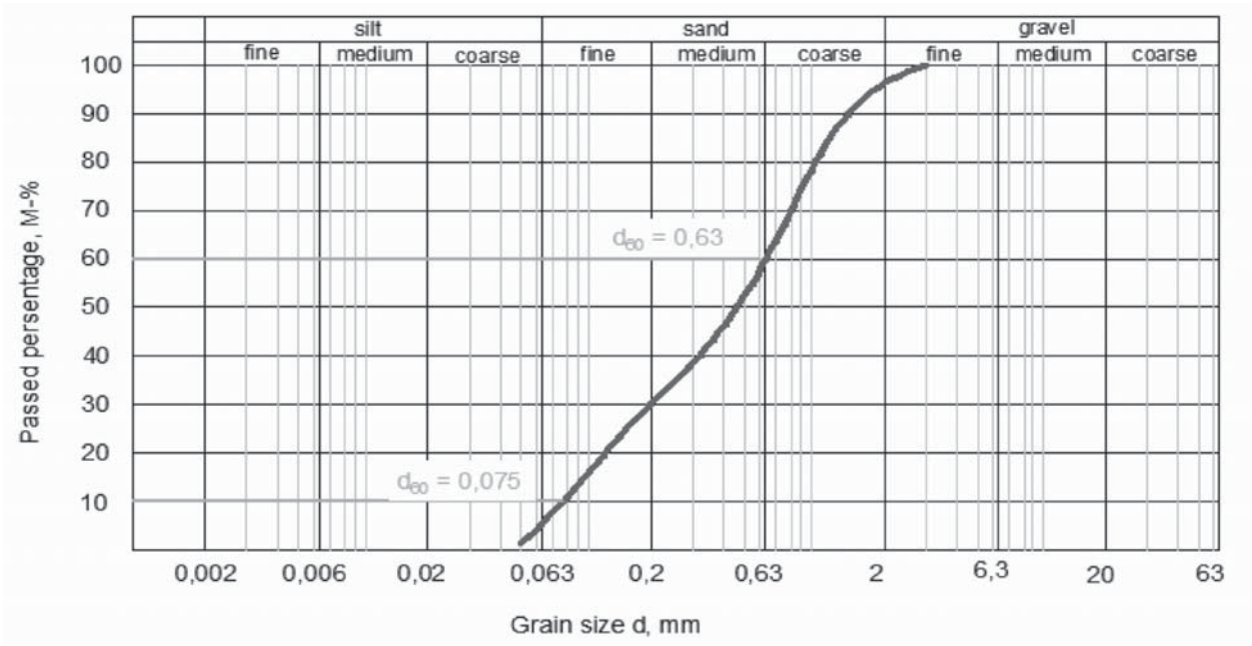

Fig. 4. Grain-size distribution

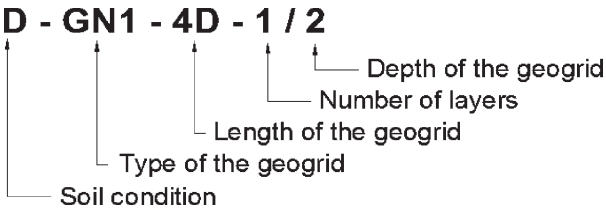

The aim of the conducted tests was to define the influence of one-, two- and three-layered reinforcement on the behaviour of the sand. The effect of the length of the geogrid b=n.D was also investigated. A total of nine tests were carried out – each of them with its own name (s. **Fig. 5**)

Fig. 5. Test name

The reinforcement was implemented by PVC grid with cell dimension 5U5 mm and tensile strength T_{max}=2 kN/m for s_T=20%. The geogrid was noted as GN1.

Results

It was adopted to obtain the bearing capacity by the tangent method by Terzaghi (shortly "tt"-method). The experimental results (points in the coordinate system "s-q") were approximated by a smooth curve. The value of q_u was defined as the load corresponding to the intersect point between the tangents. As a comparison the values of the allowable bearing capacity were also given. The settlement levels were s=8%.D and s=10%.D.

Table 1. Summary – settlement vs. load

Load q	**D–X–X–X–X/X**	**D–GN1–2D–1/2**	**D–GN1–2D–2/2**	**D–GN1–2D–3/2**	**D–GN1–3D–1/2**	**D–GN1–3D–2/2**	**D–GN1–3D–3/2**	**D–GN1–4D–1/2**	**D–GN1–4D–2/2**	**D–GN1–4D–3/2**
kN/ml	mm	mm	mm	mm	mm	mm	mm	mm	mm	mm
0	0,00	0,00	0,00	0,00	0,00	0,00	0,00	0,00	0,00	0,00
25	1,64	1,60	1,52	1,48	1,04	0,84	0,74	0,54	0,44	0,34
50	2,91	2,55	1,98	1,86	1,45	1,37	1,02	0,82	0,73	0,47
75	3,48	3,15	2,75	2,67	1,64	1,43	1,35	1,20	0,97	0,63
100	4,11	3,95	3,32	3,23	1,97	2,01	1,67	1,47	1,35	0,98
125	4,92	4,75	3,89	3,86	2,41	2,26	1,83	1,65	1,58	1,32
150	5,93	5,14	4,98	4,89	3,14	3,18	2,56	1,93	1,84	1,56
175	7,15	5,94	5,81	5,74	3,88	3,59	3,24	2,78	2,06	1,87
200	8,28	7,02	6,57	6,39	4,63	4,38	4,17	3,41	3,04	2,54
225	10,15	8,44	7,48	7,52	5,73	6,03	5,02	4,75	3,82	3,26
250	12,61	10,98	10,08	9,75	7,86	7,68	6,89	6,63	5,36	5,11
275	15,44*	13,83	12,62	12,08	10,64	10,22	9,91	9,02	8,56	8,12
300	Coll	Coll	Coll	Coll	Coll	Coll	Coll	Coll	Coll	Coll
**) The settlement for q=275 kN/ml -15,44 mm is extrapolated.*										

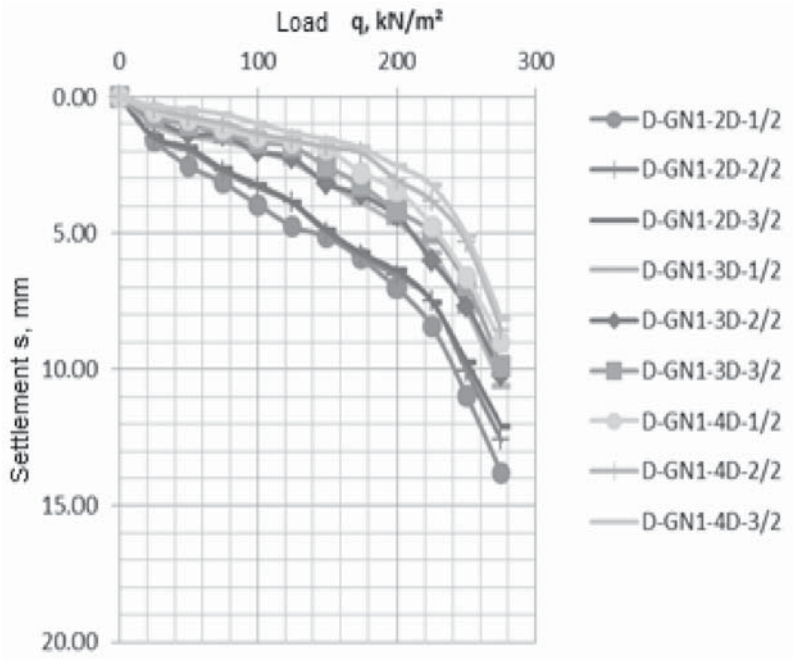

Fig. 6. Influence of the geogrid length b=n.B and the layers N=1, 2, 3 on the load-settlement curve

The obtained results for the settlements are shown in Table 1.

Fig. 6 shows all load–settlement curves. The obtained results for the settlements of the various combinations are logic as well as the type of curves. The load of failure for reinforced soil is 300 kN/ml. The settlement value for test D–X–X–X–X/X (unreinforced sand) is the result of an extrapolation. The failure occurred at the load of 275 kN/ml.

Fig. 7 shows the plots of settlement vs. load depending on the length and the layers of the geogrid. The length of the grid influences considerably on the end settlement of the reinforced soil. Compared with the settlement of the plate in the unreinforced case, the settlement decreases up to 78,6÷89,6% for b=2D and up to 52,6÷58,4% for b=4D.

Depending on the number of layers the settlement decreases from 89,6% to 78,6% for b=2.D. The reduction for b=4.D is identical – from 58,5% to 52,6%. For b=3.D the value order is kept.

The values for the bearing capacity obtained by the "tt"-method are given in **Table 2**. The allowable bearing capacity is also summarized there.

In Fig. 8 the approximation of the average results is shown. The approximation curve for the number of geogrid layers has its maximum value at $N_{opt.}$=3÷4.

The same method is used in regard to the length. Geogrid with length $b_{opt.}$=(4÷6).D can be adopted as optimum.

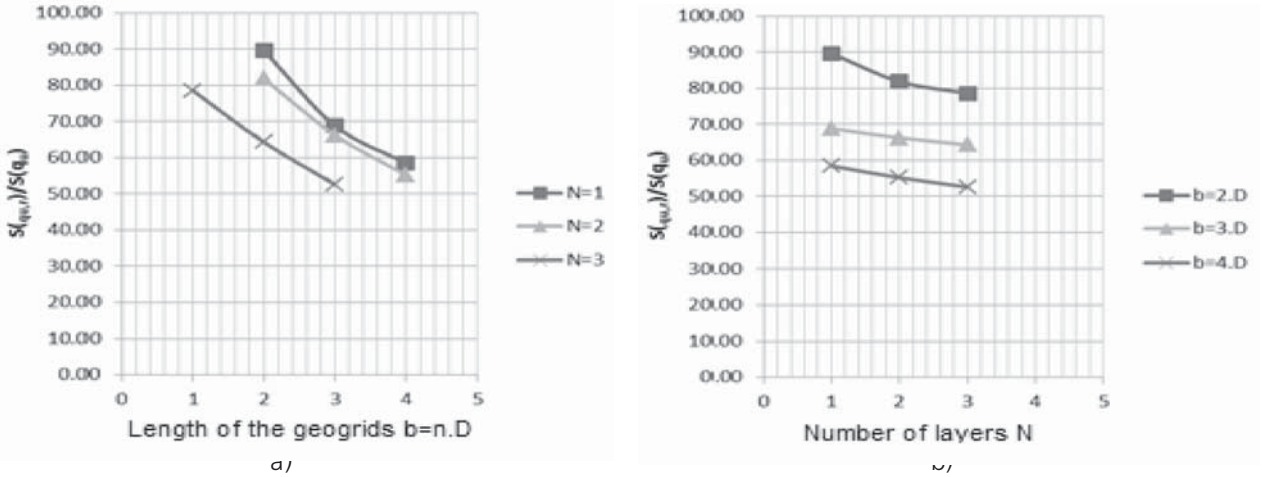

a) b)

Fig. 7. *Influence of the geogrid length b=n.B (a) and the layers N=1, 2, 3 (b) on settlement reduction in %*

Table 2. Variation of the bearing capacity depending on geogrid length b=n.B and the layers N=1, 2, 3

	D–GN1–2D–1/2	D–GN1–2D–2/2	D–GN1–2D–3/2	D–GN1–3D–1/2	D–GN1–3D–2/2	D–GN1–3D–3/2	D–GN1–4D–1/2	D–GN1–4D–2/2	D–GN1–4D–3/2
q_u, kN/ml	215.00	220.00	222.00	218.00	222.00	222.00	220.00	230.00	238.00
q_u(s=10%),kN/ml	150.00	160.00	160.00	208.00	212.00	220.00	225.00	238.00	245.00
q_u(s=8%), kN/ml	110.00	122.00	130.00	185.00	192.00	200.00	210.00	222.00	230.00

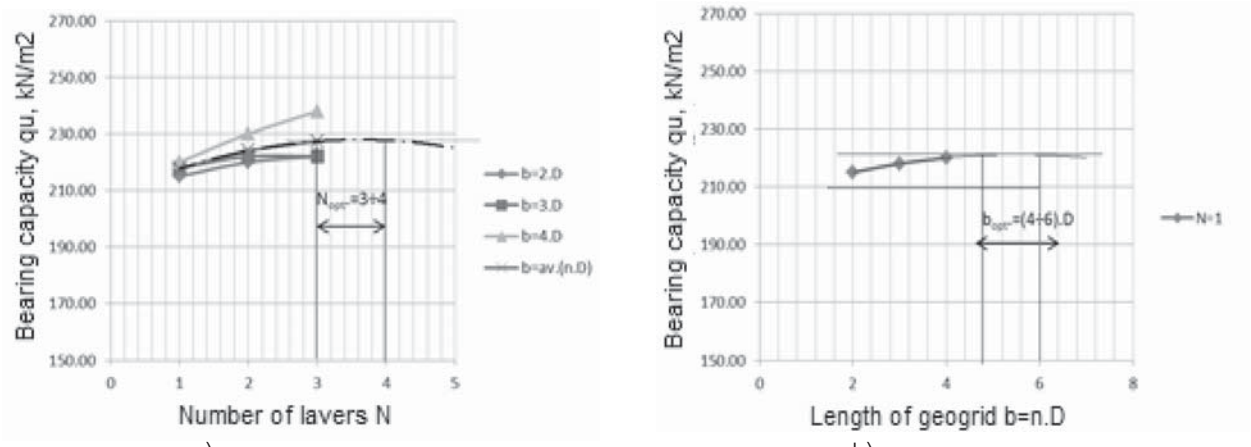

a) b)

Fig. 8. Forecast values - a) number of layers N; b) length of the geogrid

Table 3. Variation of BCR depending on geogrid length b=n.B and the layers N=1, 2, 3

	D-GN1-2D-1/2	D-GN1-2D-2/2	D-GN1-2D-3/2	D-GN1-3D-1/2	D-GN1-3D-2/2	D-GN1-3D-3/2	D-GN1-4D-1/2	D-GN1-4D-2/2	D-GN1-4D-3/2
BCRu	1.04	1.06	1.07	1.05	1.07	1.07	1.06	1.11	1.15
BCRs(s=10%)	1.20	1.28	1.28	1.66	1.70	1.76	1.80	1.90	1.96
BCRs(s=8%)	1.22	1.36	1.44	2.06	2.13	2.22	2.33	2.47	2.56

Conclusions

The effect of reinforcement (evaluated by BCR – see **Table 3**) varies from 1,04 (the shortest grids) to 1,15 (for b=4.D). The effect is largest for length 4D. The maximum value is 15%. The effect on BCR of one layer of the geogrid is the same for all the lengths. The increase of the bearing capacity from one to two layers of reinforcement is about 5% for length b=4.D. The difference in BCR between two and three layers of the geogrid is 4%.

The representation of the settlement reduction using SRF (**Fig. 9**) shows that for the same number of layers the settlement decreases with increasing the length of the reinforcement. The vertical displacements decrease with about 20% for length b=2.D, about 45% for b=3.D and up to 65% for b=3.D.

On the basis of the experimental results the following conclusion can be drawn:

- The highest values of bearing capacity are obtained for a number of layers of the geogrid N=3t4;
- The optimum length of the geogrids is found to be about $b_{opt.}$=(4÷6).D;
- The effect of the reinforcement on the settlement is considerable – SRF reaches values up to 0,3 (that means 70% reduction of the settlement);
- The effect on the bearing capacity is relatively less compared to the settlement reduction

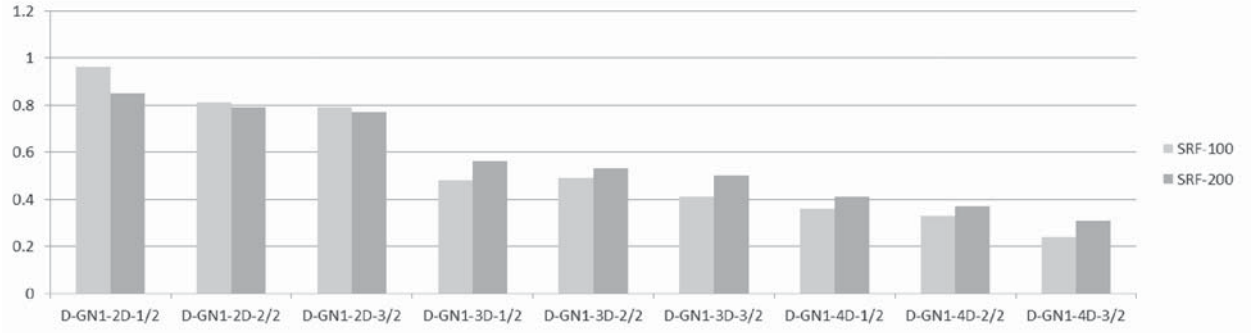

Fig. 9. Variation of SRF

– BCR-values up to 1,15.

The obtained results are comparable with the experimental observations by other researchers.

References

[1] Binquet, J., K. L. Lee. Bearing capacity tests on reinforced earth mass. *Journal of the Geotechnical Engineering Division - ASCE.* 1975, 101, 12.

[2] Guido, V. A. Comparison of geogrid and geotextile reinforced earth slabs. *Canadian Geotechnical Journal.* 1986, 23.

[3] Yetimoglu, T., J. T. H. Wu, and A. Saglamer. *Bearing capacity of rectangular footings on geogrid-reinforced sand.*.м. : Journal of Geotechnical Engineering Division, ASCE, 1994.

[4] Shin, Das. *Experimental Study of bearing capacity of a strip foundation on geogrid-reinforced sand*. Geosynthetics International, 2000, 7.

[5] Hataf, Boushehrian, Ghahramani. Experimental and Numerical Behavior of Shallow Foundations on Sand Reinforced with Geogrid and Grid Anchor under Cyclic Loading. *Transaction A: Civil Engineering.* 2010, 17, 1.

[6] Chung, W. and G. Cascante, Experimental and numerical study of soil-reinforcement effects on the low strain stiffness and bearing capacity of shallow foundation. *Journal of Geotechnical and Geological Engineering.* 2006.

[7] Puri, Kumar, Das, Prakash, Yeo. *Settlement of reinforced subgrades under dynamic loading.*

[8] Haripal, P.K., R.N. Behera, C.R. Patra. *Behavior of surface strip footing on geogrid reinforced sand bed.* Goa: IACMAG, 2008.

[9] Mohanmed, T. P. W., K. Ilamparuthi. *Performance of footing on sand bed with and without reinforcement.* Chennai : Indian Geotechnical Conference, IGS Mumbai Chapter & ITT Bombay, 2010.

[10] Patra, C.R., J. N. Mandal, B.M. Das. *California State Ultimate bearing capacity of shallow foundation on geogrid-reinforced sand.*

[11] Al-Sinaidi, R., A. H. Ali. Improvement in bearing capacity of soil by geogrid - an experimental approach. 2006 .

[12] Omar, M.T., B.M. Das, S. C. Yen, V. K.Puri, E. E.Cook, Ultimate bearing capacity of rectangular foundations on geogrid-reinforced sand. *Geotechnical Testing Journal - ASTM.* 1993.

ДРЕБНОМАЩАБНИ ОПИТИ ЗА ИЗСЛЕДВАНЕ НА ЕФЕКТА НА АРМИРАНА ПОЧВЕНА ОСНОВА

Елвина Стойнова
Катедра „Геотехника“, Университет по архитектура, строителство и геодезия
Бул. „Христо Смирненски“ 1, София

Резюме

Представени са резултатите от дребномащабни опити за изследване на носещата способност на кръгли фундаменти върху основа от армиран с геомрежа пясък. Опитите са проведени за едно-, дву- и триредово армиране при промяна на дължината на геомрежата от 2 до 4 пъти диаметъра на моделния фундамент. Резултатите се отнасят за разположени на повърхността фундаменти.

BULGARIAN ADDED VALUE TO ERA

BULGARIAN SOCIETY FOR EIGHTEENTH–CENTURY STUDIES

Antoaneta Petkova*
Sofia University "St. Kliment Ohridski", Faculty of History
*E-mail: petkova.antoaneta@gmail.com

Abstract

The aim of this article is to present the Bulgarian Society for Eighteenth-Century Studies with a special emphasis on the Annual ISECS Executive Committee Meeting and the River and River Spaces in the XVIII Century (The Danube and Other Examples) conference which is held in Sofia in August 2014.

INTRODUCTION

The Bulgarian Society for Eighteenth-Century Studies (BSECS) takes pride in being a multi- and inter-disciplinary organisation, adept at implementing new standards and approaches in teaching and researching all the cultural and political aspects of the eighteenth-century reality and their impact on the further historical development. Since its establishment in 1992, the Society unites the efforts of senior scholars in all fields of the humanities with those of their young colleagues to promote the advancement of the eighteenth century studies and to encourage scientific collaboration among Bulgarian and international researchers.

Despite the fact that the BSECS is an organisation with relatively modest income, the president of the Society Assoc. Prof. Angelina Vacheva PhD (Faculty of Slavic Studies, Sofia University), continuing the tradition inherited from the previous leader Assoc. Prof. Dr Habil Ivan Parvev (Faculty of History, Sofia University), strives to be active in hosting and organising scientific events both at the national and international levels. In this respect, at least one major conference is organised every year. Other events in the BSECS calendar include, but are not limited to, lectures and seminars.

Furthermore, the praiseworthy efforts of the BSECS to arouse students' interest in the Century of Enlightenment give their fruitful results. More and more young people take an active part in the events organised by the Society. It is equally important that BSECS tries to bring the science into the wider community by encouraging everyone to express their opinion during the discussion sessions.

All these activities are in conformity with the ideals recognised by the entire family of national societies united by the International Society for Eighteenth-Century Studies (ISECS). The ISECS meets annually and organises a congress every four years.

THE ANNUAL ISECS EXECUTIVE COMMITTEE MEETING

The BSECS is proud to have the honour of hosting the Annual ISECS Executive Committee Meeting in August 2014. This is the first time when this meeting is held in Sofia. As Assoc. Prof. Dr Habil Ivan Parvev, in charge of the organising committee, has an excellent reputation as an organizer of international forums, the expectations are that the Bulgarian society will deliver a high quality event. Thanks to the support of the Centre of Excellence in the Humanities "Alma Mater" the preparations advance at quite a fast rate although the participants have to cover their travel and accommodation expenses themselves.

The meeting will take place in Sofia from 25 to 28 of August 2014. The delegates represent thirty national organisations affiliated to the International Society for Eighteenth-Century Studies. During the events, the delegates are going to discuss the points scheduled in the agenda. Apart from the organisational and administrative questions, the meeting will open the floor for discussions about future scientific projects and more opportunities for collaboration.

RIVER AND RIVER SPACES IN THE XVIII CENTURY (THE DANUBE AND OTHER EXAMPLES) CONFERENCE

Continuing the tradition, the Annual ISECS Executive Committee Meeting is accompanied by a multidisciplinary conference which this year takes place on 27 August 2014 in Sofia University. The topic of this conference is "River and River Spaces in the XVIII Century (The Danube and Other Examples)".

The aim of the event is to cover as broad dimensions of the river understanding as possible. This means that the scholars are free to choose the topic of their presentation among environmental, political, economic, social, cultural, etc. aspects of rivers. In this respect, organisers called upon specialists with interest in different fields of study to choose one of the following sections:

"Rivers as connections in the XVIII century" and "South-Eastern Europe as a Danubian Space (environment, culture, history)".

Not coincidentally, the accent is on rivers as connectors. Namely the aim of this topic is to prompt a response why rivers, as a natural phenomenon, are not only landmarks but also objects that unite people and determine their common culture. Equally important, the topic gives the researchers freedom to express what they consider important about rivers and provokes wider discussions.

Judging by the number of proposals received, there is a serious scientific interest in this topic. Further information about the conference could be found on the web-site of the BSECS (http://bulgc18.com/index.php?pageid=9).

FUTURE EXPECTATIONS

As it has already been mentioned, the Eighteenth-century study congress is organised once every four years. The next one is going to take place in Rotterdam next year where the Bulgarian Society intends to present the published volume of the conference papers as a result of the events in Sofia in 2014.

The ultimate goal which the BSECS sets is to host a congress which, according to ISECS data, will attract between 600 and 1200 participants. This is a challenge BSECS is ready to encounter. It is believed that the high quality of the events organised in August 2014 will prove this.

CONCLUSION

In conclusion, the BSECS is a small but important organisation in the family of the eighteenth-century specialists worldwide. It has important contributions to promote the advancement of the eighteenth-century studies. On account of the international recognition, the Bulgarian Society was given the honour of hosting major events in 2014.

БЪЛГАРСКО ОБЩЕСТВО ЗА ПРОУЧВАНЕ НА XVIII В.

Антоанета Петкова
Софийски университет „Св. Климент Охридски",
Исторически факултет

Резюме

Целта на настоящата статия е да представи Българското общество за проучване на XVIII в. с акцент върху Годишното събрание на изпълнителния комитет на Международното дружество и конференцията „Реки и речни пространства през XVIII в. (Дунав и други примери)", които ще бъдат проведени в София през август 2014 г.

MADE IN BULGARIA WITH EUROPEAN SUPPORT

CARBON–BASED NANOCOMPOSITES WITH INTERMETALLIC Cu–Sn NANOPARTICLES AS ANODE MATERIALS IN Li–ION BATTERIES

Ivania Markova, Vladislava Stefanova, Olivier Chauvet*, Tihomir Petrov, Valentina Milanova, Ivan Denev, Snejanka Uzunova

University of Chemical Technology and metallurgy

8, Kl. Ohridski blvd., 1756 Sofia, Bulgaria

*Institut of materials, Nantes, France

E-mail:vania@uctm.edu

Abstract

Results obtained during the second phase of the Contract DVU 02/98 " Porous nanocomposite electrodes for a new generation of electrochemical power sources based on carbon foam and metal nanoparticles", funded by the Bulgarian Science fund of the Ministry of Education and Science are presented. Intermetallic Cu-Sn nanoparticles are synthesized through a borohydride reduction with $NaBH_4$ in a mixture from aqueous solutions of $CuCl_2.2H_2O$ and $SnCl_2.2H_2O$ in a ratio Cu:Sn=2:3. Intermetallic nanoparticles are also synthesized by a "template" technique with a support (carbon foam, carbon powder, graphite), and carbon-based nanocomposites are obtained. Studies are carried out by scanning electron microscopy (SEM) and X-ray diffraction (XRD) analysis in order to investigate the influence of different supports used on the morphology, structure, and phase composition of the synthesized composite materials. Phases of Cu_6Sn_5 and $Cu_{10}Sn_3$ are formed, and they are in correspondence with the phase diagram of the binary Cu-Sn system. The prepared porous nanocomposites which consist of a C-foam matrix and Cu-Sn nanoparticles are electrochemically tested by cyclic voltammetry in the solution of 1M LiCl and 1M KOH performed with Gamry galvanostat-potenciostain a three-electrode Dr. Bob's cell. Nanocomposite materials with a different carbon matrix (graphite, carbon powder, carbon foam), and Cu-Sn nanoparticles are tested as anodes in Li-ion batteries. The influence of the carbon matrix on the electrochemical behavior of these composites is investigated. When Cu_6Sn_5 alloy is deposited on carbon foam, the composite has 40% higher cyclability on the 30^{th} cycle. The conducted electrochemical tests show that the obtained composites which consist of a carbon matrix and Cu-Sn nanoparticles are suitable anode materials as an alternative to graphite in lithium-ion batteries.

INTRODUCTION

In recent years many authors are involved in investigations on alternative electrode materials for a new generation of electrochemical power sources. Efforts are concentrated on the production of carbon-based composite materials which will have better characteristics than those of the conventional anodes (graphite or alloys). Metal alloys and intermetallic compounds based on tin (Sn), antimony (Sb), and silicon (Si) are synthesized because of their potential use as an alternative material of the graphite electrode in Li- ion batteries. These materials are characterized by high specific capacity compared to that of the graphite. The requirements for the high specific capacity of the electrode material ,

while maintaining a high cyclability, cannot be answered by pure elements such as Sn, Sb, Si etc. Cycle properties of Sn can be improved by adding subcomponents which alloy with Sn and form intermetallic compounds such Sn_2Fe, Sn_2FeS , Cu_6Sn_5, Co-Sn (CoSn, $CoSn_2$, Co_3Sn_2) and Ni_3Sn_x (Ni_3Sn, Ni_3Sn_2, Ni_3Sn_4) [1,2]. For example, negative electrodes based on Sn have a higher specific capacity (993 mAh g^{-1}) than that of carbon materials (e.g., 372 mAh g^{-1} for graphite). However, in the "charge-discharge" cycle their volume changes due to phase transformations and it leads to stress conditions which cause cracking or destruction of the tin electrode . This negative effect could be reduced by creating two- or multi-phase electrodes, and also by reducing the size of the base material (electrode). In bi- or multiphase electrodes the active material is usually surrounded by an inert layer that serves as a buffer, increasing the mechanical stability of the electrode. The resistance of the electrode material can also be improved by modifying the structure with additional elements, which are arranged at the boundaries of the grains and increase the strength of the material, and its resistance to breaking as well.

Cu-Sn, Co-Sn and Ni-Sn intermetallic compounds can be used as electrode materials in Li-ion batteries [3, 4]. K.D. Kepler and his colleagues have found that lithium (Li) can be implemented in Cu_6Sn_5 alloy forming $Li_xCu_6Sn_5$ system [5]. This material has a theoretical mass capacity over 350 $mAhg^{-1}$ and significantly higher volumetric capacity corresponding to 1655 $mAhml^{-1}$ compared to commercial LiC_6 electrode material. Various methods are used in order to obtain nanosized alloys with different morphology. T. Sarakonsri and coworkers have proposed a method for preparation of intermetallic compounds such as InSb, Cu_6Sn_5 and Cu_2Sb materials for negative electrodes in lithium batteries by solution reduction of transition metal salts and non-metal salts with fine zinc powder [6].

A relatively new approach is preparation of composites which combine the stability of graphitized carbon with a material showing a large capacity towards lithium. Thus, a high energy matrix with stable electrochemical parameters is obtained.

In the new energy storage systems an inert electrode matrix is the unifying unit (for both anode and cathode). It plays a role of a micro reaction module which simultaneously serves as a current collector, and a reservoir for electrolyte and reaction products. The weight of the electrodes based on classic Ni or Cu supports with a coarse structure can be reduced by their replacement with porous fine grained electrode materials known in the literature as *foam*. These foams have micro pores, which helps to increase energy and power density of the electrodes. Porous carbon-based nanocomposites which consist of carbon foam (C-foam) and metal nanoparticles can be obtained. Their potential use is in current electrochemical power sources, as well as in other areas, such as biotechnology, biology, medicine, solar cells and others.

Accordingly, the main goal of DVU 02/ 98 Project is to obtain porous nanocomposite electrodes for a new generation electrochemical current sources based on carbon foam and metal nanoparticles [7-10]. In connection to this the purpose of this study is to carry out physico-chemical investigations and electrochemical tests of carbon-based nanocomposites with Cu-Sn nanoparticles obtained by a template synthesis through a borohydride reduction and to establish the influence of the carbon matrix type on the electrochemical behavior of these composites.

EXPERIMENTAL SET–UP

Iintermetallic Cu-Sn nanoparticles are synthesized as an active ingredient of the resulting nanocomposites through a borohydride reduction with 0.5M NaBH4 in a mixture of aqueous solutions of the corresponding chloride salts (0.2M $CuCl_2.2H_2O$ and 0.2M $SnCl_2.2H_2O$) at a ratio Cu:Sn=2:3 using a "template" technique with a carrier in the sequential mode of introducing the reaction solutions (the precursors and the reducing agent) at room temperature and atmospheric pressure. Citric acid, $(HOOCCH_2)_2C(OH)COOH$ is used as a complex agent. Cu-Sn nanoparticles are synthesized in-situ in the pores of a modified C-foam and in the pores formed between the carbon grains. Carbon-based nanocomposite materials are obtained as a result. After completion of the reduction process the samples were fil-

tered, washed with distilled water and ethanol and dried in vacuum for 24 h at 100 °C.

The morphology, structure, and phase composition of the obtained intermetallic nanoparticles synthesized with C-based support were examined by a scanning electron microscopy (SEM) and X-ray diffracrion (XRD). The SEM images were made with a JEOL 6400F (Japan) SEM microscope at accelerating voltage of 7 kV, and also with a JEOL JSM 5300 (Japan) SEM microscope at accelerating voltage of 20 kV. X-ray diffraction patterns of all samples are collected within the 2θ range from 10^{o} to 95^{o} with a constant step 0.03^{o} and counting time 1 s/step on Philips PW 1050 diffractometer using CuKα radiation.

Electrochemical behavior of the synthesized Cu_xSn_y alloy and the C-based composites (C/Cu_xSn_y) as positive electrodes (anodes) in Li-ion battery is investigated in a three-lectrode cell using a computer controlled laboratory cycling equipment BA500 Series Battery Analyzer. For the electrochemical study a composite material representing a matrix from inactive carbon foam covered with a nanocrystalline Cu-Sn alloy is prepared. The amount of the alloy compared to the carbon matrix is 90%.

The tested nanocomposite electrodes are prepared by mixing of 50% of the active component and 50% of Teflonized Acetylene Black (TAB-2). The mixture is pressed (981 MPa) onto a copper foil substrate with a diameter of 15 mm. Li foil is used as a negative electrode. The electrolyte is a mixture of 1M LiPF6, ethylene carbonate (EC) and diethyl carbonate (DEC) (1:1). The water content in the electrolyte is under 30 ppm. Test cell is assembled in argon-filled glove box. The cell is cycled at room temperature and a constant current density of 0.2 $mA.cm^{-2}$ between 0.01 – 1.5 V towards Li^{+}/Li.

The obtained porous nanocomposite materials based on C-foam and metallic (Cu, Sn)/ intermetallic (Cu-Sn) nanoparticles are investigated as working electrode in aqueous solution of 1M LiCl and 1M KOH by cyclic voltammetry. The experiments are carried out in a Gamry cell (three-electrode Dr. Bob's cell) with a capacity of 200 cm^3 at room temperature without stirring the electrolyte. The working electrode area is 2 cm^2. The counter electrode (≈2 cm^2) is made of platinum. A calomel reference electrode (Hg/Hg_2Cl_2) is used. Its potential, compared to a normal hydrogen electrode, is E_{SCE} = 0.244 V. The experiments are carried out with a computer-controlled Gamry potenciostat-galvanostat Model G 300ZRA. The Gamry Framework PHE 200 program is used. The scane rate was 10mVs-1. In most cases scanning started from the potential of the reference calomel electrode and was counted until a sufficiency negative potential was reached, at which the reaction of hydrogen release is assumed to start. After that the scanning direction was reversed and scanning was carried out up to the selected potential in the anode zone.

RESULTS AND DISCUSSION

1. Physical–chemical study of carbon–based composite materials with intermetallic Cu–nanoparticles. SEM and XRD results

Fig. 1 (a-d) presents XRD patterns of the on Cu-Sn nanoparticles and their C-based composites. Carbon powder (C-powder), carbon foam (C-foam) and graphite (C-F) are used as a carbon matrix.

XRD pattern of Cu-Sn nanoparticles prepared by a reductive precipitaion proves the formation of one main phase of $Cu_{10}Sn_3$ (Fig. 1-a). In the case of Cu-Sn nanoparticles synthesized using C-foam as a support a phase of $Cu_{10}Sn_3$ is formed, too (Fig. 2-b), but phases of Cu and Sn are also observed, as well as the presence of the carbon phase is proved. When C-powder is used as a carrier for the Cu-Sn nanoparticles synthesis, the diffraction pattern consists of two phases: major phase of Cu_6Sn_5 and the impure phase of Cu_2O (Fig. 2-c). The presence of carbon phase is also improved. The X-ray diffraction pattern of the nanocomposites based on Cu-Sn nanoparticles and graphite as a support has proven the existence of three phases: the major phases of Cu_6Sn_5 and $Cu_{10}Sn_3$ and a little impure phase of Cu_2O, as shown in the Fig. 2-d. A carbon phase is also indicated.

In Fig. 2(a-d) SEM images of Cu-Sn nanoparticles synthesized through a chemical reduction and their carbon (C)-based composites at a different magnification are shown.

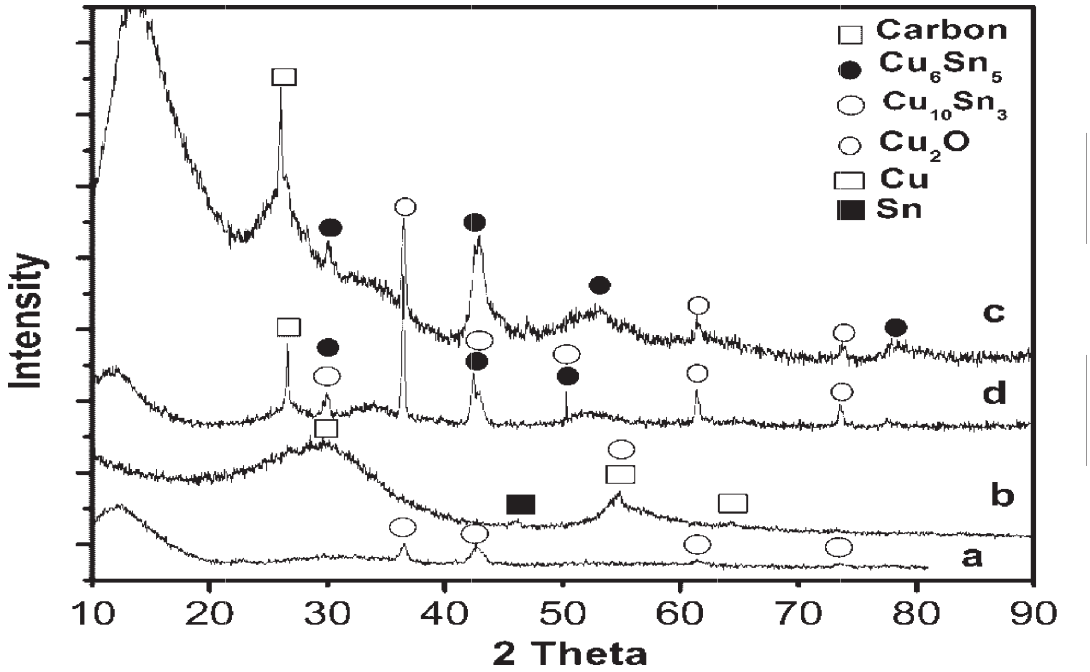

Fig.1. XRD pattern of: a-Cu-Sn nanoparticles, b-C-foam/Cu-Sn nanoparticles, c-C-powder/CuSn nanoparticles, d-C-F/Cu-Sn nanoparticles

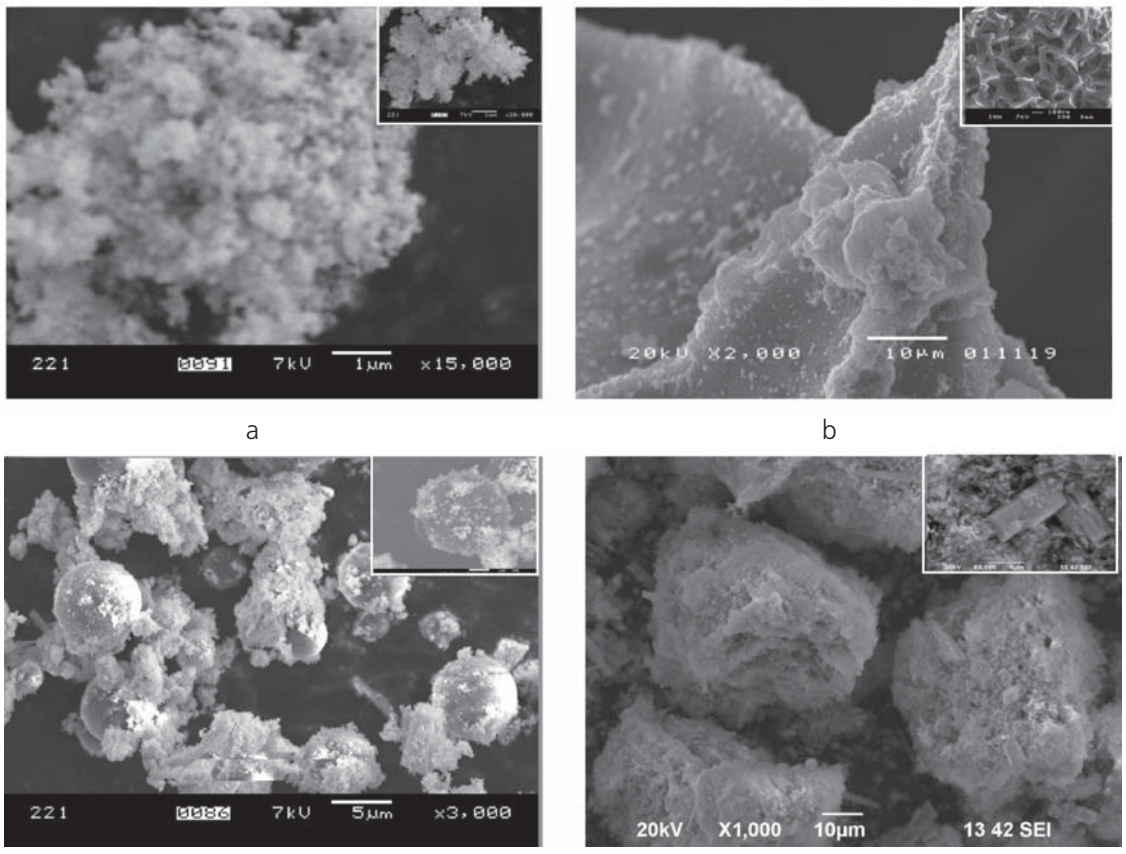

a b c d

Fig. 2. SEM image at a different magnification: a-Cu-Sn nanoparticles, x15000, b-C-foam/Cu-Sn nanoparticles, x2000, b-C-powder/Cu-Sn nanoparticles, x3000, c-CF/Cu-Sn nanoparticles, x1000

On the SEM images of nanosized Cu-Sn powder and their C-based composites, shown in Fig. 2, it can be seen that the morphology of the samples have some differences. The Cu-Sn nanoparticles synthesized through a borohydride reduction in water solutions (Fig. 1-a) are too small to be identified and aggregate to large aggregations randomly. It could be contributed to that the strong reducing agent $NaBH_4$ in combination with an intense stirring during the reductive process creates a large number of nuclei, which limited the growth of graines. Small particles with a high surface energy tend to aggregate spontaneously to decreasing their energy. In the case of C-foam matrix (Fig. 1-b) it can be seen that the nanoparticles also exhibit a tendency to aggregate as a result of a high developed surface due to the particle nanosize.When C-powder is used as a matrix for the nanoparticle template synthesis, smaller particles and bigger ones are grown on the C-grain surface (Fig. 1-c). On the SEM images of Cu-Sn nanoparticles synthesized using the graphite (C-F) support shown in Fig. 1-d, graphite grains irregular and flake in form are observed. Aggregated Cu-Sn particles obtained together with and between the graphite flakes can be detected. The Cu-Sn particle size according to the SEM images is 40 to 60 nm. The Fig. 1-d demonstrates microparticles in size of 50-60 μm due to the aggregation of nanoparticles together with the C-flakes in the case of graphite support. Plates of Sn in size of 5.5x1.5x10 μm are also observed (the small picture in the right corner in Fig. 1-d).

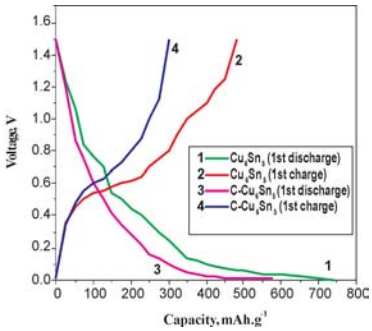

Fig. 3. Initial charge/discharge curves of Li/Cu_6Sn_5 alloy and Li/C-Cu_6Sn_5 composite cells

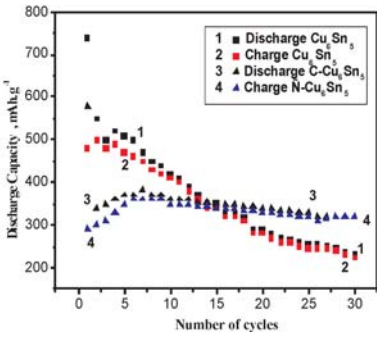

Fig.4. Cycling performance of Cu_6Sn_5 alloy and C-Cu_6Sn_5 composite electrodes

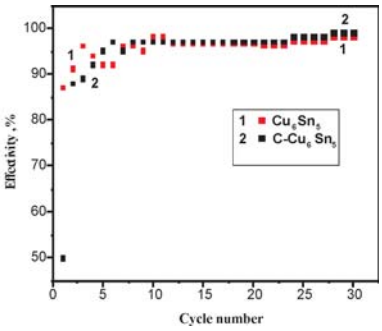

Fig. 5. Coulombic efficiencies *vs.* number of cycles for the Cu_6Sn_5 alloy and C-Cu_6Sn_5 composite electrodes

2. Cycling electrochemical tests of the obtained nanocomposite materials based on C–foam and Cu–Sn nanoparticles as anodes in Li–ion batteries

The charge/discharge curves of the initial cycle for $Cu_{10}Sn_3$ alloy and C/Cu-Sn composites are shown in Fig. 3. A higher initial discharge/charge capacity has the Cu_6Sn_5 alloy (740 mAh.g^{-1} and 480 mAh.g^{-1}, respectively) and a lower capacity - the C-Cu_6Sn_5 composite (580 mAh.g^{-1} and290 mAh.g^{-1}, respectively). The reversible capacity at the 30th cycle is higher for the C-Cu_6Sn_5 composite (322 mAh.g^{-1}), while for the Cu_6Sn_5 alloy it is lower (230 mAh.g^{-1}) (Fig. 4).

Different electrochemical behavior of the both electrodes is due to their different phase composition and microstructure. In the case of the Cu_6Sn_5 alloy conditions of the destruction of the active material and loss of contact between separate particles which leads to the capacity loss are created during the initial lithation.

The higher reversible capacity in the case of the C-Cu_6Sn_5 composite is due to the forming of the stable microstructure of the active material using inactive carbon foam, which prevents destruction of the material during the cycling process and minimizes losses of the contact between the particles.

The dependence of the efficiency vs. the cycle number for the both electrodes is presented in Fig. 5. The initial efficiency of the electrodes based on Cu_6Sn_5 alloy is 87%, while for the electrodes based on C-Cu_6Sn_5 composites it is 50%. During the cycle process the efficiency increases till 98% for the alloy and 99% for the compos-

ite.

The Cu_6Sn_5 alloy deposited on the modified commercial C-foam exhibits a cyclability improved with 40% on the 30 cycle. The choice of a suitable matrix (modified C-foam) and optimization of the conditions for the Cu_6Sn_5 alloy synthesis could bring to essential improvement of its electrochemical behavior. These porous nanocomposite materials are potential anode material and could be used as alternative material to the graphite electrodes in Li-ion batteries. They are expected to have improved their capacity.

3. Electrochemical behaviour of the obtained composite materials based on C–foam and metallic (Cu, Sn)/intermetallic (Cu–Sn) nanoparticles carried out with Gamry Insruments in a Dr. Bob's cell

Obtained composite materials based on C-foam and metallic (Cu, Sn)/intermetallic (Cu-Sn) nanoparticles were investigated by the method of cyclic voltammetry, carried out with Gamry Instruments in a Dr. Bob's cell, where model conditions in a liquid electrolyte - 1M LiCl with a concentration of Li^{1+} ions equivalence to those in 1M $LiPF_6$ in Li-ion battery are created in order to be electrochemically studied as anodes. Cycling voltammograms (CVA) are performed at room temperature at potential range from 0.0 to 2.0 V at the scan rate of 10 mVs^{-1}. The cycling voltammograms on the investigated samples - C-foam and composites on its basis with Cu, Sn and Cu-Sn nanoparticles in different electrolytes (1M LiCl, 1M KOH) are shown in Figs. 6-9.

Figure 8 (figure 6 is a part of this figure) shows the recoded curves, obtained in the solution of 1M LiCl. Curve 1 shows the results ob-

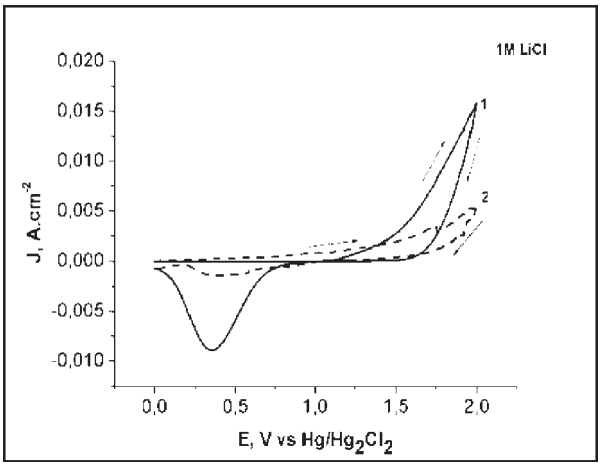

Fig. 6. Cycling voltammograms in 1M LiCl on: 1-C-foam, 2-C-foam/Cu-Sn nanoparticles

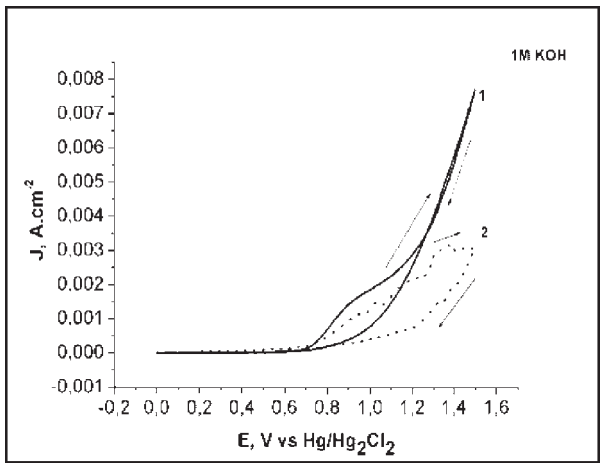

Fig. 7. Cycling voltammograms in 1M KOH on: 1-C-foam, 2-C- foam/Cu-Sn nanoparticles

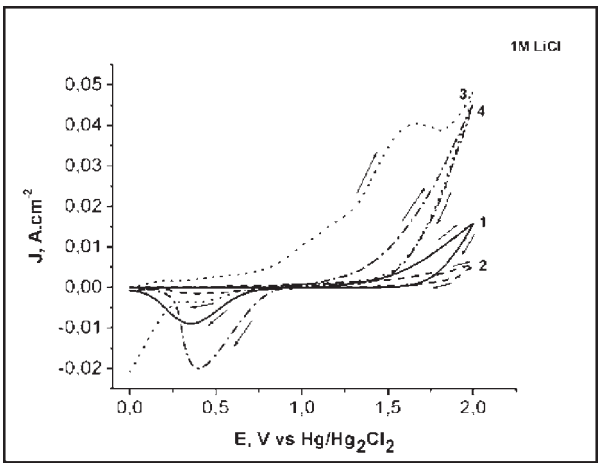

Fig. 8. Cycling voltammograms in 1M LiCl on: 1-C-foam, 2-C-foam/Cu-Sn nanopar-ticles, 3-C-foama/Cu nanoparticles, 4-C-foam/Sn

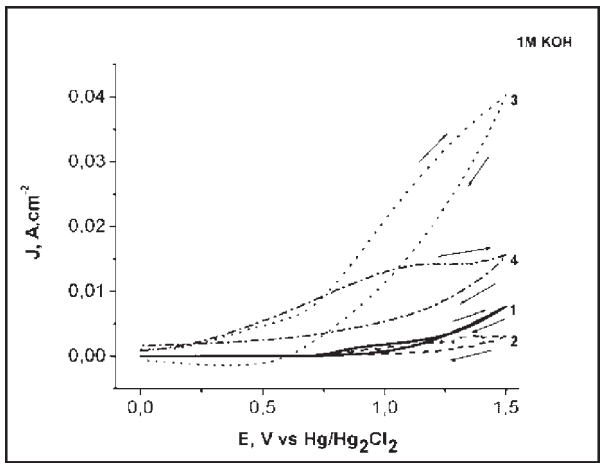

Fig. 9. Cycling voltammograms in 1M KOH on: 1-C-foam, 2-C-foam/Cu-Sn nano-particles, 3-C-foama/Cu nanoparticles, 4-C-foam/Sn

tained onto C-foam. The oxidation process starts at the 1.2 V and at the reversive scan a cathodic peak (negative current) around 300 mV is detected. This process most probably is connected with some chemical changing of the chloride or oxides formed at the scanning of potentials from 0 to 2 V. The behavior onto the covered by Cu-Sn nanoparticles carbon foam shows the suppression of the above mentioned processes – oxidation as well as the reduction process. The sample doped with the Cu (curve 3) nanoparticles indicates very aggressive process of oxidation as well the same could be detected with doped only by Sn nanoparticles (curve 4). Taking a look onto the curves obtained in the KOH (Figure 7 and 9), it should be noted that the main difference is an absence of a cathodic peak. It is obvious that it happens due to the reduction of passive layers, formed during oxidation process in the solution of LiCl. It may be concluded that the reaction rate of the oxidation process is the smallest in the case of sample doped with Cu-Sn nanoparticles.

Conclusion

Intermetallic Cu-Sn nanoparticles with a carbon-based support are synthesized through a borohydride reduction with $NaBH_4$ in an aqueous solution of the corresponding chloride salts at a mass ratio Cu:Sn=2:3 at room temperature and atmospheric pressure. The used "template" technique for the synthesis of the nanoparticles is an effective way for a direct preparation of nanocomposites type carbon-based matrix/nanoparticles. Citric acid used as a complex agent is important for the formation of nanoparticles on C-grains surface or in the pores between the C-grains. Electron microscopic studies indicate that the resulting composite material (intermetallic alloy powder) has a morphology which is typical of alloy materials. The particles have irregular shape and tend to aggregate, which is typical of the nanostructured state. The nanoparticles have a size of 40 to 80 nm, while the aggregates of the nanoparticles have a size in the range of 200-300 мm. The used supports (C-powder, graphite, C-foam) slightly affect the morphology of the particles during their formation. In relation to the dispersion of the nanoparticles, graphite is the most suitable support. XRD analysis proves the formation of phases of Cu, Sn, Cu_6Sn_5, $Cu_{10}Sn_3$, and carbon. The mass ratio Cu:Sn=2:3 set in the synthesis of intermetallic nanoparticles does not affect the shape and morphology of the particles, but it is determining for the phase formation. The obtained phases are in accordance with the phase diagram of the binary Cu-Sn system.

The influence of the active ingredient on the specific capacity and the cyclic performance of the synthesized nanocomposite materials are followed by charge-discharge curves. The Cu_6Sn_5 alloy deposited on a modified commercial C-foam exhibits an improved cyclability with 40% of the 30th cycle. While being electrochemically tested, it is found out that the obtained Cu-Sn intermetallic nanoparticles and the composites based on them are suitable composite materials for preparation of electrodes in advanced electrochemical power sources.

Acknowledgement

This Project DVU 02/98 is supported by the National Research Fund of the Republic of Bulgaria at the Ministry of Education, Youth and Science.

References

[1] M. Salavati-Niasari, M. Bazarganipour, F. Davar, Nanosized Cu_6Sn_5 alloy prepared by a co-precipitation reductive route, *Polyhedron,* 29 (2010) 1796-1800.

[2] J. Wolfenstine, S. Campos, D. Foster, J. Read, W.K. Behl, Nanoscale Cu_6Sn_5 anodes, *Journal of Power Sources*, 109 (2002) 230-233.

[3] Xiao-Yong Fan, Fu-Sheng Ke, Guo-ZhenWei, Ling Huang, Shi-Gang Sun, SnlCo alloy anode using porous Cu as current collector for lithium ion battery, Journal of Alloys and Compounds, 476 (2009) 70s73.

[4] H. Groult, H. El Ghallali, A. Barhoun, E. Briota, C.M. Julien, F. Lantelmea, S. Borensztjand, Study of Co–Sn and Ni–Sn alloys prepared in molten chlorides and used as negative electrode in rechargeable lithium battery, Electrochimica Acta, 56 (2011) 2656d2664.

[5] K.D. Kepler, J.T. Vaughey, M.M. Htackarey, *Elecrochem. Solid State Lett.,* 2, 7 (1999) 307.

[6] T. Sarakonsri, C.S. Johnson, S.A. Hackney, M.M. Thackeray, Solution route synthesis of InSb, Cu_6Sn_5 and Cu_2Sb electrodes for lithium batteries, *Journal of Power Sources*, 153 (2006) 319–327.

[7] Ivania Markova, Tihomir Petrov, Ivan Denev,

Snejanka Uzunova, Radostin Nikolov, Vladislava Stefanova, Olivier Chauvet, Synthesis and Physico-chemical study of porous nanocomposites based on carbon foam and Cu/Cu-Sn nanoparticles for Li-ion baterry electrode materials, *Advances in Bulgarian Science,* National Center for information anddocumentation, Annual 2012, pp. 37-47, Sofia, Eds. by Kamen Velev, Vanya Grashkina, Yana Popova, Lyubov Racheva, Milen Angelov, Katia Stoilova, Lyudmila Velkova, ISSN: 1312-6164.

[8] V. Milanova, T. Petrov, I. Denev, I. Markova, Nanocomposites based on intermetallic nanoparticles template synthesized using different support, Journal of Chemical Technology and Metallurgy, issue *60th Anniversary of the UCTM*, 48, 6 (2013) 12-20, ISSN1311-7629, www.uctm.edu.

[9] T. Petrov, I. Markova-Deneva, O. Chauvet, I. Denev, Synthesis and study of porous carbon foam/ Cu(Cu-Sn) nanoparticles composites for electrode materials, Proc. of the 9th Int. Conf. on Multi-Mat. Micro Manuf., 2012, pp.105-108, ISBN:978-981-07-3353-7.

[10] T. Petrov, V. Milanova, I. Denev, I. Markova, Electrochemical behavior of porous nanocomposites based on carbon foam and intermetallic Cu-Sn nanoparticles, *Proceedings of the 10th Int. Conf. on Multi Materials Micro Manufacture,* 8-10 Octsber 2013, San Sebastian, Spain, Eds. by Sabio Azcarate and S. Dimov, pp.137-140, ISBN 978-981-07-7247-5, doi: 10.3850/978-981-07-7247-5_332.

ВЪГЛЕРОДНО-БАЗИРАНИ НАНОКОМПОЗИТИ С ИНТЕРМЕТАЛНИ Cu-Sn, НАНОРАЗМЕРНИ ЧАСТИЦИ КАТО АНОДНИ МАТЕРИАЛИ В Li-ЙОННИ БАТЕРИИ

Иваня Маркова, Владислава Стефанова, Оливие Шове*, Тихомир Петров, Валентина Миланова, Иван Денев, Снежанка Узунова
Химико-технологичен и металургичен университет
Бул. "Кл. Охридски" 8, София 1756, България
*Институт по материали, Нант, Франция

Резюме

Представени са резултати от втория етап на проекта „Порести нанокомпозитни електроди за ново поколение електрохимични източници на ток на базата на въглеродна пяна и метални наночастици", финансиран от Фонд „Научни изследвания" към Министерството на образованието, младежта и науката. Синтезирани са интерметални Cu-Sn наноразмерни частици чрез борхидридна редукция с $NaBH_4$ в смес от водни разтвори съответно на $CuCl_2.2H_2O$ и $SnCl_2.2H_2O$ при отношение Cu:Sn=2:3. Интерметални наноразмерни частици са синтезирани и чрез "template" техника с помощта на носител (въглеродна пяна, въглероден прах, графит), при което са получени въглеродно-базирани нанокомпозитни материали. Проведени са изследвания със сканираща електронна микроскопия (SEM и рентгено-дифракционен (XRD) анализ, за да се изучи влиянието на различните въглеродни носители върху морфологията, структурата и фазовия състав на тези композитни материали. Получени са фази на Cu_6Sn_5 и $Cu_{10}Sn_3$, които са в съответствие с диаграмите на състояние на бинарната Cu-Sn система. На получени порести нанокомпозитни материали, представляващи матрица от С-пяна и Cu-Sn наноразмерни частици, са проведени електрохимични тестове чрез циклична волтамперометрия в електролит на 1M LiCl и 1M KOH с апаратура Gamry галваностат-потенциостат в триелектродна клетка на Dr. Bob's. На нанокомпозитни материали с различна въглеродна матрица - въглеродна пяна и Cu-Sn наноразмерни частици, са проведени електрохимични изпитания като аноди в Li-ионни батерии. Изследвано е влиянието на въглеродната матрица върху електрохимичното поведение на тези композити. При отлагане на Cu_6Sn_5 сплав върху въглеродна пяна се подобрява циклируемостта на сплавта с 40% на 30-и цикъл. Проведеният електрохимичен тест показва, че получените композитни материали с въглеродна матрица и Cu-Sn наноразмерни частици са подходящи за анодни материали, алтернатива на графита в литиево-йонни батерии.

EQUAL IN EUROPEAN RESEARCH AREA

BULGARIAN VIPs

Prof. ANDRIANA ANTONOVA NEYKOVA, PhD

Faculty of History, Department Archives and Applied Historical Studies,
Sofia University "St. Kliment Ohridski"
Phone: +359 2 8502 101, Fax: +359 2 9463 022, E-mail: adi_n@abv.bg

Professor of Archival Science and Documentaries at the Faculty of History at Sofia University. Author of the monograph "Archives and the Society" and a number of research papers in the area of archival science, archeography and history and development of the Bulgarian university archival science as a professional educational model.

Professor Andriana Neykova is a successor and continuer of the best traditions and achievements of the Bulgarian historical and archival school. She is an innovator and generator of ideas, which assigns her a deserved place among the most prominent representatives of the contemporary archival thought. She has a leading role for the establishment, consolidation and modernization of the subject "Archival Science and Documentaries" at Sofia University "St. Kliment Ohridski".

Education and career

Prof. Andriana Neykova, PhD was born on 14th February 1949 in Sofia. In 1973 she graduated with excellent marks from Sofia University "St. Kliment Ohridski" majoring in history and immediately after that she started working at the Central State Historical Archives, now Central State Archives. In 1974 she was taken on the staff as a full-time post-graduate student at the Department of ***Archival Science and Auxiliary Historical Subjects*** of the Faculty of History at Sofia University. In 1980 she defended her dissertation paper on the following topic: "Archeographic Problems of the Documentary Heritage of the Bulgarian National Revival (1878-1978)". Within the period 1977-1979 she was an assistant in Archival Science at the Faculty of History of Sofia University. Having won a competition, she started working as a research scholar in the Scientific research laboratory of archival science and documentaries SRLASD established in 1979 as part of the former Chief Department of Archives at the Council of Ministers, presently Archives State Agency. During that period she took part in the development of important methodological regulations and standards of the archival science and documentaries. In 1984 she was appointed head of SRLASD. In 1986 she won the competition for assistant in archival science at the Faculty of History of Sofia University. In 1992 she attained the academic rank of ***associate professor*** with her paper "Ideas and programs for tracing and publishing of written sources of Bulgarian history". She is a member of the editorial staff of the Bulletin of state archives (1993-1996). Since 2001 she has been an expert at the National Education and Accreditation Agency. Within the period 2003 – 2006 she was a member of the specialized sci-

entific council of the new and newest history. In 2012 she occupied the academic position of ***professor*** at the Faculty of History at Sofia University.

Areas of teaching and research experience

The main areas of teaching and research are fundamental and topical issues of archival theory, history of archives, archeography, documentary and archival management, history and development of the Bulgarian university archival science as a professional educational model, European information professional archival standards of description.

Publications

Prof. Neykova published in 2007 the monograph "Archives and the Society". She has published over 80 research papers in specialized scientific journals. Her works are part of the contemporary Bulgarian specialized literature and contribute to the clarification of the specification in the development of our archival knowledge and the national archival system within the context of the general historical process and compared with the long-lasting traditions and the level of the leading foreign archival schools and practices.

Teaching and research projects

Within the period 1986-2002 the academic career of Prof. Neykova at the Faculty of History at Sofia University was connected with the educational process carried out within the framework of specialization in ***Archival science*** at the Department of ***Archival science***. During those years she worked hard for implementation of her idea for establishment of the university subject ***Archival science and documentaries***. In 2003 this project was officially accredited in the three stages of our higher education, namely: Bachelor, Master and PhD degrees. The past 12 years since the launching of the subject ***Archival science and documentaries*** have been inextricably bound up with the research and lecturing activities of Prof. Neykova. It is a well-known fact that during that period she read the main profiled lectures for the Bachelor's and Master's programs of the subjects ***Archival science and documentaries*** and ***History*** not only at Sofia University but also in other higher educational establishments which have educational courses in archival science, even though in separate subjects for now. Her general lecturing activity shows that she participates seriously in all stages of the higher education, which assigns her a leading role in the teaching of archival science in our country. She was a director of studies of more than 160 graduates and post-graduate students, as well as PhD students, including foreigners. These achievements are a categorical testimonial of the formation of an entire school of students and successors of the ideas and efforts of Prof. Neykova to ensure high quality professional university education and qualification in archival science. She is a scientific advisor of the one of its kind departmental ***Electronic library of archival science and documentaries.*** The name of professor Neykova is associated with the first ***University archival readings***, the beginning of which was marked on 18th April 2005. Under her leadership within the period 2005-2013 seven scientific conferences dedicated to topical problems of theoretical archival science, archival institutions, the profession of "archival scientist" and the university archival science were held. In the period of 1991-1993, Prof. Neykova participated in the international TEMPUS project for implementation of information technology in professional training of Archivistics.

Prof. LYUDMIL YORDANOV SPASOV, PhD, DSc

Faculty of History and Phylosophy, Department of History and Archaeology,
"Paisii Hilendarski" Plovdiv University
Phone: +359 32 261 268, E-mail: lyspasov@abv.bg

Born May 8, 1949, in the village of Yakimovo, district of Montana, Republic of Bulgaria. In 1971 graduates in History from the "St. Cyril and St. Methodius" University of Veliko Tarnovo. Works on issues of modern history of Bulgaria, Russia and the Balkans. Author of more than 10 monographies, 8 textbooks and over 130 papers. Regular member of the Union of the Scientists in Bulgaria.

Academic career:

1974 – Assistant; 1978 – Senior Assistant; 1981 – Chief Assistant; 1985 – Associate Professor; 2008 – Professor.

In 1980 received PhD in History of Bulgaria with dissertation entitled "The Government of the Bulgarian Agrarian National Union and the Russian Beloemigranti, 1921 – 1923".

In 2007 received scientific degree Doctor of Historical Sciences with thesis entitled "Bulgaria and the USSR, 1917 – 1944 (Politico-Diplomatic Relations)".

Teaching experience:

1974 – 1987 "St. Cyril and St. Methodius" University of Veliko Tarnovo, Associate Professor in Modern and Contemporary History of Bulgaria;

1988 – 1989 University of Forestry, Sofia;

1989 – 1995 Technical University, Sofia;

1995 – 1998 Institute of Military History to the Headquarters of the Bulgarian Army;

From 1998 to nowadays – Professor in the "Paisii Hilendarski" University of Plovdiv.

Read lectures at the Universities of Plovdiv and Veliko Tarnovo in the following disciplines: "History of Bulgarian Revival", "History of Bulgaria, 1878 – 1944", "History of the Bulgarian Diplomacy, 1878 – 1944" (these lectures are also read at the "Ivan Franko" L'viv University), "History of the Bulgarian Political Life, 1878 – 2013", "Ethnic Groups in the Balkans".

Specializations in the USSR (1976), Yugoslavia (1979/1980, 1985) and Greece (1987).

Administrative experience:

1983 – 1987 Deputy dean of the Historical faculty ("St. Cyril and St. Methodius" University of Veliko Tarnovo);

1990 – 1991 Director of Center for Education and Science (Technical University of Sofia);

2004 – 2012 Director of the "Lyuben Karavelov" Branch of the Plovdiv University.

SELECTED BIBLIOGRAPHY

Monographies: „Българо-съветски дипломатически отношения 1934-1944 г.", С., Наука и изкуство, **1987**, 205 р.; **„България,** Великите сили и балканските държави 1933–1939 г.", С., Изд. „Габи–91", **1993**, 185 р.; **„Врангеловата** армия в България 1919–1923 г.", С., Унив. изд. „Св. Климент Охридски", **1999**, 243 р.; **„История** на българите. Т. 4. Българската дипломация от древността до наши дни", С., Изд. „Знание" и Книгоизд. къща „Труд", **2003**, 695 р., съавт.: В. Тошкова, В. Трайков и Е. Александров); **„България** и СССР 1917-1944 г. (Политико-дипломатически отношения)". В. Търново, Фабер, **2008**, 550 р.; **Сто** неща, които трябва да знаем за историята на България 1878–1945 г. С., Световна библиотека, **2008**, 80 р.; **Македония**, земя българска. С., Световна библиотека, **2009**, 80 р., съавт. Пл. Павлов; **Освободителни** борби, армия и

войни. С., Световна библиотека, **2009**, 80 р.; **От** Добри Желязков до АЕЦ Козлодуй. С., Световна библиотека, **2009**, 80 р.; **Политика** и дипломация. С., Световна библиотека, **2009**, 80 р.

Studies and articles: Certain New Aspects of the Preparations for the April 1876 Uprising (The Role Played in Them by Oton Ivanov). – B u l g. hist. rev., **1976**, N 4, 74-77; **Bulgarian** Participation in the 1877-1878 Russo-Turkish War of Liberation - Southeastern Europe. – L'E u r o p e du Sud-Est, 6, Pt. 2, **1979**, 154p170, съавт.: П. Горанов; **La Sebie** et la question de Danube a la Conférence de Londres de 1871. – E t. balk., **1980**, № 4, 74-85; **Георги Бенковски** и възстановяването на българската държавност. – И с т. прегл., **1982**, № 1, 21-29; **Projets** de pacte de la mer Noire a la veille de la Deuxiime guerre mondiale. – E t. balk., **1982, L'URSS** et les relations bulgaro-turques a l'époque de 1934 a 1938. – E t. balk., **1983**, № 3, 58-76; **Дейността** на българските правителства за въоръжаване на войската 1919-1939 г. – В о е н н о и с т. сб., **1984**, № 6, 43–69; **СССР** и болгаро-турецкие отношения (сентябрь 1939 – март 1941 г.). – E t. hist., 12, **1984**, 251–272; **Les Projets** d'un Pacte méditerranoen et l'Entente balkanique 1934 – 1937. – E t. balk., **1987**, № 2, 3–19; **La Serbie** et le différend territorial bulgaro-roumain (janvier – août 1913). – E t. balk., **1987**, **Русские** ученые - белоэмигранты в Болгарии (1920-1930 годы). – B u l g. hist. rev., **1992**, № 4, 107-112; **La Conférence** a Montreux de 1936 et les pays balkaniques. – E t. balk., **1993**, № 1, 3-19; **Българо**-югославският пакт за нерушим мир и вечно приятелство от 24 януари 1937 г. – И з в. ВИНД, 61, **1998**, 145-183, co-author: Цв. Спасова; **Намесата** на Сърбия в Руско-турската война от 1877-1878 г. – И з в. ВИНД, 63, **1998**, **СССР,** България и Балканският пакт 1934–1940 г. – Във: Р о с с и я – Болгария: векторы взаимопониманиа. XVIII-XXI вв. Российско-болгарские научны е дискусии. М., **2010,** 404-427; **La petite** France et l'adhésion de la Bulgarie a la Société des Nations (1920). – E t. balk., **2011.**

AWARDS

PYTHAGORAS AWARDS '2013 FOR SIGNIFICANT CONTRIBUTIONS TO SCIENCE

The fifth annual ceremony for handing the Pythagoras awards for science took place in Sofia on May 21, 2013. The ceremony was hosted by Corresponding Member Professor Nikolay Miloshev, Minister of education, youth and science. Welcome address was given by Mr. Rosen Plevneliev, President of the Republic of Bulgaria.

Pythagoras awards for science have gained recognition as a prestigious annual event distinguishing best Bulgarian researchers. This year a number of 12 researchers were rewarded with prizes in 10 categories.

The **Grand Pythagoras Prize for young scientist** was shared between two chemists: **Assistant Professor Dr. Nikolay Georgiev** from the University of Chemical Technology and Metallurgy and **Assistant Professor Dr. Petko Denev** from the Institute of Organic Chemistry with Centre of Phytochemistry at the Bulgarian Academy of Sciences. Both received Pythagoras statuette and money prize of 5 000 BGN. They prizes were presented by the President, Mr. Rosen Plevneliev.

Minister Miloshev as host of the event presented the **Grand Prize for successful manager of international projects**, Pythagoras statuette and 10 000 BGN money prize to **Corresponding Member Professor DSc Toni Spasov** from the Faculty of Chemistry and Pharmacy at the "St. Clement of Ohrid" Sofia University.

There were four prizes for established researchers in the various areas of science. They were given as follows: **Prize for established researcher in the field of technical sciences** to **Corresponding Member Professor DSc Krasimir Atanasov** from the Institute of Biophysics and Biomedical Engineering at the Bulgarian Academy of Sciences; **Prize for established researcher in the field of biomedical sciences** to **Professor DSc Lyudmila Georgieva** from the Department of Medical Microbiology at the Medical University of Sofia; **Prize for established researcher in the field of natural and mathematical sciences** to **Professor DSc Georgi Vaisilov** from the Faculty of Chemistry and Pharmacy at the "St.

Clement of Ohrid" Sofia University; **Prize for established researcher in the field of social and humanitarian sciences** to **Professor DSc Sava Grozdev** from the Institute of Mathematics and Informatics at the Bulgarian Academy of Sciences.

Honors for research team with implemented developments in business were awarded to **Associate Professor Dr. Pavlinka Dolashka** from the Institute of Organic Chemistry with Centre of Phytochemistry at the Bulgarian Academy of Sciences.

A **special award for outstanding contribution to science** was presented to **Academic Professor DSc Dechko Dechkov** from the Institute of Electrochemistry and Energy Systems at the Bulgarian Academy of Sciences.

Each of the listed winners received crystal Pythagoras plaquettes and 5 000 BGN prize money.

Special awards for outstanding contribution to natural sciences were given to **Associate Professor Dr. Leander Litov** from the Faculty of Physics of the "St. Clement of Ohrid" Sofia University and to **Professor Dr. Vladimir Genchev** from the Institute for Nuclear Research and Nuclear Energy at the Bulgarian Academy of Sciences.

Prize of the Bulgarian Science Fund was handed to **Professor Dr. Hristo Beloev** from the "Angel Kanchev" University of Ruse.

Each of the last scientists received crystal Pythagoras plaquettes and 2 500 BGN prize money.

ARTICLES

RECENT PUBLICATIONS OF BULGARIAN SCIENTISTS

Title: **Zones of interculturality and linguistic identity: tales of Ladino by Sephardic Jews in Bulgaria**
Authors: Fay, R. [1], Davcheva, L[2].
Source: Language & Intercultural Communication. Vol. 14 Issue 1 (Jan. 2014), 24-40.
Author Affiliations: [1]The Manchester Institute of Education, The University of Manchester, Manchester, UK
[2]AHA Moments, Centre of Intercultural Learning, Education and Research, Sofia, Bulgaria
ISSN: 1470-8477

Title: **Colloidal origin of colloform–banded textures in the Paleogene low–sulfidation Khan Krum gold deposit, SEBulgaria**
Authors: Marinova, I.[1], Ganev, V.[1], Titorenkova, R.[1]
Source: Mineralium Deposita. Vol. 49, Issue 1, (Jan.2014), 49-74
Author Affiliations: [1]Institute of Mineralogy and Crystallography, Bulgarian Academy of Sciences, Acad. G. Bonchev Str., Bl. 107 1113 Sofia, Bulgaria
ISSN: 0026-4598

Title: **Morphological variation, genetic diversity and genome size of critically endangered Haberlea (Gesneriaceae) populations in Bulgaria do not support the recognition of two different species**
Authors: Petrova, G.[1], Dzhambazova, T.[1], Moyankova, D.[1], Georgieva, D.[1], Michova, A.[2], Djilianov, D.[1], Möller, M.[3]
Source: Plant Systematics & Evolution. Vol. 300, Issue 1, (Jan. 2014), 29-41
Author Affiliations: [1]Agrobioinstitute, 8 Draghan Tsankov Blvd 1164 Sofia Bulgaria
[2]Laboratory of Haematopathology and Immunology, National Specialized Hospital for Active Treatment of Haematological Diseases, Sofia, Bulgaria
[3]Royal Botanic Garden Edinburgh, 20A Inverleith Row Edinburgh EH3 5LR S cotland, UK
ISSN: 0378-2697

Title: **The state of public affairs in Bulgaria**
Authors: Mihova, M.[1]
Source: Journal of Public Affairs (14723891). Vol. 14, Issue 1, (Feb. 2014), 76-83
Author Affiliations: 1EPPA SA
ISSN: 1472-3891

Title: **Characterization of the chemical composition of archaeological glass finds from South–Eastern Bulgariausing PIXE, PIGE and ICP–AES**
Authors: Lesigyarski, D.[1], Šmit, Ž., Zlateva-Rangelova, B.[1], Koseva, K.[2], Kuleff, I.[1]
Source: Journal of Radioanalytical & Nuclear Chemistry. Vol. 295, Issue 3, (Mar. 2013), 1605-1619

Author Affiliations: [1]Faculty of Chemistry and Pharmacy, University of Sofia, 1 'James Bourchier' blvd 1164 Sofia Bulgaria
[2]Faculty of History, University of Sofia, 15 'Tsar Osvoboditel' blvd 1504 Sofia, Bulgaria
ISSN: 0236-5731

Title: **Three–point observation in the troposphere over Sofia–Plana Mountain,** Bulgaria
Authors: Evgenieva, T.[1], Wiman, B.[2], Kolev, N.[1], Savov, P.[3], Donev, E.[4], Ivanov, D.[4], Danchovski, V.[4], Kaprielov, B.[1], Grigorieva, V.[1], Iliev, I.[5], Kolev, I.[1]
Source: International Journal of Remote Sensing. Vol. 32, Issue 24, (20 Dec. 2011), 9343-9363
Author Affiliations: [1]Institute of Electronics, Laser Radars Laboratory, Bulgarian Academy of Sciences, Bulgaria
[2]Environmental Science and Technology Section, Linnaeus University, Sweden
[3]Department of Physics, University of Mining and Geology 'St. Ivan Rilski', Bulgaria
[4]Department of Meteorology and Geophysics, Faculty of Physics, Sofia University 'St. Kliment Ohridsky', Bulgaria
[5]Central Laboratory of Solar-Terrestrial Influences, Bulgarian Academy of Sciences, Bulgaria
ISSN: 0143-1161

Title: **Out–of–pocket payments for health care services in Bulgaria: financial burden and barrier to access**
Authors: Atanasova, E.[1,2], Pavlova, M.[2], Moutafova, E.[1], Rechel, B.[3], Groot, W.[2,4]
Source: European Journal of Public Health. Vol. 23, Issue 6, (Dec. 2013), 916-922
Author Affiliations: 11 Department of Health Economics and Management, Faculty of Public Health, Medical University, Varna, Bulgaria
22 Department of Health Services Research, CAPHRI, Maastricht University Medical Center, Faculty of Health, Medicine and Life Sciences, Maastricht University, Maastricht, The Netherlands
33 European Observatory on Health Systems and Policies, London School of Hygiene and Tropical Medicine, London, UK
44 Top Institute for Evidence-Based Education Research (TIER), Maastricht University, Maastricht, The Netherlands
ISSN: 1101-1262

Title: Distribution of chestnut blight and diversity of Cryphonectria parasitica in chestnut forests in Bulgaria
Authors: Risteski, M.[1], Milev, M.[2], Rigling, D.[3], Milgroom, M.[4], Bryner, S.[3], Sotirovski, K.

Source: Forest Pathology. Vol. 43, Issue 6, (Dec. 2013), 437-443
Author Affiliations: [1]Univerzitet 'Sv. Kiril i Metodij' Faculty of Forestry
[2]Faculty of Forestry, Department of Forestry, University of Forestry
[3]WSL Swiss Federal Research Institute
[4]Department of Plant Pathology and Plant-Microbe Biology, Cornell University
ISSN: 1437-4781

Title:	**First detection of OXA-24 carbapenemase-producing Acinetobacter baumannii isolates in Bulgaria**
Authors:	Todorova, B., Velinov, T.[1], Ivanov, I.[1], Dobreva, E.[1], Kantardjiev, T.[1]
Source:	World Journal of Microbiology & Biotechnology. Vol. 30, Issue 4, (Apr. 2014), 1427-1430
Author Affiliations:	[1]National Center of Infectious and Parasitic Diseases (NCIPD), 26, Yanko Sakazov Blvd 1504 Sofia, Bulgaria
ISSN:	0959-3993

Title:	**Paleoenvironmental application of Taxodium macrofossil biomarkers from the Bobov dol coal formation,** Bulgaria
Authors:	Stefanova, M.[1], Ivanov, D.[2], Simoneit, B.[3]
Source:	International Journal of Coal Geology. Vol. 120, (Dec. 2013), 102-110
Author Affiliations:	[1]Institute of Organic Chemistry, Bulgarian Academy of Sciences, Acad. G. Bonchev Str., bldg. 9, BG-1113 Sofia, Bulgaria [2]Institute of Biodiversity and Ecosystem Research, Bulgarian Academy of Sciences, Acad. G. Bonchev Str., bldg. 23, BG-1113 Sofia, Bulgaria [3]Department of Chemistry, Oregon State University, Corvallis, OR 97331, USA
ISSN:	0166-5162

Title:	**Essential and toxic microelement profile of walnut (Juglans regia L.) cultivars grown in industrially contaminated area — Evaluation for human nutrition and health**
Authors:	Arpadjan, S.[1], Momchilova, S.[2], Elenkova, D.[1], Blagoeva, e.[3]
Source:	Journal of Food & Nutrition Research. Vol. 52, Issue 2, (2013), 121-127

EVENTS

THIRD INTERNATIONAL CONGRESS OF BULGARIAN STUDIES

Between 23rd and 26th of May 2013 at "St. Clement of Ohrid" Sofia University take place the **Third International Congress of Bulgarian Studies**. It was attended by 475 scientists, which represented more than 130 universities, research institutions and centers from 45 countries of the world. Having in mind that it's impossible for such an event to be sufficiently summarized, in the following lines are outlined only the main groups of activities.

The scientific program of the Congress was divided in plenary reports per sections, four main sections (each of them with several subsections) and four round tables.

Plenary reports were presented by **Acad. Prof. Vasil Gjuzelev** ("The Last Quarter of a Century in Bulgarian Medieval Studies"), **Assist. Prof. Alberto Alberti** ("Tarnovo Gospels in the 14th century and Byzantine Text: So Close, So Far Away"), **Assoc. Prof. Veselin Tepavicharov** ("Problems of the Transition in Bulgaria after 1989: Ethnopolitical Projections"), **Assoc. Prof. Eero Suvilehto** ("Krali Marko and Kalevala: Epics as Part of National Identity"), **Prof. Mihail Nedelchev et alii** ("The New Bulgarian Studies"), **Prof. Celina Juda** ("People's Republic of Bulgaria as a Palimpsest: «Alternative» Literature for Memory and Identification in the Experience of Authors Working outside of Bulgaria"), **Prof. Habil. Ruselina Nitsolova** ("Some Results from the Grammaticalization in Bulgarian Morphology"), **Dr. Johanes Reinhart** ("Old Bulgarian and the Reconstruction of Proto-Slavic Verb").

The Sections and their subsections were as follows: **History and Archaeology** ("Bulgarian Lands in Antiquity", "Bulgarians in the Middle Ages", "Bulgarian Lands and the Bulgarians in the 15th – 19th Century", "New Bulgarian History", "Contemporary Bulgarian History", мEconomics"), **Culture and Society** ("Anthropology, Sociology, Culturology", "Bulgarian Diaspora", "Comparative Ethnology", "Bulgarian Ethnology"), **Bulgarian Literature** ("History of Bulgarian Literature", "Bulgarian Literature in European and World Context", "Modern Bulgarian Literature") and **Bulgarian Language** ("History of Bulgarian Language", "Modern Bulgarian Language: Comparative and Contrastive Studies", "Dialectology", "Modern Bulgarian Language: Phonetics and Grammar", "Modern Bulgarian Language: Norm, Communications, Mentality", "Bulgarian Studies Abroad: Translation and Bulgarian Language Teaching", "Bulgarian Language: Lexicology and Lexicography").

The round tables were organized around the topics of: "Cyril and Methodius Studies", "Bulgarian Studies", "Digitalization" and "The Golden Age of Tsar Simeon: Policy, Religion, Culture".

UPCOMING CONFERENCES

5 – 7 March 2014
10th Energy Efficiency and Renewable Energy Congress and Exhibition for South–East Europe
Inter Expo Center, Sofia, Bulgaria
Web site: http://via-expo.com/en/pages/ee-re-congress

24 – 26 May 2014
4th World Congress of
Total Intravenous Anaesthesia and Target Controlled Infusion
Sofia, Bulgaria
Web site: http://tiva-tcicongress.com

28 – 31 May 2014
21st European Congress on Obesity
National Palace of Culture, Sofia, Bulgaria
E-mail: eco2014@easo.org
Web site: http://eco2014.easo.org

5 – 9 June 2014
2nd International Conference
Agriculture and Food 2014
Elenite Holiday Village, Burgas, Bulgaria
E-mail: agriculture@sciencebg.net
Web site: http://www.sciencebg.net/en/conferences/agriculture-and-food

8 – 12 June 2014
23rd International Conference
Ecology and Safety 2014
Elenite Holiday Village, Burgas, Bulgaria
E-mail: ecology@sciencebg.net
Web site: http://www.sciencebg.net/en/conferences/ecology-and-safety

11 – 15 June 2014
16th International Conference
Materials, Methods and Technologies 2014
Elenite Holiday Village, Burgas, Bulgaria
E-mail: mmt@sciencebg.net
Web site: http://www.sciencebg.net/en/conferences/materials-methods-and-technologies

17 – 26 June 2014
14th International Multidisciplinary Scientific
GeoConference & EXPO SGEM 2014
Flamingo Grand Congress Center, Albena Resort & SPA, Bulgaria
Phone: (+359) 2 975 3982
Fax: (+359) 2 874 1088
Skype Name: SGEM_Office
E-mail: sgem@sgem.org
Web site: http://www.sgem.org

19 – 22 June 2014
25th World Congress on
Videourology & Advances in Clinical Urology
Sofia, Bulgaria
E-mail: info@videourology2014.com
Web site: http://www.videourology2014.com/welcome.html

26 – 28 June 2014
8th National Conference on Chemistry
Chemistry for Sustainable Development
University of Chemical Technology and Metallurgy, Sofia
Phone: (+359) 2 870 20 88
Fax: (+359) 2 870 75 23
E-mail: bioreac@bas.bg
Web site: http://8ncc.unionchem.org/index.php

27 – 28 June 2014
International Conference on
Computer Systems and Technologies
Ruse, Bulgaria
E-mail: JKalmukov@gmail.com
Web site: http://www.compsystech.org

1 – 5 September 2014
13th International Conference
Economy and Business 2014
Elenite Holiday Village, Burgas, Bulgaria
E-mail: economy@sciencebg.net
Web site: http://www.sciencebg.net/en/conferences/economy-and-business

2 – 7 September 2014
International Multidisciplinary Scientific Conferences on
Social Sciences and Arts
Albena, Bulgaria
Phone: (+359) 2 975 3982
Fax: (+359) 2 874 1088
E-mail: sgem@sgemsocial.org
Web site: http://sgemsocial.org

4 – 8 September 2014
5th International Conference
Education, Research and Development 2014
Elenite Holiday Village, Burgas, Bulgaria
E-mail: erd@sciencebg.net
Web site: http://www.sciencebg.net/en/conferences/education-research-and-development

7 – 11 September 2014
8th International Conference
Language, Individual and Society 2014
Elenite Holiday Village, Burgas, Bulgaria
E-mail: lis@sciencebg.net
Web site: http://www.sciencebg.net/en/conferences/language-individual-and-society

8 – 11 September 2014 16th international conference on
Harmonisation within Atmospheric Dispersion Modelling for Regulatory Purposes
Riviera Holiday Club, Varna, Bulgaria
Phone: (+359) 2 980 17 95; (+359) 896 700 949
E-mail: dani@cim.bg
Web site: http://www.harmo16.org

10 – 14 September 2014 3rd International Conference
Media and Mass Communication 2014
Elenite Holiday Village, Burgas, Bulgaria
E-mail: media@sciencebg.net
Web site: http://www.sciencebg.net/en/conferences/media-and-mass-communication

2 – 5 October 2014 XIV National Congress of
Cardiology
Golden Sands Resort, Varna, Bulgaria
Phone: (+359) 2 988 80 35; (+359) 895 737 820
Fax: (+359) 980 60 74
E-mail: denitza@cim.bg
Web site: http://en.14cardiocongress.com

30 – 31 October 2014
Scientific Conference
Geography and Regional Science
Pazardzhik, Bulgaria
Phone: (+359) 2 979 3943; (+359) 2 979 3304
E-mail: bulgeo2014@gmail.com; bulgeo2014@abv.bg